Geochimica et Cosmochimica Acta

JOURNAL OF THE GEOCHEMICAL SOCIETY

xecutive Editors

C. W. CORRENS, *Göttingen.* E. INGERSON, *Austin, Texas.* L. R. WAGER, *Oxford.*

ditors

L. H. AHRENS, *Capetown.* S. R. NOCKOLDS, *Cambridge.* H. C. UREY, *La Jolla, Calif.*
JOHN VERHOOGEN, *Berkeley, Calif.* A. P. VINOGRADOV, *Moscow.*
F. E. WICKMAN, *Stockholm.*

CONTENTS VOLUME 15, No. 3 DECEMBER 1958

R. J. W. McLAUGHLIN: Geochemical partition in two illitic clays 165

J. P. FORSMAN and J. M. HUNT: Insoluble organic matter (kerogen) in sedimentary rocks 170

E. C. WALKER, F. CUTTITTA and F. E. SENFTLE: Some natural variations in the relative abundance of copper isotopes 183

A. E. RINGWOOD: The constitution of the mantle—III. Consequences of the olivine–spinel transition 195

THELMA ISAACS and RUSTUM ROY: The α–β inversions in eucryptite and spodumene 213

IRVING FRIEDMAN and ROBERT L. SMITH: The deuterium content of water in some volcanic glasses 218

M. D. KARKHANAVALA: On radioactive uraniferous iron oxides 229

S. A. EL WARDANI: Marine geochemistry of germanium and the origin of Pacific pelagic clay minerals 237

Book Review:

"Gmelins Handbuch der anorganischen Chemie. 8 Auflage. System Nummer 28: Calcium. Teil A—Lieferung 2." (reviewed by C. W. CORRENS) 255

Papers to be published in future issues 256

UNIVERSITY OF HAWAII LIBRARY

PERGAMON PRESS LONDON • NEW YORK • PARIS • LOS ANGELES

GEOCHIMICA ET COSMOCHIMICA ACTA

EXECUTIVE EDITORS

PROF. C. W. CORRENS (1959) *Sedimentpetrographisches Institut der Universität, Lotzestr.* 13, *Göttingen, Germany*
PROF. E. INGERSON (1959–1960) *Department of Geology, University of Texas, Austin* 12, *Texas, U.S.A.*
PROF. L. R. WAGER, F.R.S. (1959–1961) *Department of Geology and Mineralogy, The University, Oxford, England*

EDITORS

PROF. L. H. AHRENS (1959–1960) *Department of Chemistry, University of Capetown, Rondebosch, Cape Province, South Africa*
DR. S. R. NOCKOLDS (1959) *Department of Mineralogy and Petrology, The University, Cambridge, England*
PROF. H. C. UREY, For. Mem. R. S. (1959) *University of California, La Jolla, California, U.S.A.*
DR. JOHN VERHOOGEN (1959–1961) *Department of Geology, University of California, Berkeley, California, U.S.A.*
PROF. A. P. VINOGRADOV (1959–1961) *Vernadsky Institute, Moscow, U.S.S.R.*
PROF. F. E. WICKMAN (1958) *Naturhistoriska Riksmuseets, Mineralogiska Avdelning, Stockholm* 50, *Sweden*

EDITORIAL ADVISORY BOARD

EUROPE

T. BARTH, *Oslo*
L. CAPDECOMME, *Toulouse*
E. J. CONWAY, *Dublin*
P. ESKOLA, *Helsinki*
P. GALLITELLI, *Modena*
A. HADDING, *Lund*
O. HAHN, *Göttingen*
H. W. HARVEY, *Plymouth*
F. HEIDE, *Jena*
A. HOLMES, *Edinburgh*
W. Q. KENNEDY, *Leeds*
PH. H. KUENEN, *Gröningen*
S. LANDERGREN, *Stockholm*
F. MACHATSCHKI, *Vienna*
A. MUIR, *Harpenden*
J. ORCEL, *Paris*
E. RAGUIN, *Paris*
K. RANKAMA, *Helsinki*
E. REINHARD, *Basle*
TH. G. SAHAMA, *Helsinki*
C. E. TILLEY, *Cambridge*
T. VOGT, *Trondheim*
W. WAHL, *Helsinki*

AMERICAN CONTINENT

A. F. BUDDINGTON, *Princeton*
D. GUIMARAES, *Belo Horizonte*
G. E. HUTCHINSON, *New Haven*
B. H. MASON, *New York*
F. WHIPPLE, *Cambridge*
R. WILDT, *New Haven*

FAR EAST

T. WATANABE, *Tokyo*

Publishing Offices: Pergamon Press Ltd., 4 & 5 Fitzroy Square, London W.1 (EUSton 4455)

Four issues per volume, three volumes per year

Subscription *per annum* (including postage) (A) £18. (U.S.A. $51.00); (B) For individual subscribers who certify that the Journal is for their private use, £7. 7s. (U.S.A. $21.50). Members of the Geochemical Society, or non-members who occasionally publish papers in the Journal, £3. 11s. 6d. (U.S.A. $10.00) *per annum.*

Payment must be made in advance

Back numbers, £10 (U.S.A. $28.00) per volume

Copyright © 1958 Pergamon Press Ltd.

PERGAMON PRESS LTD.

4 & 5 FITZROY SQUARE, LONDON W.1 122 EAST 55TH STREET, NEW YORK 22, N.Y.

PRINTED AT THE UNIVERSITIES PRESS, BELFAST, NORTHERN IRELAND

Geochimica et Cosmochimica Acta, 1958, Vol. 15, pp. 165 to 169. Pergamon Press Ltd. Printed in Northern Ireland

Geochemical partition in two illitic clays

R. J. W. McLaughlin
T. & R. Boote Ltd., Burslem, Staffs

(*Received* 1 *February* 1958)

Abstract—Chemical data for both major and minor elements are given for sand, silt and clay fractions of two illitic clays. The gradations are traced and geochemical enrichment discussed.

Introduction

The term illite was originally proposed as a general name for the widely distributed clay mineral content of argillaceous sediments. The general relation was to the mica group and type formula $(OH)_4K_y(Al,Mg,Fe)_{4-6}$ $(Si_{8-y}Al_y)O_{20}$ (Grim, Bray and Bradley, 1937; Grim, 1939).

The samples selected for treatment were those chosen by the American Petroleum Institute, Project 49 (1951), namely nos. 35 and 36. For convenience these numbers have been retained in this paper. No. 35 is from $3\frac{1}{2}$ miles S of Fithian, Illinois, on the SE bank of Salt Fork Creek, W $\frac{1}{2}$ section 31, Township 19 N, Ranch 13 W in Vermilion Co. The clay outcrops along the creek beneath the coal seam. No. 36 is from 7 miles E of Morris, Illinois, Goose Lake area, NW $\frac{1}{2}$ NE, $\frac{1}{4}$ section 11, Township 33 N, Range 8 E, in Grundy Co. The clay occurs in a clay pit and lies above the three underclays which are separated by minor coal seams.

After a preliminary treatment with hydrogen peroxide to oxidize any carbonaceus material present, the illitic clays were separated into various size-fractions by dispersal in distilled water, using a small quantity of sodium hexametaphosphate to aid dispersion. The subsequent separation into fractions was by gravitational settling for sand (>20 μ equivalent spherical diameter [esd]) and centrifugal means for silt (2–20 μ esd) and clay (<2 μ esd). Settlement of the clay fraction is achieved by adjusting the pH slightly. All fractions were thoroughly washed with distilled water before drying with alcohol and acetone. Analysis was by classical methods for major elements and spectrographic for the minor elements. In the case of the latter, estimation was semi-quantitative, and the method used was similar to that described by Nockolds and Allen (1953) with the exception that the standards used were prepared mixtures in which composition corresponded to average composition of the materials investigated.

Results

It should be pointed out in advance that the rigorous pre-treatment of the samples precludes any concentrations described as due to base exchange or absorption phenomena. This facet of the chemistry of these clays is therefore not discussed. The figures presented in Table 1 show some interesting features. There are, as might be expected, anomalous figures in the sand fractions, thus no. 35 contains a considerable excess of calcium (present as calcium carbonate) and no. 36 contains a considerable excess of iron (present as pyrite).

The increase in quantity of the mineral illite with decreasing grain-size is best exhibited by the aluminium figures, for although the potassium rises also, it does not do so to such a marked extent. These features are best demonstrated by calculating silicon/aluminium ratios. The potassium/aluminium ratios are not

Table 1. Element concentrations (p.p.m.) of fractions of two illitic clays

	35			36			S†	A†
	Sand	Silt	Clay	Sand	Silt	Clay		
$Si^{+4} \times 10^2$	2357	2820	2380	1673	2978	2484		0·42
$Al^{+3} \times 10^2$	445	936	1357	77	750	1247		0·51
$Ti^{+4} \times 10^2$	34	65	47	21	54	51		0·68
$Fe^{+3} \times 10^2$*	746	332	423	2678	424	394		0·64
$Mg^{+2} \times 10^2$	36	60	30	54	110	18		0·66
Mn^{+2}	396	223	54	281	—	—		0·80
$Na^{+1} \times 10^2$	68	57	18	6	10	10		0·97
$Ca^{+2} \times 10^2$	1157	187	39	14	42	48		0·99
$K^{+1} \times 10^2$	142	342	354	22	384	414		1·33
Ga^{+3}	—	5	7	—	5	7	2	0·62
Cr^{+3}	100	180	180	100	250	340	2	0·63
V^{+3}	22	95	130	22	400	800	5	0·74
Sn^{+4}	—	—	25	—	—	10	10	0·71
Li^{+1}	12	80	40	2	40	40	1	0·68
Ni^{+2}	50	50	22	200	100	50	2	0·69
Co^{+2}	10	10	8	25	10	8	3	0·72
Zr^{+4}	100	100	45	100	100	45	10	0·79
Y^{+3}	17	22	17	—	17	10	3	0·92
Sr^{+2}	320	220	140	140	320	320	2	1·12
Pb^{+2}	65	30	—	—	30	30	6	1·20
Ba^{+2}	300	650	650	650	400	300	5	1·34
Rb^{+1}	320	700	700	—	700	1000	30	1·47
Ag^{+1}	—	—	—	T	—	—	0·5	1·26
Si/Al	5·29	3·01	1·70	21·7	3·97	2·00		
Al/K	3·13	2·74	3·83	3·50	1·95	3·01		
K/Na	2·09	6·00	19·7	3·66	38·4	41·4		

* Ferrous iron was not determined.

† S = sensitivity, A = ionic radii in Å.

— = below sensitivity. Be^{+2}, $S = 30$; La^{+2}, $S = 13$; Mo^{+4}, $S = 2$; Cs^{+1}, $S = 15$; Sc^{+3}, $S = 8$; are all —.

constant either because of extraneous minerals influencing their trend or because the actual clay mineral does vary in potash content. It is difficult to demonstrate any points with the sand fraction because of the known contaminants. The silt fraction is, however, relatively clear of admixture (except for silica) and in this fraction the Al/K ratios are lower than in the clay fractions. As no extraneous minerals high in potash can be found (by X-ray analysis) the inference is, therefore, that the clay mineral of the silt fraction is richer in potassium than that in the more fine-grained material. If this is so then it may arise by two methods. Either

during deposition there were deposited two distinct types of illite, the coarser approximating to degraded mica or sericite, or during compaction there has been some recrystallization. This latter is favoured by the evidence of slickensiding and parallelism of larger clay mineral fragments in thin section (especially no. 36). This would mean, therefore, that during recrystallization more aluminium for silicon substitution would occur in the tetrahedral layers with consequent increase in charge of the layers and subsequent entry of relatively more potassium to balance such charge. This hypothesis is also substantiated by the higher magnesium content (presumably in the octahedral layers) and also titanium. Furthermore, the older the sediment consisting of illite, the better crystallized is the material, (Grim, Dietz and Bradley, 1949), and Nagelschmidt (1944) has shown that illite from consolidated shales is more resistant to molecular dilation along the *z*-axis (using calcium chloride) than that in recent unconsolidated sediments. The evidence would therefore point in favour of some recrystallization becoming operative and this does indicate that the substitution of aluminium for silicon takes place under relatively low conditions of shear.

In both major and minor elements there is, in the cases of specific elements, a tendency to concentrate in the silt fraction. This is true for silicon, titanium, magnesium, lithium and yttrium. This same behaviour with specific elements has also been observed in fractionated soils (McLaughlin, 1955). The higher content of manganese in the coarse fraction as against the finer fraction is presumably due to minute amounts of manganese dioxide associated with the sand grains.

The behaviour of the minor elements and their relationships to the major elements is as follows. Gallium follows aluminium and therefore is concentrated in the clay fraction. Tin, chromium and especially vanadium are concentrated in the clay fractions and are presumably following the iron in the octahedral layers of the lattice. There are specific trace elements which are concentrated in the coarser fractions and these are: nickel and cobalt, following the iron and presumably present in the sesquioxide coatings and pyrite impurity; zirconium, probably as minute fragments of zircon. The behaviours of barium and strontium are opposed in the two specimens, but a consideration of ionic sizes suggests that in no. 35 the strontium is higher in the coarse fraction because of the calcium carbonate impurity and higher in no. 36 fine fraction because here it is being absorbed by the fine grained material, for the larger the ionic size the more strongly an ion will be absorbed. Thus in both specimens the barium is high in the clay fractions because, like rubidium, it is following potassium. The anomaly of high barium content of the sand fraction in no. 36 is no doubt due to liberation of sulphuric acid from the pyrite and subsequent precipitation of the very insoluble barium sulphate. The trace of silver recorded in no. 36 sand is believed to be associated with the pyrite impurity.

Discussion

The figures derived for the partition of the elements amongst the various size fractions shed some interesting light upon the palaeographic conditions operative during formation. It is known that illite (the predominant mineral present) may be formed from other clays. Thus many investigators, (Caillère and Hénin,

1948; Volk, 1938; Aleshin, 1948; and Barshad, 1950) have shown that a material similar to illite is produced from potassium-saturated montmorillonite when dried at approximately 110°C. Similarly Dietz (1942) and Grim, Dietz and Bradley (1949) have shown that illite is being formed at the present day by diagenesis of material on the ocean bottom, thus kaolinite is lost slowly and montmorillonite very slowly by the processes of halmyrolysis. It should be noted, however, that Norin (1954) in his investigations on sediments from the central Tyrrhenian Sea showed that glass fragments and feldspar showed little sign of alteration, but illite was present in the finer fractions. At the present day illite is being formed in considerable quantities under conditions of temperate weathering, semi-tropical or tropical weathering tending to cause lateritization. It is generally agreed that free-draining acid conditions favour kaolinite formation and water-saturated alkaline conditions favour montmorillonite formation. It is also generally agreed that illite is formed under conditions where there is an excess of lime and both nos. 35 and 36 are associated with calcareous bands (Caillère, Petter and Oberlin, 1956). There are therefore four possibilities of formation of the sediments investigated:

(1) Diagenesis from other clays, e.g. kaolinite.
(2) Alteration from sericitic material.
(3) Direct precipitation *in situ*.
(4) Direct formation by weathering and subsequent transportation.

The figures in Table 1 for minor elements shed some light upon which of these possibilities is correct. If (1) were correct this would assume that either the kaolinite was rich in such elements as vanadium, chromium, etc., or such elements were rich in the slowly percolating solutions operative during diagenesis. It seems difficult to credit the former of these two possibilities in view of the known low adsorptive power of kaolinite. Furthermore, one might expect some remnant of relict structure, but the illite is always poorly defined in crystal outline. There is also no apparent source of the potassium-rich solutions necessary to effect the change, nor any remnant kaolinite. If (2) were correct then it would seem reasonable to assume that such material would be comparatively coarse (silt or sand) and yet the greater part of the specimens are of very fine grade. If hypothesis (3) were correct then the results of precipitation would be very fine-grained and would, of necessity, form fairly slowly, as laboratory experiments of synthesis have shown. This would not accord with the presence of excess quartz in the coarser fractions, which must have entered by the normal processes of the sedimentary cycle, and thus mitigates against any explanation of origin as due to very slow accumulation of material by precipitation *in situ*. Furthermore, there are associated coal seams and the lithology is strongly indicative of deposition in a littoral zone.

The evidence is strongly in favour of hypothesis (4) and under this the material would have been derived from normal processes of erosion upon land. The conditions at the time must therefore have been temperate and certainly not tropical or sub-tropical. The illite presumably represents weathered material, perhaps from soils, which has been transported and deposited. The occurrence of calcareous bands is highly suggestive of a marine environment, and the very fine grain-size

of much of the clay need not, of necessity, indicate slow accumulation due to deep-water but be merely a reflection of the nature of the material being supplied at the time, for the clay–mineral illite is normally very fine-grained. The titanium and zirconium figures would indicate that little admixture of material from foreign sources occurred, for these values are lower than those usually encountered in sedimentary clays. This is perhaps indicative of deposition in semi-landlocked embayments of the sea and hence the associated plant detritus.

References

Aleshin S. N. (1948) *Dokl. Akad. Nauk SSSR* **61,** 693–695.
Barshad I. (1950) *Amer. Min.* **35,** 225–238.
Caillère S., Hénin S. and Meriaux S. (1948) *C. R. Acad. Sci., Paris* **226,** 680–681.
Caillère S., Petter G. and Oberlin A. (1956) *Bull. Soc. France. Minér.* **79,** 174.
Dietz R. S. (1942) *Amer. Min.* **27,** 219–220.
Grim R. E. (1939) *J. Amer. Ceram. Soc.* **22,** 141–151.
Grim R. E., Bray R. M. and Bradley W. F. (1937) *Amer. Min.* **22,** 813–829.
Grim R. E., Dietz R. S. and Bradley W. F. (1949) *Bull. Geol. Soc. Amer.* **60,** 1785–1808.
Kerr P. F. (Editor) (1951) *Reference Clay Minerals.* American Petroleum Institute Project 49.
McLaughlin R. J. W. (1955) *Geochim. et Cosmochim. Acta* **8,** 109–130.
Nockolds S. R. and Allen R. (1953) *Geochim. et Cosmochim. Acta* **4,** 105–142.
Nagelschmidt G. (1944) *Miner. Mag.* **27,** 59–61.
Norin E. (1954) *Bull. Geol. Instn. Upsala* **39,** 279–284.
Volk G. (1938) *Soil Sci.* **45,** 263–276.

Geochimica et Cosmochimica Acta, 1958, Vol. 15, pp. 170 to 182. Pergamon Press Ltd. Printed in Northern Ireland

Insoluble organic matter (kerogen) in sedimentary rocks*

J. P. Forsman† and J. M. Hunt
Jersey Production Research Company, Tulsa, Oklahoma, U.S.A.

(*Received* 25 *November* 1957)

Abstract—Kerogen was isolated, by techniques developed in this study, from twenty-one rock samples representing a wide variety of geologic ages, rock types, and environments of deposition. These techniques make it possible to separate relatively mineral-free kerogen from rocks containing trace amounts of organic matter and to obtain reliable measurements of physical and chemical properties of kerogen. The two types of kerogens recognized in this study appear to be controlled by the nature of the original living matter deposited with the sediments, although metamorphic forces also appear to have affected the properties of kerogen. Hydrogenolysis of different kerogens results in soluble products varying appreciably in amount and type.

Previous studies (Hunt, Stewart and Dickey, 1954; Hunt and Jamieson, 1956) have shown that a large majority of sedimentary non-reservoir rocks contain from a few hundredths to 5 per cent of organic matter. Two general types of organic matter are recognized in these rocks. *Soluble organic matter*, usually 5 to 15 per cent of the total, is isolated by extraction of the rock with organic solvents. This material, which resembles petroleum in constitution as well as in appearance, can be separated into paraffin–naphthene hydrocarbons, organic compounds containing nitrogen, sulphur or oxygen, and "asphaltenes." These types of compounds all have their counterparts in petroleum (Hunt and Jamieson, 1956).

Relatively little attention has been given to the *insoluble organic matter* or *kerogen* of a sedimentary rock, despite the fact that it accounts for most of the total organic content. Several investigators have carried out chemical studies of kerogen in oil shales and torbanites (reviewed by Himus, 1949), but only a few papers have appeared on kerogen in less organic-rich marine rocks (Breger and Deul, 1953–1956; Takahashi, 1935).

The present study of kerogen in sedimentary rocks of marine origin was undertaken to determine certain of its chemical and physical properties that could lead to a better understanding of the processes involved in the formation of petroleum. However, before any of the various properties of kerogen could be measured, it was first necessary to isolate the kerogen from the inorganic constituents of the rock.

Procedures

The isolation procedures used in this study (Fig. 1) were based on the methods first used by the Bureau of Mines (Guthrie, 1938) and later developed by Dancy and Giedroyc (1950). Briefly, the method consisted of treating with an excess of acid a quantity of pulverized and solvent-extracted rock (Hunt and Jamieson, 1956) sufficient to yield at least 1 g of kerogen. The initial acid treatment varied according to the lithology of the samples. Carbonates and calcareous shales were

* Paper read before the Division of Analytical Chemistry, 131st Meeting, ACS, Miami, Florida, April 1957.

† Present address: Esso Research and Engineering Co., Linden, N.J., U.S.A.

best digested with hydrochloric acid to remove soluble calcium and magnesium which otherwise would form insoluble precipitates in subsequent treatments. Following the hydrochloric acid step, the insoluble residue was successively digested with cold and with hot concentrated hydrofluoric acid to remove alumina-silicates and quartz.

Early in the investigation, it was recognized that, in contrast to kerogen-rich oil shales, the isolation of organic matter from the more common types of marine

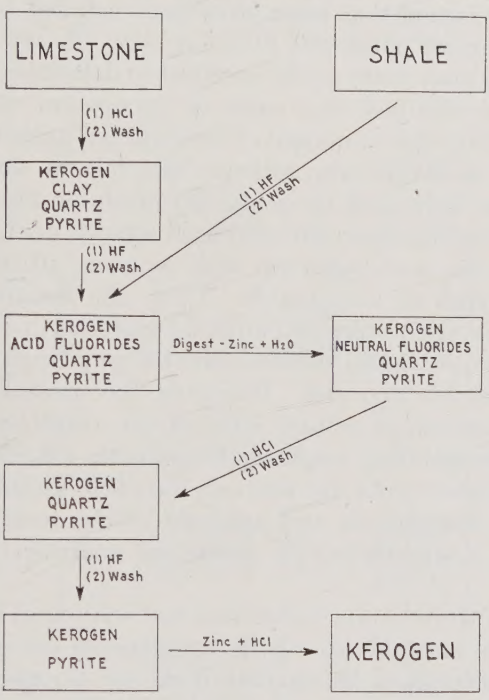

Fig. 1. Flowsheet for isolation of kerogen.

shales presented special problems. These were caused by the fact that the more typical marine shales contain much less organic matter than oil shales, and thus the hydrofluoric acid-insoluble minerals generally exceed the organic content. Accordingly, a considerable amount of effort was expended in improving techniques of isolation and in devising new methods for reducing the ash content.

The more difficultly soluble inorganic material encountered in this investigation was of two general types. These were: (1) insoluble minerals such as pyrite and zircon and (2) complex fluorides formed during the reaction of hydrofluoric acid with clay minerals and feldspars.

Of the first type, pyrite proved to be the most troublesome because it was abundant in nearly all of the samples. Pure pyrite is readily soluble in concentrated nitric acid, but the drastic effects of the reagent on organic matter precluded its use in this investigation. For a few samples, the size of the pyrite particles was large enough that physical methods such as heavy liquid flotation could be used in their separation. In all other cases, an improvement of the

zinc–hydrochloric acid method devised by Himus and Basak (1949) was used. This technique was found to be very effective in dissolving pure pyrite, but the presence of organic material appeared to inhibit the reaction. Consequently, several treatments with this reagent were generally necessary.

The second class of insoluble material consisted of a number of complex fluorides of various types. In a few cases, the identity of these products was established by the comparison of X-ray diffraction spectra of digestion residues with synthetic material. These compounds that were identified included potassium fluosilicate, aluminum oxyfluoride, and potassium fluoaluminate. X-ray diffraction lines were found in some samples that could not be ascribed to definite compounds. However, indirect evidence was obtained that some of the spectra might be attributed to mixtures of complex fluorides composed of ferrous iron, ammonium ion, and hydrogen with such metals as aluminium, calcium, magnesium, and potassium.

Several techniques were used for removing insoluble fluorides. Each of these methods, which included digestion with hot hydrochloric acid, hot water extraction, and treatment with zinc and water or with aqueous alkalis, were found to be specific for certain types of compounds. Thus, the treatments used and their sequences depended on the nature of inorganic material in the residues.

Dancy and Giedroyc (1950) recommend the use of sodium carbonate for the decomposition of insoluble fluorides. However, the present work indicated that the addition of potassium or sodium salts to the reaction mixtures causes the formation of the corresponding insoluble fluosilicates (M_2SiF_6). Ammonium carbonate is preferred since it does not form an insoluble fluosilicate.

Table 1 lists the descriptions and analyses of the rock samples used in this investigation; Table 2 summarizes the elemental analytical data on the kerogen isolates.

Three examples of the combined chemical and analytical attack on the problem of removing the more insoluble inorganic components are given in the following sections. The first example, a black shale from the Eocene Wilcox of Louisiana, illustrates the use of X-ray diffraction in the identification of inorganic impurities and in following their removal at various stages of concentration. The second sample, an argillaceous limestone from the Duvernay shale of Alberta, gives some of the refinements in technique developed during the course of the work. The isolation of kerogen from a metamorphosed rock of Texas is included as the third example because it shows a modification in technique which is useful for the more graphitic samples.

Black shale

Portions of pulverized shale were placed in 2 l. Monel beakers, and 50 per cent hydrofluoric acid was added slowly in order to prevent loss of material by frothing. After digestion on a steam bath, the contents of the two beakers were diluted with water; the solid residue was collected in a basket-type centrifugal filter and washed with water until only traces of fluoride were detected in the filtrate (lead chloride test). The moist filter cake was transferred to Monel beakers, and, after a second treatment with hydrofluoric acid, the gelatinous, dark-brown insoluble residue was centrifuged and washed with dilute hydrochloric acid in polyethylene bottles.

Table 1. Description and analyses of rocks used in kerogen isolation

Lab. serial no.	Formation	Sample locality			Depth (ft)	Lithology	Age	Analyses of extracted rock		
		Well	Location	State				Organic C %	Kjeldahl N %	Total S %
6529	Cherokee	TCO # 1 Winchell	6–36S–5E	Kansas	3136–47	blk. sh.	Pennsylvanian	1·73	0·11	1·01
6412	Hoxbar	TCO # 1 Garrett	32–11N–25W	Oklahoma	10687–8	dk. gry. sh.	Pennsylvanian	0·65	0·15	0·03
593	Woodford	TCO # 2 Moore-Daniel	36-26N-5W	Oklahoma	5785–92	blk. sh.	Mississippian	4·19	0·20	3·30
13210	Frontier	TCO # 1 State Burke	36-37N-79W	Wyoming	5800*	dk. gry. sh.	Upper Cretaceous	1·79	0·13	1·61
609	Caney	TCO # 1 Moss Wilson	8–1N–1W	Oklahoma	7495–500	blk. sh.	Mississippian	3·51, 3·45	0·27, 0·28	1·9, 2·0
6875	Wilcox	TCO # 2 Clyde Graham	48–6N–9E	Louisiana	6120-24	blk. sh.	Eocene	0·86	0·08	0·13
13211	Monterey	Ohio Oil Co.	12-25S–12E	California	4497–517	gry. sh.	Miocene	2·03	0·14	1·57
12967	Lower Duvernay	Calif. Std.	4–53N–25W4	Alberta	5530	calc. sh. to arg. ls.	Devonian	7·63	0·2	1·73
		Winterburn Province						0·74	0·064	0·52
7678–80	Morrison	TCO Govt. Steele Creek	28-26N–82W	Wyoming	3429-47	red to grn. sh.	Jurassic	0·11	0·12	0·16
12976	Phyllite	Humble # 1 Carroll	Falls Co.	Texas	3677	phyllite		0·22	0·10	0·07
12974	Green River	NH Canyon (outcrop)		Utah	—	mahogany "shale" (marl)	Eocene	12·40	0·48	1·72
12975	Green River	(Outcrop)	27–11–10E	Utah	—	papery "shale" (marl)	Eocene	18·33	0·39	1·56
982	Traverse	TCO # 2 Louis Stevens	15–13N–18W	Michigan	1716–20	ls.	Devonian	0·53	0·04	0·02
7762	Ste. Genevieve	TCO # 2 Sellers	19–0–23	Kentucky	2510	ls.	Mississippian	0·036	0·017	0·18
7695	Madison	TCO Govt. Steele Creek	28–26N–82W	Wyoming	5794–5	pink dolo.	Mississippian	0·04	0·06	0·01
12973	Collier	(quarry spl.)	Near Mt. Ida	Arkansas	—	blk. ls.	Cambrian	0·16	0·012	0·14
9561	La Luna	Totumal 141–3	—	Colombia	8177	blk. ls., arg.	Cretaceous	3·73	0·26	1·12

*Approximate

To remove insoluble acid fluorides, the dried residue was taken up with water, an excess of powdered zinc was added, and the mixture was digested over-night on the steam bath. After washing by centrifugation and decantation, the sample was acidified with hydrochloric acid and washed again.

Sieving of the moist residue through a 200-mesh screen separated the material into two fractions: a very fine, dark-brown solid, and coarse, very black particles. Subsequent treatments of the fine fraction included digestion with zinc, a digestion

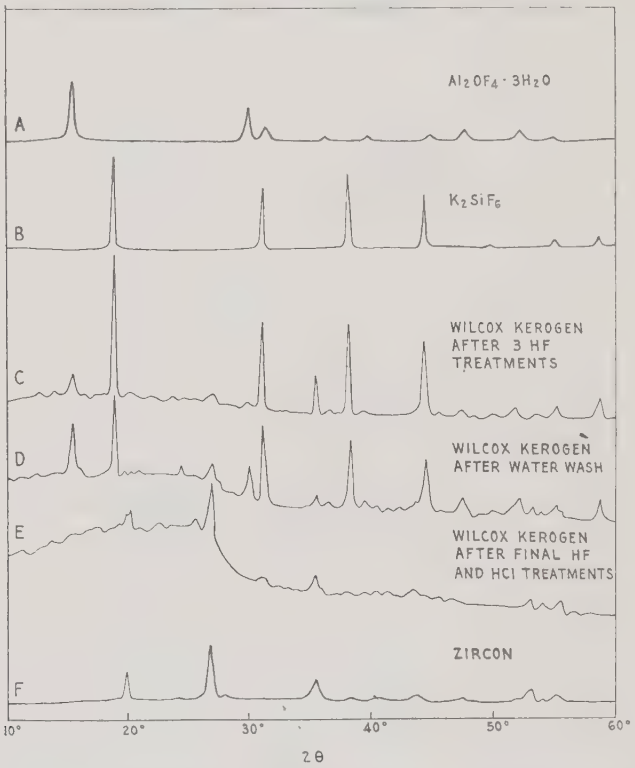

Fig. 2. X-ray diffraction spectra of Wilcox kerogen and inorganic impurities. Cu*K* radiation.

with hydrofluoric acid, and digestions with hydrochloric acid. A qualitative X-ray diffraction analysis showed the presence of about 30 per cent of potassium fluosilicate (K_2SiF_6) and a small amount of aluminium oxyfluoride ($Al_2OF_4 \cdot 3H_2O$). (Compare Figs. 2A, B, and C.)

To remove the potassium fluosilicate, the kerogen concentrate was washed with hot water until no precipitate was obtained on addition of *iso*propyl alcohol to the filtrate. Spectrum (Fig. 2D) of the kerogen showed the presence of zircon, aluminium oxyfluoride, and some potassium fluosilicate.

After additional digestions with hydrofluoric and dilute hydrochloric acid, an X-ray diffraction analysis of the residue showed the absence of fluorides but revealed the presence of a considerable amount of zircon (see Fig. 2F). Separate experiments with zircon indicated that chemical dissolution of the mineral could

be effected only under drastic conditions, and no attempt was made to remove this mineral from the kerogen sample.

The coarse black material retained by the sieve was digested successively with hydrofluoric acid, powdered zinc, and hydrochloric acid. The X-ray diffraction spectrum of the material showed the presence of a considerable amount of unidentified inorganic material, here assumed to be insoluble fluorides.

Elemental analyses obtained on the fractions isolated from the Wilcox shale are given in Table 2.

Table 2. Elemental analyses of kerogen

Lab. serial no.	Name	Organic carbon %	Organic factor* %	Hydrogen %	Kjeldahl nitrogen %	Oxygen %	Total sulphur %	Ash %	Total† %
6529	Cherokee sh.	71·93	1·16	4·17	2·01	5·43	2·43	21·44	107·41
6412	Hoxbar sh.	30·04	—	2·40	0·84	—	1·71	—	—
593	Woodford sh.	65·60	1·17	4·96	2·51	3·68	10·73	16·29	103·77
13,210	Frontier sh.	68·88	1·22	5·14	0·14	10·16	5·36	8·53	98·21
609	Caney sh.	57·70	1·29	5·08	2·24	9·33	11·46	13·28	99·09
6875	Wilcox sh.								
	Kerogen fines	71·17	1·25	4·82	0·16	12·77	0·35	4·04	93·31
	Coarse kerogen	54·63	1·31	4·38	2·22	10·62	1·92	20·91	94·68
	Lignites	59·86	—	5·37	0·35	—	—	23·79	—
13,211	Monterey sh.	40·72	1·24	4·12	1·35	4·24	20·52	33·33	104·28
12,967	Duvernay								
	Calc. sh.	64·19	1·16	6·19	1·08	3·29	16·22	13·19	104·16
	Arg. ls.	63·03	1·18	6·98	1·41	3·06	8·68	19·32	102·48
7678–80	Morrison sh.	23·05	1·39	2·24	1·37	5·40	15·15	58·18	105·39
12,976	Phyllite	87·30	1·08	2·82	0·18	3·58	0·29	5·16	99·33
12,974	Green River (mahogany) sh.	73·46	1·25	9·09	2·51	6·97	2·33	8·11	102·47
12,975	Green River (papery) sh.	76·65	1·25	9·53	1·46	8·22	1·91	10·17	107·94
982	Traverse ls.	68·63	1·22	8·03	1·32	5·77	8·98	16·02	108·75
		74·36	1·15	5·46	1·96	3·52	12·72	17·35	115·37
7762	Ste. Genevieve ls.								
	Kerogen in ls.	53·48	1·26	4·21	1·88	7·56	7·87	22·90	97·90
	Kerogen in stylolite	40·97	1·29	3·65	2·03	6·28	7·38	41·95	102·26
7695	Madison dolo.	65·06	1·16	3·68	1·60	5·12	2·16	22·25	98·87
12,973	Collier ls.	76·58	1·05	2·17	0·79	1·22	0·14	13·49	94·39
9561	La Luna ls.	64·35	1·14	5·18	1·44	2·26	7·26	9·29	89·78

* Organic factor equals percentage of total organic matter divided by percentage of organic carbon.
† Totals in excess of 100 are probably caused by the contribution of inorganic sulphur (as pyrite) in both the ash and the sulphur analyses. Values less than 100 are probably due to inorganic matter (fluorides) that volatilize during ashing.

Argillaceous limestone, Duvernay shale, Alberta

Portions of the pulverized, organic solvent-extracted rock were placed in 1 l. polyethylene beakers; and, after wetting the samples with *iso*propyl alcohol, concentrated hydrochloric acid was added in portions to the stirred alcohol-rock slurry. The moist acid residues obtained by centrifugation were combined in a polyethylene beaker, and 50 per cent hydrofluoric acid was added in portions. Distilled water was added, and the liquid phase was separated from the residue by centrifuging and decanting.

To remove insoluble fluorides formed during the hydrofluoric acid treatment, excess sodium carbonate solution was added to the residue, and the mixture was allowed to stand until evolution of carbon dioxide had ceased (1 day). The centrifuged residue was digested for 2 days with dilute hydrochloric acid and washed with distilled water. Inorganic substances detected by X-ray diffraction analyses were pyrite (large amount) and calcium fluoride.

To remove the pyrite, *iso*propyl alcohol and concentrated hydrochloric acid were added to the washed kerogen residue. To this mixture an excess of powdered

zinc was added in approximately 5 g portions. The pyrite was dissolved as evidenced by the evolution of hydrogen sulphide and appearance of ferrous iron in the water–alcohol mixture. After evolution of gas had ceased, the liquid phase was removed by centrifugation and the zinc–hydrochloric acid reaction was repeated three times. The formation of hydrogen sulphide took place during the fourth treatment. The kerogen residue from the fourth zinc–hydrochloric acid reaction was washed with water, centrifuged, and then dried at 100°C. Pyrite was the only impurity detected by X-ray diffraction analysis.

Table 3. Elemental material balance
(Argillaceous Limestone, Duvernay shale, Alberta)

	Organic carbon	Total nitrogen	Total sulphur
Wt. (%) of element in extracted rock	0·74	0·062	0·52
Wt. (g) of element in 237·5 g rock	1·8	0·15	1·2
Wt. (%) of element in kerogen concentrate	64·19	1·08	16·22
Wt. (g) of element in 3·0 g concentrate	1·9	0·032	0·49
Amount of element recovered (%)	105	21	41

The data in Table 3 show that reasonable agreement was obtained in the carbon material balance, and the decrease in the weight of sulphur was consistent with loss of pyrite and other sulphides during various stages of concentration of the kerogen. Most of the nitrogen lost during isolation of the kerogen was probably ammonia, and possibly some extraction of basic nitrogen organic compounds occurred.

Metamorphosed shale (phyllite)

Portions of the pulverized and organic solvent-extracted rock were placed in 1 l. polyethylene beakers; 35 per cent hydrofluoric acid was added, and, after heating for several days on the steam bath, the residue was centrifuged. Zinc and water were added and the mixtures were allowed to stand. After the slow evolution of gas had ceased, the liquid was removed by centrifugation and the excess zinc was dissolved by treatment with concentrated hydrochloric acid. This treatment dissolved some of the pyrite as evidenced by the evolution of hydrogen sulphide and the appearance of ferrous iron (thiocyanate test after oxidation with hydrogen peroxide) in the reaction mixture.

After additional treatments with hydrofluoric acid and with zinc, a mechanical separation of the kerogen from remaining inorganic matter was accomplished in the following manner. The sample was agitated in a Waring Blendor with a mixture of *n*-heptane and water and poured into a separatory funnel. On standing, most of the inorganic material settled to the bottom, whereas the black organic matter remained at the interface of the water–heptane layers. The solid inorganic

matter was drawn off, and the kerogen was filtered and dried. An X-ray diffraction spectrum of the sample showed the presence of about 10 per cent of quartz plus some unidentified material.

The remaining quartz was removed by digestion with 50 per cent hydrofluoric acid in the steam bath. The X-ray diffraction pattern of the washed residue (Fig. 3) indicated that some graphite was present.

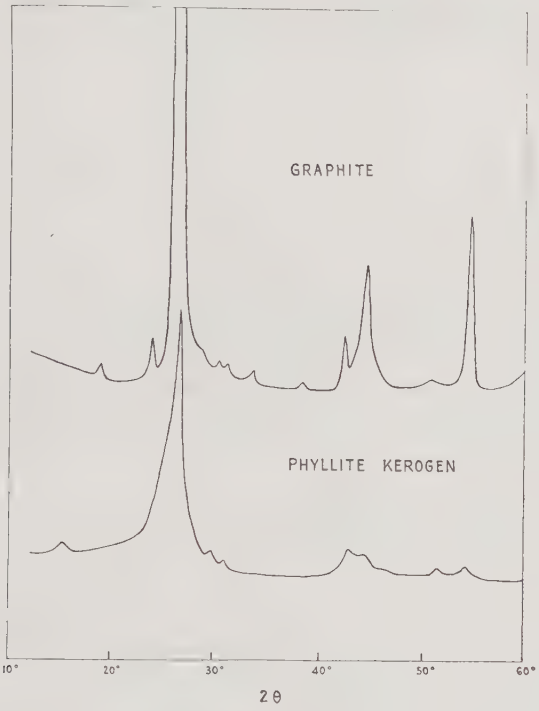

Fig. 3. X-ray diffraction spectra of phyllite kerogen and pure graphite. CuK radiation.

Results and Discussion

Physical characteristics

Kerogens isolated from typical marine rocks were obtained as very fine, amorphous, soft powders that varied from dark brown to jet black in colour, many showing a marked resemblance to coal dust. When the samples were heated in open test tubes, usually little or no oily distillate was formed. This behaviour is distinctly different from that exhibited by oil shales, which under the same conditions yield substantial amounts of oily distillates.

Refractive indices of the powdered kerogen samples were determined by the oil immersion method at 450× magnification. Table 4, which lists these measurements, also includes indices of a few coals, asphaltites, and mineral waxes.

Typical coals and asphaltites show a fairly uniform increase in refractive index with decreasing hydrogen–carbon atomic ratio. While a few kerogen samples appeared to follow this relationship, the refractive indices of most of the kerogens

Table 4. Refractive indices of kerogens, coals and asphaltites

Kerogen	Refractive index	Asphalt and coal	Refractive index†
Frontier	1·73	Anthracite coal	1·80
Traverse*	1·73	Bituminous coal	1·75
Caney	1·64	Subbituminous coal	1·70
Woodford	1·61	Albertite	1·66
Green River (mahogany)	1·60	Lignite	1·63
Traverse*	1·57	Gilsonite	1·61
Green River (papery)	1·50	Wurtzilite	1·57
		Ozokerite	1·53

* Separate fractions obtained during acid treatment, in which part of the kerogen floated on the surface of the acid mixture

† Hunt *et al.* (1954): Lowry (1945).

were lower than predicted. This effect may have been caused by fluoride contaminants, whose refractive indices are somewhat lower than those of kerogen.

Specific gravity measurements were made by the pycnometer method in *iso*propyl alcohol at 25°C. Table 5 lists the specific gravities, corrected for mineral content,* of several kerogen samples, together with corresponding data for a few coals, asphaltites, and mineral waxes.

Table 5. Corrected specific gravities of kerogens, coals and asphaltites

Sample	Specific gravity†	Sample	Specific gravity†
Traverse*	1·51	Anthracite coal	1·4 –1·8
Cherokee	1·39	Bituminous coal	1·2 –1·5
Green River (papery)	1·38	Albertite	1·07–1·10
Traverse*	1·32	Wurtzilite	1·05–1·07
Green River (mahogany)	1·22	Gilsonite	1·03–1·10
Frontier	1·22	Ozokerite	0·85–1·0
		Peat, dried	0·84

* See footnote, Table 4.

† Kerogen data corrected for mineral content. Data for asphalts and coals taken from Abraham (1945) and Lowry (1945).

For recording the infra-red spectra of kerogens, scattering was minimized by grinding samples under *iso*propyl alcohol in a mortar. The resultant fine powders were then deposited in the form on thin films on salt block cells, using a technique previously developed in this laboratory (Hunt and Turner, 1953). Absorption peaks were noted at several wavelengths; however, because of the weak absorption,

* Corrections were made with the assumption that the major impurities were pyrite (sp. gr., 5·0) and inorganic fluorides (mean sp. gr., 2·8). Pyrite in the samples were estimated from iron and sulphur determinations; the identity and quantity of fluorides were determined from X-ray diffraction and emission spectrographic analysis.

no marked differences were observed between any of the spectra. The two non-marine (Green River) kerogens had slightly more intense peaks at wavelengths of 3·5 and 6·9 μ, indicating that these samples have less condensed and more paraffinic structures than typical marine kerogens.

Chemical composition

The results of the elemental analyses show that, in all of the kerogen samples, carbon, hydrogen, and oxygen are the major constituents. On an atomic basis, nitrogen is less abundant, but nevertheless it constitutes an integral part of the

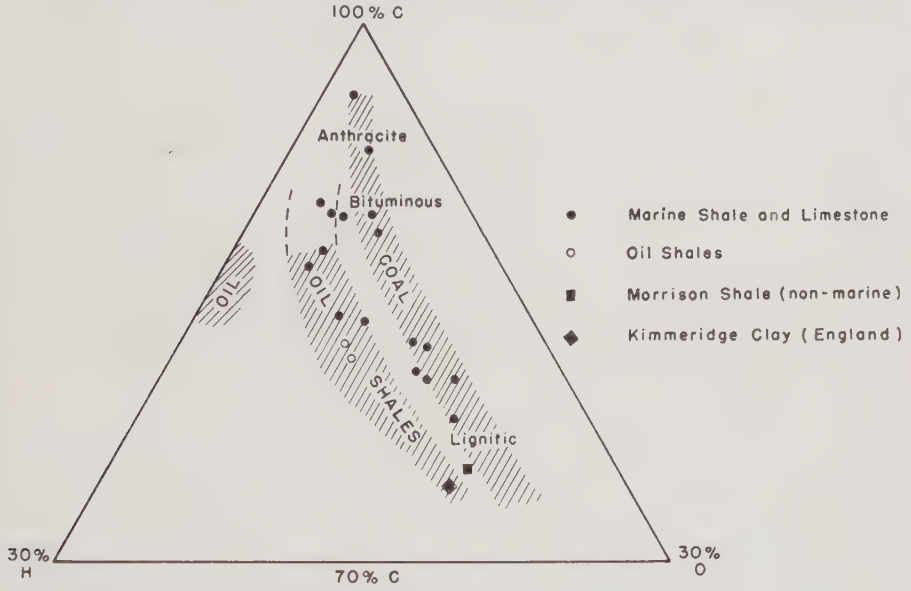

Fig. 4. Distribution of carbon, hydrogen and oxygen in kerogen.

kerogen molecule. Organic sulphur was presumed to be present in all of the kerogens but, because of residual pyrite, the organic sulphur content could not be determined accurately. In a few instances, it was established that the total sulphur was considerably greater than could be attributed to inorganic sulphur alone.

All the samples analysed by emission spectrography contained a number of metallic constituents some of which may have been combined chemically with the kerogen. No attempt was made in the present study to demonstrate the presence of metallo–organic substances.

In the triangular diagram (Fig. 4), the solid circles express the composition of the kerogens on an ash-, nitrogen-, and sulphur-free basis. Also shown in the diagram is a coal band, which represents the composition of coals in various stages of maturity or metamorphism (Bangham, 1950). The shaded area entitled "oil shales," which lies parallel to and left of the coal band, represents literature data for kerogens isolated from approximately thirty samples of oil shales and torbanites of various ages and localities (Himus, 1951).

Two points of geologic interest are provided by the data in Fig. 4. First, it is

apparent that there are two broad types of kerogen in marine rocks. Members of one type have elemental compositions that are comparable to oil shales and torbanites, whereas the other type is scarcely distinguishable from coal. Both limestone and shale kerogens are included in each of these types.

The second point of importance is the suggestion that kerogen changes in elemental composition in a manner similar to that which has taken place in coals. The evidence for the change in rank is: (1) the distribution of members of each of the two types along the lengths of the oil shale and coal bands, respectively; (2) the fact that anthracite-like kerogens were found in two highly metamorphosed rocks but not in the relatively unmetamorphosed rocks; and (3) the progressive change in hydrogen–carbon atomic ratios and fixed carbon values of kerogen (Forsman and Hunt, in press).

A few of the kerogen samples did not fall into either of the two categories. The first of these, the Morrison shale kerogen, appears to have a composition intermediate to that of a very low-rank coal or lignite and that of the Kimmeridge clay of England (Dancy and Giedroyc, 1950). The three other unclassified samples lie well to the left of the coal band, but almost directly above the oil shale region. Although oil shale analyses that fall in this region are lacking, it is probable that the oil shale band should be extended upward toward 100 per cent carbon, the hypothetical end-product of all sedimentary organic matter. The proposed extension, which is shown as dashed lines in Fig. 4, includes two of the three remaining samples.

During the concentration of kerogen, large losses of the original nitrogen content of the rock occurred, although the recovery of organic carbon generally exceeded 90 per cent. Because of the high ratio of nitrogen lost to carbon lost, most of the nitrogen must have been removed during acid extraction as ammonium ion rather than as organic nitrogen. For shales, the average nitrogen loss based on rock weight was 0·09 per cent; for calcareous shales, 0·05 per cent; and for limestones, 0·02 per cent. These values agree with the prediction that the amount of ammonia in a rock increases with increasing clay content.

Carbon/nitrogen ratios of the kerogen samples generally fell in the range of 25–60. A few kerogen samples, notably those from metamorphosed rock, contained only traces of nitrogen.

Although kerogens differ appreciably in elemental composition, it is apparent that elemental analyses reflect only gross differences between kerogens. Because of the possibility that two kerogens of identical elemental composition might have entirely different structures, it was desirable to find a method that would yield some information concerning structural differences between kerogens. One of the more promising methods appeared to be hydrogenolysis at high temperatures, a process that is employed in the commercial liquefaction of coal.

In the present work, seven representative samples, including four kerogens, one coal, and two shales, were subjected to uncatalysed hydrogenolysis in a 1000 ml stainless steel Aminco super-pressure vessel. Preliminary experiments indicated that hydrogenolysis in the presence of *n*-heptane would yield up to 200 per cent more soluble material than in the absence of solvent. With pure heptane, extensive cracking and some polymerization took place at 450°C; whereas, at

380°C, no significant change in boiling point occurred. Consequently, hydrogenolysis of kerogen was carried out at the latter temperature. Other reaction conditions were: maximum pressure, 2700–3100 lb/in^2; time, 12–20 hr. The soluble products, which were obtained in yields varying between 18 and 87 per cent, were further separated into types of organic compounds by the standard solubility-alumina chromatography method used at this laboratory (Hunt and Jamieson, 1956).

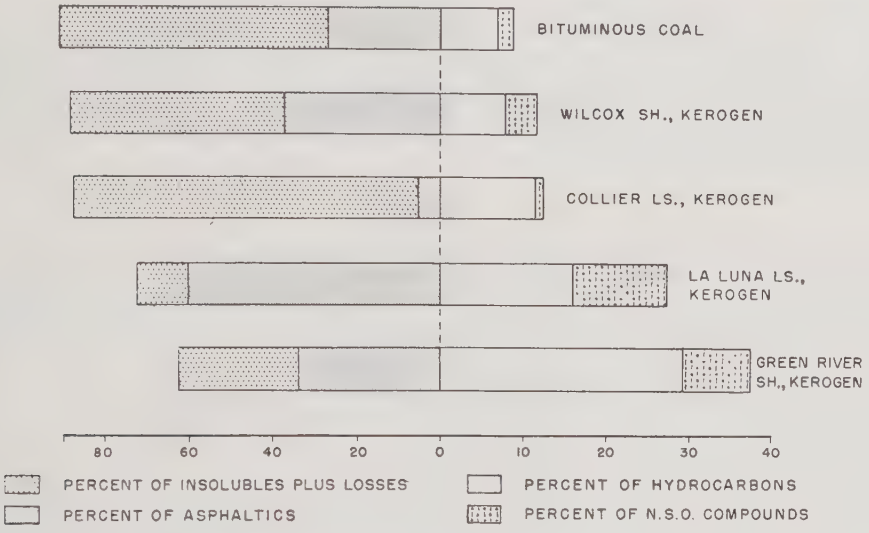

Fig. 5. Distribution of hydrogenolysis products of kerogen and coal.

The results of the hydrogenolysis of four kerogens and one coal, presented graphically in Fig. 5, show that there are very marked differences to be found between kerogens. For example, in the total amount of kerogen converted to soluble products, both the La Luna and Green River (mahogany shale) samples are clearly different from the Wilcox kerogen. The hydrogenolysis products of the La Luna and Green River kerogens are, in turn, dissimilar in their hydrocarbon and asphaltic contents. Unlike the other kerogens, the soluble products from the Cambrian Collier limestone consisted predominantly of hydrocarbons, and over four-fifths of this kerogen resisted attack by hydrogen.

Table 6. Distribution of hydrocarbon types in kerogen hydrogenolysis products

Sample	Paraffin–naphthenes/aromatics
Bituminous coal	0·13
Wilcox kerogen	0·10
Collier kerogen	1·60
La Luna kerogen	0·65
Green River kerogen	1·20

In view of the wide variations in the results obtained with different kerogen samples, the marked similarity between the hydrogenolysis products of the Wilcox kerogen and of the coal appears especially significant.

In Table 6, differences between the kerogens may also be seen in the ratio of paraffins plus naphthenes to aromatics in the soluble products. The resemblance between the bituminous coal and the Wilcox kerogen again appear in this data.

Acknowledgements—Special thanks are due: G. E. C. Wear, of the Products Research Division, Esso Research and Engineering Company, for the Unterzaucher oxygen analyses of the kerogen samples; to P. V. Smith, Jr. and M. C. Brenneman, Chemicals Research Division, Esso Research and Engineering Company, for preliminary hydrogenolysis work; and to C. G. Claypool and F. E. Dollarhide, of the Jersey Production Research Company for the X-ray and hydrogenolysis data, respectively. The authors wish to express their gratitude to P. A. Dickey for his many constructive suggestions.

References

Abraham H. (1945) *Asphalts and Allied Substances* (5th Ed.). Van Nostrand, New York.

Bangham D. H. (Editor) (1950) *Progress in Coal Science*. Interscience, New York.

Breger I. A. and Deul M. (1953) *U. S. Geol. Surv. T. E. I. Prog. Repts.* **390,** 161–2; (1953–4); **440,** 141–2; (1954) **490,** 178–82; (1954–5) **540,** 187–90; (1955) **590,** 264–7; (1955–6) **620,** 264–6.

Deul M. (1956) *Bull. Amer. Assoc. Petrol. Geol.* **40,** 909–17.

Dancy T. E. and Giedroyc V. (1950) *J. Inst. Petrol.* **36,** 593–603; 607–23.

Forsman J. P. and Hunt J. M. *Insoluble Organic Matter (Kerogen) in Sedimentary Rocks of Marine Origin*. In press.

Guthrie B. (1938) *U.S. Bur. Mines, Bull.* **415**, 105–17.

Himus G. W. (1951) Observations on the composition of kerogen rocks and the chemical constitution of kerogen. *Oil Shale and Cannel Coal* Vol. 2. Institute of Petroleum, London.

Himus G. W. and Basak G. C. (1949) *Fuel* **28,** 57–65.

Hunt J. M. and Turner D. S. (1953) *Analyt. Chem.* **25,** 1169–74.

Hunt J. M., Stewart, F. and Dickey P. A. (1954) *Bull. Amer. Assoc. Petrol. Geol.* **38,** 1671–98.

Hunt J. M. and Jamieson G. W. (1956) *Bull. Amer. Assoc. Petrol. Geol.* **40,** 477–88.

Lowry H. H. (Editor) (1945) *Chemistry of Coal Utilization* Vol. 1, pp. 310–27. John Wiley, New York.

Takahashi Jun-ichi (1935) *Sci. Repts. Tohoku Univ.* Ser. 3. **1,** 63–156.

Geochimica et Cosmochimica Acta, 1958, Vol. 15, pp. 183 to 194. Pergamon Press Ltd. Printed in Northern Ireland.

Some natural variations in the relative abundance of copper isotopes*

E. C. Walker, F. Cuttitta and F. E. Senftle
U.S. Geological Survey, Washington, D.C.

(*Received* 22 *May* 1957)

Abstract—The relative isotopic abundance of copper has been measured in a number of minerals and a few plant materials. Suites of samples from Michigan and the Colorado Plateau have been examined in more detail to determine if local variations due to isotopic exchange or diffusion could be found. The relative isotopic abundance of copper in specimens from several other localities was also determined. The variations noted were small but in some cases were felt to be significant because they were larger than the experimental error (0·1 per cent in the ratio). A total spread of −1 to +8 parts per mil compared to the standard was found in the specimens tested.

Introduction

As Rankama (1954) has pointed out, little attention has been paid to the possibility of terrestrial fractionation of copper isotopes. The mass difference of the copper isotopes is small and no large variations can be expected. Brown and Inghram (1947) have compared the isotopic composition of copper from Canon Diablo meteorite with two terrestrial copper samples and obtained 2·244, 2·236, and 2·234 for the Cu^{63}/Cu^{65} ratio, respectively. They felt that this difference of a little less than 0·5 per cent was within their experimental error and hence was not significant.

Regardless of the small fractionation anticipated, it would be of interest if a real variation of this order of magnitude could be established with improved accuracy of the measurements. Copper is relatively easily dissolved by slightly acidic aqueous solutions, and hence is free to move about. One would, therefore, expect a greater possibility of finding isotopic fractionation of copper by such processes as exchange reactions or diffusion than if the copper were relatively insoluble. It is now well established that exchange reactions can, and do, cause isotopic fractionation in some of the lighter elements. However, small variations in isotopic abundance due to a diffusion process, if detectable, will probably be localized and will occur chiefly in the minor constituent of the host rock (Senftle and Bracken, 1955).

Effects of such local fractionation processes are likely to be masked in a bulk deposit or specimen of such an element. For instance, in a similar investigation of the variation of the zinc isotopes in nature by Blix, Ubisch and Wickman (1957) no variations were noted. However, only bulk zinc-bearing minerals were investigated, and small variations may have been masked.

The present investigation was undertaken to determine whether significant variations of the Cu^{63}/Cu^{65} ratio occur in nature, particularly in specimens where these fractionation processes are suspected to have taken place, that is, where the abundance of copper was relatively low. Special efforts have been made to keep the experimental error less than 0·1 per cent at the 95 per cent confidence level.

* Publication authorized by the U.S. Geological Survey and the Division of Research of the U.S. Atomic Energy Commission.

Method of Analysis

A 60°, 6 in. radius mass spectrometer of the Nier type was used. The ion current was measured by a vibrating reed electrometer and recorded by an automatic recorder. Manual magnetic scanning was used for peak selection and the null point method was used to determine the ratios. The bulk-out potential was obtained by placing two Dekapot potentiometers alternately across a 1·2 V mercury cell. These potentiometers have an accuracy of better than ±0·05 per cent of their nominal value, a linearity of ±0·01 per cent, and a resolution of better than 0·0002 per cent. The potentials obtained in this way were used to buck-out the two

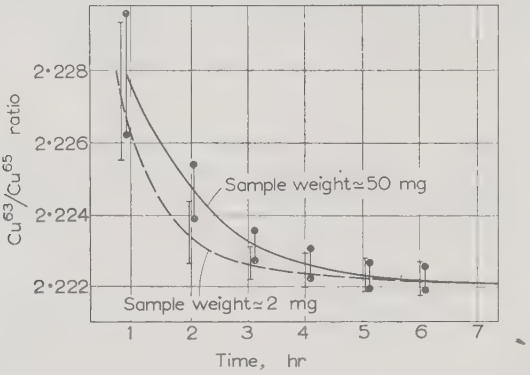

Fig. 1. Variation of Cu^{63}/Cu^{65} ratio with time and sample weight.

peaks. The ratio of the resistance of the potentiometers, which is proportional to the ratio of the ion currents, is used as the ratio of the peak heights. Using this system, at least fifty ratios were taken for each measurement completed.

Although the $[Cu^{63}]^+$, $[Cu^{65}]^+$, and $[Cu^{63}I]^+$, $[Cu^{65}I]^+$ peaks were well resolved and gave good intensity, they were not as reliable as the $[Cu_2I_2]^+$ peaks. It was found difficult to remove completely the background contamination peaks from the $[Cu]^+$ and $[CuI]^+$ peaks, and at times an unexplained instability was observed. More stable operation and negligible background effects were observed in the higher mass region of $[Cu_2I_2]^+$ peaks. Another feature in favour of the $[Cu_2I_2]^+$ peaks is the formation of a $[Cu^{63}/Cu^{65}I_2]^+$ peak. This peak is about the same size as the $[Cu^{63}{}_2I_2]^+$ peak, whereas the $[Cu^{63}I]^+$ peak is about twice that of the $[Cu^{65}I]^+$ peak. Less error is incurred in measuring two peaks of the same relative magnitude.

It was further noted that the ratio of Cu^{63}/Cu^{65} varied with time as shown in Fig. 1. When the ion source is first turned on, the light isotope is preferentially removed, probably owing to diffusion processes at the surface of the sample itself. After a short while equilibrium is approached resulting in the much lower slope observed in the figure. When smaller samples are used, equilibrium is reached in a somewhat shorter time (Fig. 1). To obtain a greater reproducibility, the mass spectrometer was always run for the same length of time for all samples of approximately the same weight. For instance, with a full sample charge the instrument was allowed to run for 4 hr before any data were collected, and then all of the data were collected during the 3½ hr that followed. For samples of less than a full furnace

charge, only weighed amounts were used, which yielded curves similar to curves such as shown in Fig. 1. Although analysis would start at a somewhat earlier period for the smaller samples, the samples reported here were all done after 4 hr. In this way data were obtained from that section of the curve with a fairly constant and nearly zero slope. This waiting period also allowed sufficient time for the magnet to stabilize, and thus minimize any drift error from this source.

Reagent grade, copper (I) iodide was used as a working standard, and the National Bureau of Standards copper (II) oxide sample no. 29 was used as a primary reference. Table 1 indicates the reproducibility of the results on the

Table 1. Cu^{63}/Cu^{65} ratios for the working standard

Date run	Cu^{63}/Cu^{65} ratio	Date run	Cu^{63}/Cu^{65} ratio
8/11/55	2·223	2/1/56	2·222
10/25/55	2·223	2/16/56	2·223
11/1/55	2·224	3/28/56	2·222
12/13/55	2·223	4/18/56	2·223
1/19/56	2·223	4/27/56	2·222
1/17/56	2·223	12/7/56	2·223

working standard sample. The average Cu^{63}/Cu^{65} ratio obtained on this standard, 2·223, is smaller than the value of 2·236 obtained by Brown and Inghram (1947), but is reasonably close to 2·220 obtained by White and Cameron (1948). All results were taken in the equilibrium portion of the curve (Fig. 1), so the copper isotope ratios are lower than those obtained from data taken within an hour or so after the instrument was turned on. This different technique may help to explain the higher ratio found by Brown and Inghram. All analyses are referred to the National Bureau of Standards reference sample no. 29 on which was obtained a Cu^{63}/Cu^{65} abundance ratio of 2·223, the same as on the working standard. As far as possible, either the working standard or the National Bureau of Standards reference sample was run before and after each unknown sample.

To avoid contamination, the samples were prepared as suggested by Myers and Barnett (1953), and Barnett *et al.* (1955). The ground samples were freed of carbonates and organic matter by ignition at 900° to 950°C. The ignited samples were then brought into solution by means of aqua regia and converted to chlorides. The metals of the hydrogen sulphide group were precipitated with H_2S at a pH 0·5, using as a carrier lead in which copper could not be detected spectrographically. Separation of the copper from most of the sulphide metals was accomplished by the precipitation of copper (II) cupferrate (Furman, Mason and Pekola, 1949) in ice-cold dilute HNO_3 using electrolytic iron as a carrier followed by an extraction of the copper by 6N NH_4OH (Baudisch, 1938). Copper was not detected spectrographically in the insoluble cupferrates. The copper was further purified by precipitation as copper (I) thiocyanate. All processes were made as quantitative as possible and at least 10 mg of copper were prepared from each unknown sample.

Copper (I) iodide was prepared from a solution of the isolated copper (as the

sulphate). In the present method, SO_2 was used as the reducing agent and a solution of reagent grade KI as the source of iodide ions. Special precautions (Lean and Whatmough, 1898; Fernelius, 1946) were taken to remove all traces of moisture from the copper (I) iodide. The prepared iodide varied from a grey-white to a tan-white crystalline powder that remained practically unchanged for indefinite periods of time if kept dry. Spectrographic analyses affirmed the purity of the prepared copper (I) iodides. Copper (I) iodide was used in all the mass spectrometric analyses.

To check the reproducibility of the chemical procedures, the National Bureau of Standards reference sample copper oxide no. 29 was converted to the iodide. The standard preparation of the copper (I) iodide as described above was generally followed, but in several cases drastic chemical procedures were used to see if any fractionation occurred. As is shown in Table 2 no fractionation was evident in any of these trials.

Table 2. Tests of chemical fractionation using National Bureau of Standards reference sample CuO no. 29

Date prepared	Type of preparation	Cu^{63}/Cu^{65} ratio
12/17/56	Standard preparation*	2·223
4/10/57	Standard preparation* but only 2 mg processed for isotopic analysis	2·223
4/10/57	Standard preparation*	2·223
4/12/57	Electroplating plus standard preparation*	2·223
4/15/57	Electroplating, precipitation, chemical displacement with Al followed by standard preparation*	2·223

* See text for details of standard preparation.

Because of the good reproducibility of the combined chemical procedures and the mass spectrometric measurement, the error in the ratios is considered to be less than 0·1 per cent in the mean at the 95 per cent confidence level. For example, the sample with the widest range of ratios had a probable error of ±0·6 part per mil at the 95 per cent confidence level, or an error of 0·06 per cent.

The results are quoted as the deviation, Δ, from the standard ratio (Cu^{63}/Cu^{65} = 2·223) in parts per mil (‰), where

$$Cu^{63}/Cu^{65}\ (\text{sample}) = \frac{2{\cdot}223\ (\text{standard})}{1 + (\Delta/1000)}$$

An enrichment of the heavy isotope or the light isotope is indicated by a positive or negative number, respectively.

Analytical Results

Samples from White Pine mine, Ontonagon County, Michigan

The rocks of the White Pine copper mine, described in detail by White and Wright (1954), represent a geologic environment in which isotopic fractionation

of copper may have taken place. Copper, in the form of both chalcocite and the native metal, is finely disseminated in several layers in the lowermost 25 ft of the Nonesuch shale. The statigraphic distribution of copper and grades typical of the different layers in the mine area are shown diagrammatically in Fig. 2. The beds dip

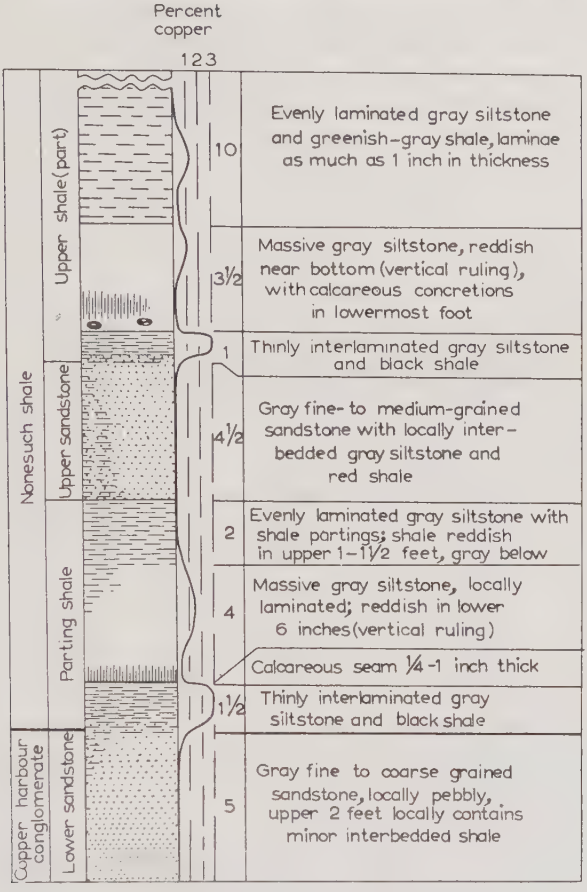
Percent copper
1 2 3
Nonesuch shale
Upper shale (part)
Upper sandstone
Parting shale
Lower sandstone
Copper harbour conglomerate
10
3½
1
4½
2
4
1½
5
Evenly laminated gray siltstone and greenish-gray shale, laminae as much as 1 inch in thickness
Massive gray siltstone, reddish near bottom (vertical ruling), with calcareous concretions in lowermost foot
Thinly interlaminated gray siltstone and black shale
Gray fine- to medium-grained sandstone with locally interbedded gray siltstone and red shale
Evenly laminated gray siltstone with shale partings; shale reddish in upper 1–1½ feet, gray below
Massive gray siltstone, locally laminated; reddish in lower 6 inches (vertical ruling)
Calcareous seam ¼–1 inch thick
Thinly interlaminated gray siltstone and black shale
Gray fine to coarse grained sandstone, locally pebbly, upper 2 feet locally contains minor interbedded shale

Fig. 2. Typical stratigraphic section of cupriferous zone, White Pine area, Michigan (White and Wright, 1954, Fig. 3).

5° to 10° E and are cut, in places, by steeply dipping to vertical joints and small faults, along some of which calcite and other vein minerals have been deposited. Some of the joints contain films of chalcocite or native copper, particularly where they cut the more highly cupriferous layers.

If the joints have acted as channelways for the introduction of the copper, movement of copper was from the joint into the rock; conversely, if the copper in joints is a product of lateral secretion of copper that was already in the rock before the joint formed, movement was from the rock into the joint. To the extent that diffusion played a part in the migration of the copper, there might be enough isotopic fractionation to give evidence for one or the other direction of migration. Convincing evidence for the direction of migration would greatly reduce the present range of speculation on the possible origin of the deposit.

As an exploratory test, three sets of samples (Sets A–C, Table 3) were picked, each set consisting of a specimen of chalcocite or copper coating a joint face, and a specimen of the cupriferous wallrock $\frac{1}{2}$–$1\frac{1}{2}$ ft from the joint, at the same stratigraphic position as the specimen from the joint. Sample no. 2 contains visible specks of native copper, but the other specimens of wallrock contain only chalcocite. These specimens were isotopically analysed; the results are given in Table 3.

Table 3. Isotopic abundance of copper from White Pine mine, Ontonagon County, Michigan

Set	Sample no.	Sample description	Cu (%)	Cu^{63}/Cu^{65} (‰)
A	1	Native copper in joint	≈100	+3·0
	2	Host rock 20 in. from joint	≈1	+0·3
B	3	Chalcocite in joint	≈80	−1·1
	4	Host rock 6 in. from joint	≈0.1	+0·1
C	5	Chalcocite in joint	≈80	−0·4
	6	Host rock 8 in. from joint	≈1	+1·3
D	10	Chalcocite from calcite veinlet	42·5	0·0
	11a	Host rock next to veinlet	0·60	+1·5
	11b	Host rock $\frac{3}{4}$in. from veinlet	0·75	+2·9
	11c	Host rock $1\frac{1}{2}$ in. from veinlet	0·59	−1·2
	11d	Host rock $2\frac{1}{4}$ in. from veinlet	1·4	0·0
	11e	Host rock 3 in. from veinlet	0·66	+1·1
	12	Chalcocite from another veinlet	2·7	0·0

Set A. From massive, very finely laminated dark-grey siltstone, about $3\frac{1}{2}$ ft above base of parting shale. Drift W-19, 25 ft west of Drift A.
Set B. From thinly laminated dark-grey shale about 1 ft above base of parting shale. Drift N5, 70 ft north of Drift E1.
Set C. From same layer as Set A. Drift N5, 50 ft north of Drift E1.
Set D. From interlaminated grey siltstone and shale about $4\frac{1}{2}$ ft above base of parting shale. Between Drifts N24 and N26 on W27. Specimen 12 is from another veinlet at the same locality, about 4 ft above base of parting shale in massive dark-grey siltstone.

In Sets B and C, the lighter isotope is slightly more abundant in the specimens from the joints than in the associated host rock. If this relation held generally throughout the deposit, it would suggest that a fractionation process may have been operative in transporting the copper, and that the direction of diffusion was from wallrock to joint. In Set A, on the other hand, in which both specimens contain native copper, the suggested direction of diffusion is from joint to wallrock. This difference in behaviour could be most simply interpreted as follows: chalcocite was present in the beds before the joints were formed, and some of it migrated into the joints during or after their formation. Native copper was introduced into the rocks after the formation of the joints, and these joints acted as channelways. This later stage of mineralization might be connected with the introduction of native copper and chalcocite into the sandstone beds above and below the parting shale; White and Wright (1954, p. 706–708) present evidence that much of the

copper in the sandstone beds was introduced after the rocks were deformed. The present data are insufficient, however, to make these interpretations at all conclusive, and serve mainly to show the kind of interpretation that can be made should the results be confirmed by a larger number of samples.

Because of the inconclusive results obtained when the distance between samples from joint and host rock was $\frac{1}{2}$–$1\frac{1}{2}$ ft, the extent of isotopic variation in the wallrock

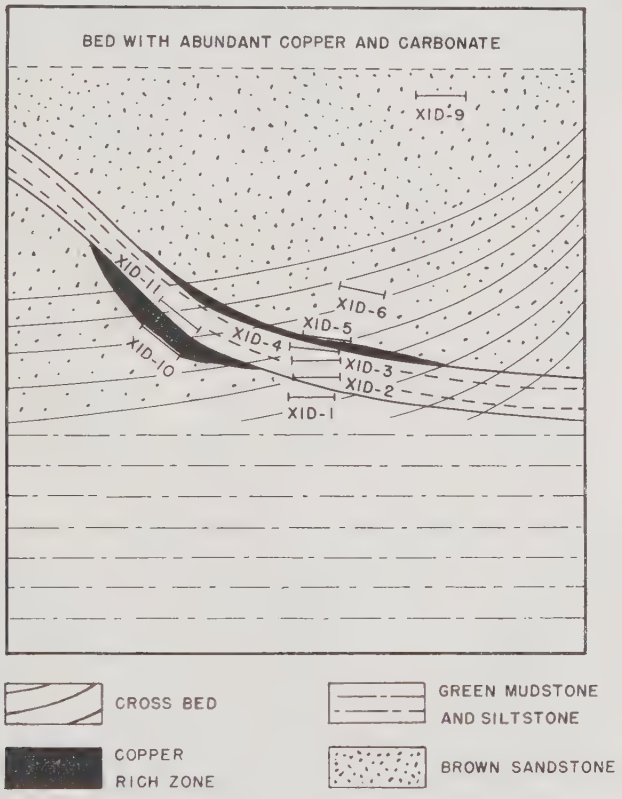

Fig. 3. Sketch of roll surface showing position of samples taken for isotopic analyses, Cougar mine, Montrose County, Colorado. (See Table 4.)

within 3 in. of a vein was tested by a suite of more closely spaced samples (Set D, Table 3). The individual samples (nos. 11a-11e) were sawed from a block, one face of which bordered the calcite–chalcocite veinlet represented by sample no. 10; each sample was a slice parallel to the vein. It was hoped that there would be a systematic variation in isotopic composition with distance from the vein that would permit a conclusion about geologic processes involved. As shown in Table 3, the differences in isotopic composition are small and show no systematic variation.

Samples from Cougar mine, Montrose County, Colorado

Uranium and vanadium ores on the Colorado Plateau generally occur in flat-lying tabular bodies parallel to the bedding of the sandstone. Occasionally these bodies are undulating and cut across the bedding planes. Where the ore body

crosses the bedding plane and exhibits a sharp interface between the ore and barren sandstone, the term "roll" has been applied to the ore body. These "rolls" have been the subject of investigation for many years, and although there have been several theories about their formation, no one theory will completely explain all the features embodied in this type of deposit (Shawe, 1956). Some isotopic measurements were made to determine if fractionation occurred in the roll.

A suite of nine samples was taken in and adjacent to a uranium-rich roll in the Cougar mine, Montrose County, Colorado. The position of the samples is shown in Fig. 3. The ore cuts across the bedding planes in a brown sandstone. It is highly

Table 4. $\Delta Cu^{63}/Cu^{65}$(‰), and analytical data (%), for samples from a roll, Cougar mine, Montrose County, Colorado

Constituent	Sample								
	XID-1	XID-2	XID-3	XID-4	XID-5	XID-6	XID-9	XID-10	XID-11
$\Delta Cu^{63}/Cu^{65}$ (‰)	0·02	0·9	2·0	2·6	2·5	−0·7	−0·5	−0·2	0·2
U (%)	0·51	0·25	0·29	0·86	0·29	0·002	0·002	0·042	0·35
CuO (%)	0·63	0·71	0·76	0·94	3·4	0·18	0·35	0·45	1·5
Fe_2O_3 (%)	*	0·007	0·03	0·007	<0·001.	0·04	*	*	*
V_2O_3 (%)	*	3·65	5·19	3·85	8·77	0·61	*	*	*
$CaCO_3$ (%)	*	3·09	2·25	6·50	1·70	6·39	*	*	*

* Not determined.

oxidized, and the minerals present are secondary. The copper-rich zones are associated with the uranium ore and occur along the edges of the roll. The central portion of the roll contains more Fe_2O_3 than the edges. The main copper-bearing mineral is volborthite, a hydrous vanadate of copper, barium, and calcium; minor amounts of malachite and azurite are present. It may be significant that in the brown sandstone about 7 or 8 ft above the roll there is a bed with abundant carbonate and some copper minerals. This bed may originally have been the source of the copper in the roll below. Unfortunately no specimens containing copper were available from this zone.

The results for these samples (plotted in Fig. 4 and tabulated in Table 4) show an enrichment of Cu^{65} of about 2·5 ‰ within the roll. Sample XID-6, which lies just outside the roll surface, is 0·7 ‰ lighter than the standard. The enrichment of Cu^{65} within the roll is a little better than twice the experimental error. Although this is not a large enrichment, it is believed to be significant. Several possible explanations of such a pattern can be given. For instance, the copper may have migrated along the roll and undergone an exchange reaction with some copper mineral originally within the roll, or a normal copper may have been laid down within the roll, subsequently redissolved, and diffused into the host rock. The copper just outside the roll should be enriched with Cu^{63} if copper preferentially diffused out of the roll structure. The data suggest that such a mechanism might have operated, but the enrichment of the light isotope is not large enough nor are there enough determinations to support fully a theory of a mechanism.

Miscellaneous samples

As little is known about the necessarily small variations in the isotopic abundance of copper in nature, a variety of samples from different geologic environments was chosen for isotopic analysis. The localities, copper content, and change in isotopic ratio for several such samples are shown in Table 5, and are described in more detail below.

Although brochantite is a relatively rich copper mineral, the first two samples shown in the Table 5, HT-3 and GC-2, occurred as slight green stains on the host material. HT-3 was a brochantite-stained celestite sample from San Miguel

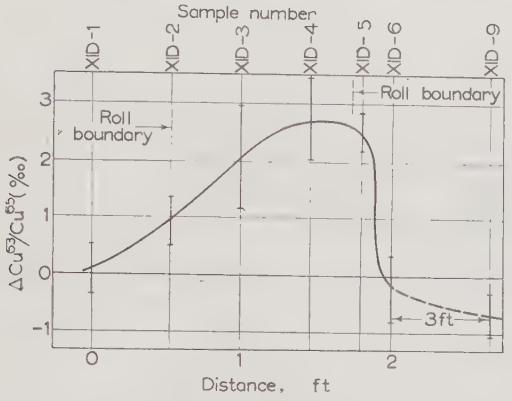

Fig. 4. Change in Cu^{63}/Cu^{65} ratio (Δ in ‰) of copper in roll structure, Cougar mine, Montrose County, Colorado.

County, Colorado, and GC-2 was a brochantite-stained sandstone from near the bottom of Grand Canyon. In both places the copper appeared as a slight green stain, and was apparently brought in by ground-water solutions. Similarly, sample M-1 was a slight chalcanthite stain found in the ore-bearing sandstone of the Monument no. 1 uranium mine, Montrose County, Colorado. These copper mineral stains are considered essentially normal as the enrichments obtained are less than 0·1 per cent, the approximate experimental error.

The next two samples, GBL-1 and TL-3, contained very little copper and were also found to have a normal abundance. The pitchblende, GBL-1, contained 100 p.p.m. of copper, and the dolomite, TL-3, contained about 14 p.p.m. of copper. Specimen TL-3 was situated about 1 ft from a lead–zinc ore body that contained about 0·03 per cent copper. There is evidence that the ore body had heated the host rock (Lovering, 1950) and that the copper in TL-3 may have diffused from that ore body. Under these circumstances TL-3 should be enriched in Cu^{63}. However, as samples of the lead–zinc ore body in the vicinity of TL-3 were unattainable for isotopic measurements, it is not certain whether or not TL-3 is enriched in Cu^{63}. Relative to the standard, however, TL-3 is normal.

The marine sediment, BM-1, exhibited the largest enrichment of Cu^{65} observed. It contained a relatively large amount of organic matter and was collected in an area where there was a pronounced anaerobic bacterial activity. The concentration of about 500 μg-atoms of copper/kg of sediment was presumably precipitated from

the sea water by the anaerobic action (Chow and Thompson, 1954). A second sample, BM-2, with much less organic matter, taken later at a point further out in East Sound where the anaerobic bacteria were less abundant, showed a normal abundance compared with the standard. As repeat runs on these specimens were made on different days and one was made on a different mass spectrometer, it is felt that the results are real. Chow and Thompson have postulated that the hydrogen sulphide produced under anaerobic conditions reacts with soluble copper

Table 5. Comparison of the $\Delta Cu^{63}/Cu^{65}$, (‰), in various specimens with the National Bureau of Standards reference sample

Sample no.	Description and location	Cu(p.p.m.)	$\Delta Cu^{63}/Cu^{65}$ (‰)
HT-3	Brochantite-stained celestite, Klondike area, San Miguel County, Colorado	*	−0·80
GC-2	Brochantite-stained sandstone, near base of Bright Angel Trail, Grand Canyon, Arizona	*	+0·27
M-1	Chalcanthite-stain in ore-bearing sandstone, Monument no. 1 mine, Arizona	*	+0·51
GBL-1	Pitchblende, Great Bear Lake, Northwest Territories	100	−0·13
TL-3	Dolomite, Chief mine, Tintic district, Utah	14	+0·27
BM-1	Marine sediment, East Sound, Orcas Island, Washington; depth 30 m, collected April 16 1955	≈3·5	+8·1
BM-2	Marine sediment, East Sound, Washington; depth 30 m collected June 1955	≈3·5	0·00
SAR-1	Seaweed (Sargassum nature), collected between (39°14′N, 67°04′W) and (37°54′N, 65°50′W)	≈200	+1·69
MD6C-1	Organic concentrate from shale, Phosphoria formation, Coal Canyon, Lincoln County, Wyoming	1000	+0·54
SP-104	Niccolite and gangue minerals, Teheran, Iran	*	+0·27
SP-104a	Pure niccolite separated from SP-104	130	−0·17
SP-104b	Gangue minerals from SP-104	20	+1·20
SP-256	Nickel ore (primarily niccolite), Cuzco, Peru	300	−0·13
OC-1	Soil sample, T1S, R12W, Pulaski County, section 4, Arkansas	10	0·00
OC-2	Leaves from oak tree in soil same as OC-1	≈18	+0·89

* Not determined.

in the sea water and precipitates copper sulphide in the bottom muds. In addition there is a further concentration of copper contained in dying organisms that are also concentrated in areas of high anaerobic activity. It is well known that biological systems do fractionate isotopes and it may be that the observed enrichment is due to the copper contained in the dead organisms.

Because of the rather large enrichment of Cu^{65} in sample BM-1, it was of interest to see if the organic matter in marine shales also contained copper which is heavier than normal. One sample of marine shale was examined, specimen

MD-6C-1, a shale from the vanadiferous zone of the phosphatic shale member of the Phosphoria formation, Coal Canyon, Lincoln County, Wyoming. The organic fraction, which was about 40 per cent richer in copper than the original sample, was separated after the procedure described by DEUL (1952), and the copper was extracted in the usual way described above. Contrary to what might be expected from the result on sample BM-1, this sample showed no significant enrichment of the heavy isotope.

Sample SP-104 was a fairly pure specimen of niccolite from Iran with a small amount of gangue. The equivalent uranium analysis of the pure niccolite fraction was 0·12 per cent, and that in the gangue fraction ran 0·41 per cent. X-ray studies indicated a small amount of a black mineral tentatively identified as uraninite in the gangue fraction. As can be seen in the table, the gangue fraction was slightly enriched in Cu^{63} compared with the pure niccolite fraction. A second niccolite, SP-256, did not show any significant enrichment of either copper isotope. The mineral and gangue fractions were not separated as in the previous sample.

Two samples of plant materials were also analysed. SAR-1, a sample of seaweed (dry weight approximately 5 lb), was collected with nets over a wide range of latitude (see Table 5). The copper extracted was found to be slightly enriched in Cu^{65} compared to the standard. The other sample of plant material, OC-2, was approximately 1 lb of dried oak leaves from a tree grown in Pulaski County, Arkansas, section 4, T1S, R12W. The copper extracted from this sample was not significantly enriched in Cu^{65} and is considered normal. A sample of soil, OC-1, in which this tree was grown was also analysed and found to be normal.

Summary

Although copper does not undergo severe fractionation in nature, there are slight variations in the abundance of the isotopes that may be significant in unravelling some geologic processes. For future investigation of the variations of isotopic abundance of the medium to heavy-mass elements, it would seem profitable to study suites of samples from localized areas where there may be some hope of interpreting a specific geologic mechanism, rather than studying widely separated samples.

Acknowledgements—We wish to acknowledge the efforts of C. H. ROACH and M. DEUL of the U.S. Geological Survey, J. R. RAND of the White Pine Copper Company, Professor T. G. THOMPSON of the University of Washington, O. M. CLARKE, Jr. of the Reynolds Metals Company, and D. R. NORTON of the Sprague Electric Company for their aid in collection of samples. Special thanks are due to W. S. WHITE of the U.S. Geological Survey for his continued interest and helpful suggestions and for permission to use Fig. 2. We are also indebted to J. FRENCH, formerly of the U.S. Geological Survey, for much of the construction and design work of the mass spectrometer. This work is part of a programme being conducted by the U.S. Geological Survey on behalf of the Division of Research of the U.S. Atomic Energy Commission.

References

BARNETT P. R., HULEATT R. P., RADER L. F. and MYERS A. T. (1955) Spectrographic determination of contamination of rock samples after grinding with alumina ceramic. *Amer. J. Sci.* **253,** 121–124.

BAUDISCH O. (1938) Über die verwendung von cupferron in der spektralanalyse. *Ark. Kemi. Min. Geol.* **12B,** No. 8, 1–6.

Blix R., von Ubisch H. and Wickman F. E. (1957) A search for variations in the relative abundance of the zinc isotopes in nature. *Geochim. et Cosmochim. Acta* **11,** 162–164.

Brown H. A. and Inghram M. G. (1947) The isotopic composition of meteoritic copper. *Phys. Rev.* **72,** 347.

Chow T. J. and Thompson T. G. (1954) Seasonal variation in the concentration of copper in the surface waters of San Juan Channel, Washington. *J. Mar. Res.* **13,** No. 3, 233–244.

Deul M. (1956) Colloidal method of concentration of carbonaceous matter from rocks. *Bull. Amer. Ass. Petrol. Geol.* **40,** No. 5, 909–917.

Fernelius W. C. (1946) *Inorganic Syntheses* Vol. II, pp. 1–4. McGraw-Hill, New York.

Furman N. H., Mason W. B. and Pekola J. S. (1949) Extraction of cupferrates. *Analyt. Chem.* **21,** 1325–1330.

Klemm A. (1943) Isotopenaureicherung durch diffusion von kupfer in silbersulfid. *Z. phys. Chem.* **193,** 29–39.

Lean B. and Whatmough W. H. (1898) New method of preparing pure oxide, preparation of cuprous iodide. *J. Chem. Soc.* **73,** 148–157; see p. 149.

Lovering T. S. (1950) The geochemistry of argillic and related types of rock alterations. *Colo. Sch. Min. Quart.* **45,** 1B, 231–260.

Myers A. T. and Barnett P. R. (1953) Contamination of rock samples during grinding as determined spectrographically. *Amer. J. Sci.* **251,** 814–830.

Rankama K. (1954) *Isotope Geology* p. 535. McGraw-Hill, New York.

Senftle F. E. and Bracken J. T. (1955) Theoretical effect of diffusion on isotopic abundance ratios in rocks and associated fluids. *Geochim. et Cosmochim. Acta* **7,** 61–76.

Shawe D. R. (1955) Significance of roll ore bodies in genesis of uranium–vanadium deposits on the Colorado Plateau. *Proc. Int. Conf. on the Peaceful Uses of Atomic Energy, Geneva*, 1955, **6,** 335–337; *U.S. Geol. Surv. Prof. Pap.* 300, 239–241.

White J. R. and Cameron A. C. (1948) The natural abundance of isotopes of stable elements. *Phys. Rev.* **74,** 991–1000.

White W. S. and Wright J. C. (1954) The White Pine copper deposit, Ontonagon County, Michigan. *Econ. Geol.* **49,** No. 7, 675–716.

Note added in proof: It is of interest to report some results obtained since the manuscript was submitted on a sample containing covellite in a digenite host. This specimen had previously been analysed for the S^{32}/S^{34} variations,* and was kindly submitted by M. L. Jensen of Yale University. In this specimen (Jensen's sample I) a variation of over 4 per cent was noted in this S^{32}/S^{34} ratio. Cu^{63}/Cu^{65} ratios were measured on the same three specimens on which he reported, but no significant variation from the standard sample has been found.

* Jensen M. L. (1957) *Econ. Geol.* **52,** 269–81.

Geochimica et Cosmochimica Acta, 1958, Vol. 15, pp. 195 to 212. Pergamon Press Ltd. Printed in Northern Ireland

The constitution of the mantle—III

Consequences of the olivine–spinel transition*

A. E. Ringwood

(*Received* 7 *November* 1957)

Abstract—Evidence on the chemical composition of the mantle is reviewed. Based upon studies of the inclusions in kimberlite pipes, intrusion of peridotites in orogenic regions, and the compositions of stony meteorites and kimberlite, it is suggested that the average composition of the mantle may approximate that of a garnet peridotite. However, the upper mantle immediately below the M-discontinuity may be poorer in sialic material and close to normal dunite–peridotite in composition.

When garnet peridotite is subjected to high temperatures and pressures a series of transitions dominated by the olivine–spinel transition occurs. Besides the olivine–spinel transition, pyroxene may invert to spinel plus coesite, whilst garnet and coesite may dissolve in the spinel at higher temperatures to form a highly disordered defect solid solution. The data in Parts I and II show that these changes should occur under the P–T conditions present in the upper 1000 km of the mantle and take place over an appreciable depth range. The position and extent of this transition range depends upon the assumed temperature distribution in the upper mantle. By choosing a suitable temperature distribution, the transition region can be made coincident with region C (Bullen) in which phase changes and inhomogeneity have been inferred on other grounds.

It is found that the proposed transition phenomena are capable of explaining the known data on seismic velocity distribution, elasticity and density in the mantle. The temperature distribution required to make the phase transition region coincident with region C is supported by recent studies of the temperature dependence of electrical conductivity in the mantle. Both convection and conduction mechanisms of heat transfer may give rise to this temperature distribution.

A specific model for the mantle is proposed.

1. Introduction

In Parts I and II of this series a study was made of the P–T conditions governing the olivine–spinel transition in forsterite and fayalite. Attention was also given to the possibility that pyroxene might break down to a spinel under pressure. The conclusion drawn was that olivines and pyroxenes would probably undergo inversion at depths of less than 1000 km in the mantle. In this paper a study is made of the consequences of these inversions and the extent to which they can account for the known properties and structure of the mantle.

Before this can be attempted, it is necessary to discuss present data on the chemical composition of the mantle, since this will determine the relative amounts of olivine and pyroxene and the extent to which the constitution of the mantle can be interpreted on the basis of phase transitions in these minerals.

2. Chemical Composition of the Mantle

At an average depth of 30 km below the continents and 5 km below the ocean basins the velocity of P earthquake waves increases suddenly to about 8 km/sec, giving rise to the Mohorovicic (M) discontinuity. This velocity essentially restricts the type of rocks which may occur in this region to dunites, peridotites and eclogites. Since the former two are closely related and differ radically from

* Paper No. 163 published under the auspices of the Committee on Experimental Geology and Geophysics and the Division of Geological Sciences at Harvard University.

eclogite, they will frequently be grouped together as "dunite–peridotite" in subsequent discussion.

Differentiation between eclogite and dunite–peridotite in the mantle cannot yet be made on physical grounds, therefore identification of the material beneath the *M*-discontinuity must depend upon geochemical and petrological arguments. At present it appears likely that most geologists favour the dunite–peridotite composition, but there have been in the past, and still are, some notable advocates of eclogites. Impetus has been given to this group by recent experiments in the high-pressure field (Kennedy, 1956; Robertson, Birch and MacDonald, 1957). It has been found that many minerals common in the crust undergo polymorphic changes to denser forms when moderate pressures are applied. It seems quite reasonable to suppose that basalt would be converted to an eclogitic assemblage at some depth (as yet unknown) in the upper mantle. The important question however is whether there is sufficient material of eclogitic composition in the upper mantle to be of geophysical significance. A substantial amount of geochemical and petrologic evidence on the composition of the upper mantle is available, and is discussed below.

(a) *The significance of crustal peridotitic intrusions and of olivine nodules in basalts*

The typical mode of occurrence of peridotites, dunites and serpentines derived therefrom is in geosynclinal regions which have undergone intense deformation. Intrusion has been controlled by major tectonic features and it is believed by many (e.g. Hess, 1955) that these bodies are derived directly from the mantle. If so, this would suggest that the upper mantle, immediately below the *M*-discontinuity is of dunite–peridotite composition.

Ross *et al.* (1954) have shown that dunite and the common olivine nodules found in basalt all over the world possess marked geochemical similarities, strongly suggestive of genetic relationship. In particular they tend to contain Ni^2 and Cr^3 in amounts considerably greater than those found in corresponding minerals from basalts. Since these elements are strongly enriched in the earliest minerals to crystallize from a magma (Wager and Mitchell, 1951) this suggests that dunite–peridotites* and olivine nodules possess a primitive, pre-basaltic origin.

Further evidence supporting the deep-seated origin of peridotites and olivine nodules is provided by the composition of diopside which usually occurs in varying amounts in this association. Ross *et al.* (1954) analysed a number of diopsides from olivine bombs and peridotites and found that they nearly always contain a substantial proportion of jadeite—up to 15 per cent. This suggests that the diopside has crystallized under pressure sufficiently high to prevent crystallization of felspars, and that as a result, the soda has entered pyroxene. It follows that olivine nodules and peridotites have been derived from the mantle, since felspars are stable in the crust.

Compared to peridotites, eclogites are exceedingly rare rocks. Their environment usually also suggests a deep-seated origin under conditions of great pressure.

* The dunite–peridotites referred to are from the typical orogenic environments. There are undoubtedly dunites and peridotites in basic complexes which have been formed by crystal settling from a parent basic magma.

This applies particularly to one of the most common modes of occurrence which is as small inclusions and schlieren in bodies of peridotite (Eskola, 1921). In this association the field and petrologic data are indicative of a genetic relationship between the two. If the peridotites come from the upper mantle the associated eclogites must also come from there. The relative abundances, however, indicate that eclogite could be only a minor constituent of the upper mantle. The association found in diamond pipes (next section) is in accord with this conclusion.

(b) *Inclusions in kimberlite pipes*

These have been described by Wagner (1914) and Williams (1932) and their geologic significance discussed. The present discussion owes much to Wagner's (1928) paper. Kimberlite pipes carrying diamonds are of frequent occurrence over 1,000,000 miles^2 of southern Africa, and are also known in India, Brazil, the United States, Siberia and Australia. In South Africa and elsewhere these pipes carry numerous xenoliths of rocks which they are known to have intruded on their journey upwards. They contain also, large numbers of xenoliths of rocks which are not known to occur in the vicinity, particularly peridotites, pyroxenites and eclogites. The presumption is that these inclusions have been derived from deeper levels in the earth, and represent a random sample of deep lying rock types cut by the pipes. This group of inclusions consists essentially of the minerals olivine, pyroxene and garnet with all gradations from peridotites through garnet peridotites and olivine eclogites to eclogite. They have been found in every known occurrence of kimberlite, and diamonds occur in these inclusions as well as in the kimberlite.

Recent thermochemical calculations by MacDonald (1954) show that given reasonable and flexible assumptions regarding temperature in the mantle, diamond would not be stable until a depth of approximately 120 km was reached. Accordingly the kimberlites may be said to have sampled the outer mantle over very large areas down to depths of at least 120 km.

It is of great significance that in all cases, *peridotitic inclusions are found to be much more common than eclogitic inclusions*. If the sampling is representative, then the outer mantle must be dominantly of peridotitic composition, with eclogite a minor, but widely distributed constituent.

The kimberlite forming the host to the above inclusions is a rock of variable composition and degree of alteration. It is noteworthy that the dominant primary mineral is magnesian olivine, which constitutes between 50 and 75 per cent of kimberlites. This suggests that the region in the mantle where kimberlite originates is one where magnesian olivine is also abundant.

(c) *Evidence from meteorites*

There is a wide belief that the average composition of the mantle may correspond approximately to that of the average stony meteorite. Justification for this belief rests upon the observation that elemental abundances of non-volatile elements in the sun, stars and meteorites are in reasonable agreement (Kuiper, 1952), and the analogy existing between the structure and composition of the earth and that of a postulated original meteoric planet.

Most recent theories of the origin of the solar system imply an originally uniform composition for the raw material (possibly dust). Birch (personal communication) has pointed out that the radioactive heat generation in chondritic meteorites closely approximates the present total heat flow from the earth divided by the mass of the mantle. This strongly suggests that the average concentrations of potassium, uranium and thorium are the same in meteorites and in the earth. Since these are known to be among the most easily fractionated elements, this indicates that there has been little relative differentiation of composition between that of stony meteorites and that of the earth's average silicate fraction. A further argument is that the assumption of a meteoritic mantle provides a satisfactory basis for theories of magma formation (Bowen, 1928) and geochemical abundances.

Table 1. Chemical composition of chondritic meteorites
(Urey and Craig, 1952)

Component	(%)
SiO_2	47·04
MgO	29·48
FeO	15·40
Al_2O_3	3·09
CaO	2·41
Na_2O	1·21
K_2O	0·09*
Cr_2O_3	0·45
MnO	0·31
TiO_2	0·14
P_2O_5	0·26

* (Ahrens, 1954)

The average composition of the silicate fraction of chondritic meteorites is given in Table 1. The analysis has been recomputed to give a "high-pressure norm", such as would probably occur under conditions existing in the mantle. Na_2O and Al_2O_3 have been computed as jadeite and garnet, and the jadeite included with pyroxene. Cr_2O_3 and TiO_2 (as Ti_2O_3) are included with Al_2O_3 whilst MnO is grouped with MgO, FeO and CaO. This latter group is treated as one unit and no attempt has been made to divide it into different kinds of pyroxenes, since complete solid solution would probably occur above 1500°C anyway. The high pressure norm is as follows:

	(%)
pyroxene	48 (incl. jadeite, 8)
olivine	44·4
garnet	7
apatite	0·6

Thus a rock of meteoritic composition would probably crystallize as a garnet peridotite under high pressure. This would be similar to some of the garnet peridotites found as inclusions in the South African diamond pipes.

The evidence from meteorites suggests that composition of the mantle might be akin to garnet peridotite. It seems however, that the amount of pyroxene relative to olivine obtained in the norms above might be somewhat high, since olivine is far more abundant in the deep-seated peridotites, kimberlites and kimberlite inclusions.

This apparent discrepancy will be considered in detail by the author in a forthcoming paper, where it is suggested that it is probably caused by a difference in the average state of oxidation of the earth and the meteoritic planet. The earth is more reduced, containing less ferrous iron than the meteoritic average. There is also evidence suggesting that the earth's core may contain about 10 per cent of silicon metal. This would be sufficient to produce a mantle containing a substantial excess of olivine over pyroxene (if the mantle was derived from an average chondritic composition by a higher degree of reduction. For the present it may be concluded that chondritic meteorite abundances suggest a mantle equivalent to a garnet peridotite, with (subject to further interpretation) olivine the dominant phase.

(d) *Chemical zoning in the mantle*

Studies of crustal peridotite intrusions and kimberlite inclusions described in Sections 2(a) and 2(b) suggested that the upper mantle immediately below the *M*-discontinuity is dominantly of peridotitic composition rather than eclogitic. However, minor amounts of eclogite are probably widespread in this region. Furthermore the data indicated that this peridotite contained very little CaO, Al_2O_3 and Na_2O.

The study of meteorite compositions (Section 2(c)) suggested that the mantle as a whole should contain substantial amounts of CaO, Al_2O_3 and Na_2O. A supply of these components in the mantle is necessary to explain the generation of basaltic magma. It is clear that these components must therefore occur below the dunite–peridotite zone, and it was shown that the material in this region would probably crystallize as a garnet peridotite. A zonal structure for the mantle therefore seems indicated, with dunite–peridotite below the *M*-discontinuity, grading downwards into primary garnet–peridotite.

Rubey (1951) has arrived at a similar conclusion from geochemical arguments. He points out that the mantle has been differentiating over geological time and supplying basalt and sialic material to the surface, resulting in continental growth. He maintains that the primary mantle material may approximate meteoritic composition (i.e. garnet–peridotite). Fractional melting of this material forms basalts which are erupted at the surface. The region where the fractional melting occurs becomes depleted in Ca, Al and Na, and therefore of dunite–peridotite composition. According to this suggestion these rocks would occur immediately below the *M*-discontinuity and would be responsible for the orogenic dunite–peridotite intrusions. However, they would grade downwards into normal mantle material (garnet–peridotite) which is the present source of basaltic magma.

This model is able to supply a satisfactory explanation of the role of eclogite. Fractional melting of primary garnet–peridotite provides material of basaltic composition. Probably much of the basalt magma would not reach the surface

but would crystallize as eclogite in pockets and widespread segregations in the primary garnet–peridotite and in the residual overlying dunite–peridotite. This would explain the ubiquitous but minor occurrences of eclogites in the diamond pipes. The width of the dunite–peridotite zone and the proportion of eclogite might vary considerably in different regions of the earth and there would be room for substantial chemical inhomogeneity in the upper mantle. Furthermore, systematic differences could well exist between continents and oceans. A thickness of from 100 to 200 km for the dunite–peridotite zone beneath continents would appear reasonable, whilst it might be substantially less under the oceans.

Birch (1952) brought forward strong evidence indicating that the mantle between 900 km and the core is homogeneous, whilst between approximately 300 km and 900 km a region of inhomogeneity occurs. This inhomogeneity may be due to changes of phase, chemical composition or both. Birch showed that the principal changes were probably polymorphic changes in the minerals present, leading to dense, close-packed structures. He also suggested that changes of chemical composition occurred. This would help to explain the large width of the transition zone.

In the following pages the author shows that the width of the transition zone and the known properties of the mantle can be explained in terms of phase changes alone. It is not necessary to assume any chemical changes.* The properties of the mantle will be discussed in terms of phase changes in a medium of primitive and uniform composition—akin to that of the garnet–peridotite previously advocated.

3. Phase Equilibria in the Mantle Involving the Olivine–Spinel Transition

In Parts I and II of this paper, some of the conditions governing the olivine–spinel transition in fosterite and fayalite were determined. Assuming plausible temperature distributions in the earth it appeared that forsterite would invert to a spinel at depths less than 1000 km, whilst fayalite was found to undergo a similar inversion at much smaller pressures (at corresponding temperatures). A thermochemical study of the stability of (MgFe) pyroxenes showed that these would break down into $(MgFe)_2SiO_4$ spinels plus coesite at maximum pressures not much greater than those required for the olivine–spinel transition in the olivine of corresponding composition. If the temperatures were sufficiently high ($\geqslant 1500°C$) the pressures required for pyroxene breakdown would become coincident with those required for the olivine–spinel transition.

In a mantle of the composition assumed in Section 2, transition phenomena will be dominated by the olivine–spinel transition because of the abundance of olivine. Furthermore since pyroxenes also break down to spinels under pressure, there can be little doubt as to the importance of the role which $(MgFe)_2SiO_4$ spinel plays in the mantle. However, there will be other components apart from MgO, FeO and SiO_2 present in the mantle and it therefore appears desirable to

* At least for the major components, which are not easily fractionated. It is possible that the distribution of some trace elements which cannot fit into existing minerals and are highly mobile may not be uniform throughout the mantle. Examples would be K, U, Th.

inquire in greater detail into the sequence of changes occurring when garnet–peridotite is placed under conditions such that an olivine–spinel transition may take place. In this respect two characteristic properties of spinels will be of particular importance.

(1) The spinel structure is stable for a very large number of ions of different size, valency and electronic structure. For example, the following ions form spinels (Gorter, 1954, with additions):

H^1	Li^1	Na^1	Cu^1	Ag^1			
Mg^2	Ca^2	Mn^2	Fe^2	Co^2	Ni^2	Zn^2	Ca^2
Al^3	V^3	Cr^3	Mn^3	Fe^3	Ga^3	Rh^3	Ir^3
Ti^4	V^4	Mn^4	Ge^4	Sn^4	Si^4		
Mo^6	W^6						

At high temperatures, spinels display a strong tendency towards solid solution among themselves. The spinel lattice is tolerant towards a very wide range of ionic substitutions. It seems quite likely that if present data on solid solution relationships were extrapolated to temperatures around from 2500°C to 3000°C, a state of complete solid miscibility would be reached between end members in most spinel systems.

(2) Spinels frequently have the ability to take compounds with ABO_3 type formulae into solid solution forming defect structures. Thus ordinary spinel ($MgAl_2O_4$) is able to form solid solutions with Al_2O_3, Fe_2O_3 and Cr_2O_3. It seems quite possible that Mg_2SiO_4 spinel would be able to dissolve some excess SiO_2 to form a defect structure (this is equivalent to dissolving some $MgSiO_3$). This process would be encouraged by high temperatures and pressures.

The possible effect of pressure and temperature on transitions in garnet–peridotite may be noted in the light of the above data. The garnet–peridotite is assumed to consist dominantly of olivine, with subsidiary pyroxene and about 10 per cent of garnet. It is emphasized however that the discussion is general and does not depend upon a detailed chemical and petrological model such as that suggested above. The following discussion applies to a mantle of any composition consisting dominantly of olivine and pyroxene, with smaller amounts of Al_2O_3, CaO, Na_2O and Cr_2O_3. The garnet–peridotite model was adopted because of reasons put forward in Section 2, and it will be convenient to discuss detailed phase changes on this model.

The olivine in the mantle contains some fayalite in solid solution—probably about 10 per cent. Because of the much lower pressure required to invert fayalite to spinel, the first spinels formed during the transition will be rich in fayalite. As pressure rises, more and more forsterite will enter the solid solution. The transition in olivine will be completed at a pressure close to that required for the pure forsterite transition.

The behaviour of pyroxene was discussed in Part II: $(MgFe)SiO_3$ will break down to spinel plus coesite at pressures somewhat higher than those required to transform olivine into spinel. At a temperature of 1500°C the pressure required to decompose pyroxene may be about one-third greater than the pressure required for the olivine–spinel transition. At higher temperatures than this the excess

pressure is decreased and may become essentially the same as that required for for the olivine–spinel transition.

Pyroxenes in the mantle will also carry some $FeSiO_3$ in solid solution. This has an effect analogous to that in olivine. $FeSiO_3$ requires smaller pressures to break down than $MgSiO_3$ and hence this transition is also spread over a transition range, forming a band. This band probably overlaps the band formed by the $(MgFe)_2SiO_4$ olivine–spinel transition.

The decomposition of pyroxene liberates coesite. At sufficiently high temperatures this may dissolve in the spinel forming a defect solid solution. The ability of spinels to form such solutions has already been discussed.

The other phase suggested to occur in the upper mantle is garnet, probably of the pyrope variety. The structures of garnet and Mg_2SiO_4 spinel are related. Both consist of oxygen ions in cubic close packing with cations filling the holes. The chief difference is that garnet contains trivalent cations, chiefly Al^3, which are not present in pure Mg_2SiO_4 spinel. It has already been pointed out, however, that all the ions which occur in garnet can also form spinels, and that spinels are capable of very wide solid solution relationships at high temperatures. Accordingly at the high temperatures occurring in the mantle it seems likely that some Ca^2, Mn^2, Cr^3, Al^3, and Ti^3 will dissolve in the spinel. This is equivalent to solid solution of the garnet phase. According to the model, there is only about 10 per cent of garnet present, and it therefore seems very possible that garnet will dissolve completely in the spinel phase at the high temperatures involved (estimated as 1500°C–3000°C in Section 7).

Summarizing this discussion it is suggested that the following transitions may occur in the material of the mantle as pressure and temperature increase with depth.

(1) Olivine → spinel	Occurs over a P–T range because of Mg–Fe solid solution
(2) Pyroxene → spinel + coesite	Occurs over a P–T range because of Mg–Fe solid solution and probably overlaps transition (1).
(3) Spinel + coesite → spinel defect solid solution	This solution encouraged by high temperatures.
(4) Spinel + garnet → spinel solid solution (or subsidiary Ca^2, Al^3, etc.)	This solid solution encouraged by high temperatures.

This discussion leads therefore to the suggestion that when the transition is completed, there will be only one phase present—essentially an Mg_2SiO_4 spinel, containing excess Si^4 Al^3 Cr^3 Ca^2 Na^1 and other minor constituents (including OH^{-1}) in solid solution. The temperature estimated for completion of this process is about 3000°C (Section 7). The spinel solid solution will be of a highly disordered, defect character, consisting essentially of a cubic close packing of oxygen ions, with Si^4 filling the tetrahedral holes, and all the other cations distributed randomly through octrahedral holes. Under the high temperatures and pressures involved it is possible that a small percentage of Si^4 ions might also occur in octrahedral

sites (disorder of ions between octrahedral and tetrahedral sites is common in spinels). Such an assemblage of ions would be as close-packed as geometry would allow and it does not seem likely that further polymorphic transitions would occur once this state was reached.

It is evident that such complex transition phenomena will take place over an appreciable pressure and temperature range. Insufficient data are available to estimate its size. It may well be in the vicinity of from 100 to 200 km at constant temperature however. Using the gradient found for the olivine–spinel transition in forsterite this would be equivalent to about 350–750°C at constant pressure.

The data obtained in Parts I and II indicated that an olivine–spinel transition and related transition phenomena should occur in the first 1000 km of the mantle for all reasonable temperature distributions. The exact position and range of the transition would depend upon the temperatures in this region.

Transition phenomena of the kind described should cause important changes in the properties of the mantle in this depth region. In the next sections a review of the physical properties of the mantle is made in order to find out whether the changes in these properties are consistent with the occurrence of the predicted olivine–spinel transition.

4. Seismic Data

The Jeffreys (1939) and Gutenberg (1948) depth–velocity curves for the mantle are illustrated in Fig. 1. The curves differ qualitatively in the shallower

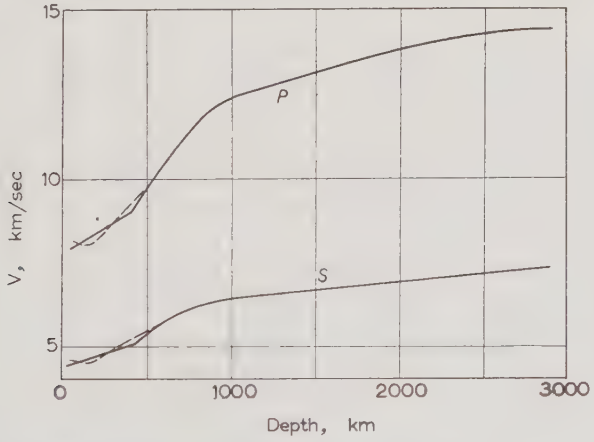

Fig. 1. Depth–velocity curves for the mantle; — Jeffreys; – – – – Gutenberg.

regions of the mantle but agree in the deeper regions. According to the classification made by Bullen (1947) on the basis of these velocity distributions, three distinct regions may be distinguished in the mantle (region *A* refers to the crust):

Region B. An outer zone where wave velocity increases at a moderate rate with depth (Jeffreys) or else it decreases slightly and then increases slowly (Gutenberg). In Jeffreys' solution this zone extends from 30 km to 412 km, in contrast to 30–200 km for the Gutenberg solution.

Region C. An intermediate zone in which both solutions indicate a region

where velocity increases very rapidly with the depth until a depth of approximately 900 km is reached.

Region D. An extensive inner zone extending fron 900 km to the core at 2900 km, where wave velocity increases at a moderate and uniform rate.

The original interpretation of the velocity distribution in the mantle gave rise to the Jeffreys–Bernal hypothesis which was discussed in Part I. Jeffreys assumed that the boundary between regions *B* and *C* was caused by a polymorphic inversion in the olivine of the mantle. It was suggested that ordinary olivine inverted to a spinel form possessing different elastic properties. In Jeffreys' original solution, a first order discontinuity due to this phenomenon was placed at 474 km but the later solution shows a second order discontinuity at a shallower depth of 413 km.

The Jeffreys–Bernal hypothesis seemed to explain most of the features of the depth–velocity curves. Thus, on this basis, region *B* was assumed to consist essentially of normal olivine whereas region *D* was regarded as the homogeneous spinel modification. Qualitatively it was noticed that the high wave velocities of this region could be explained by the probable elastic properties of a closely packed spinel modification.

Region *C* could be interpreted as a region over which the transition took place, characterized by coexisting olivine and spinel. However, advocates of this hypothesis experienced some difficulty in explaining the occurrence of such a wide transition region, since a relatively sharp transition might normally have been anticipated.

Recently, Birch (1952) investigated the structure of the mantle from a quantitative standpoint. He compared the observed variation of seismic velocity with depth, with the variation which would be expected on thermodynamic grounds in a homogeneous medium. From this comparison Birch concluded that region *B* could be homogeneous, whilst region *D* was probably homogeneous. However, the rate of increase of velocity in region *C* was too high to be consistent with homogeneity.

Birch found that the ratio of initial incompressibility (K) to initial density (σ) at room temperature for the material of region *D* was equal to about 60 $(\mathrm{km/sec})^2$. This value is much above that of any known silicate, and is only reached by closely packed oxide structures. Accordingly he suggested that region *D* consists of closely packed polymorphs of normal ferromagnesian silicates. Region *C* could be regarded as a region where the transitions from normal to tightly packed silicates took place. Possibly also some chemical changes occurred in this zone.

It appears that Birch's results in the main are consistent with the Jeffreys–Bernal hypothesis. However, the wide transitional range found by Birch was thought not easily explicable by this hypothesis. Accordingly Birch suggested that perhaps other more complex polymorphic transitions besides the olivine–spinel transition and also chemical changes might be involved.

In the previous section it was shown that other polymorphic transitions are probably involved. These are closely related to, and dominated by, the olivine–spinel transition. However, there is no need to assume a change in chemical composition in the transition width. The equilibria are complicated and the width

of the transition zone can only be found by experiment. It seems reasonable to assume that it might be 100–200 km wide at constant temperature corresponding to 350–650°C at constant pressure. It could also be substantially greater.

Such a width would be narrower than the 500–700 km inferred by Birch for the mantle. However, when the effect of temperature increase with depth in the mantle is also taken into account, there is no difficulty in meeting the geophysical requirements. The slope of the transition in forsterite was found to be about 100 bars/°C, and the slope of the whole zone will probably approximate to this, since the transition in forsterite is the controlling factor. As the temperature rises with increasing depth in the earth, the transition pressures also become higher, resulting in a further spread of the transition zone. Accordingly the final width of the zone will depend chiefly upon the temperatures assumed to occur in the mantle. In order to spread the transition zone between 300 and 900 km a temperature difference of around 1500°C is require between top and bottom. This does not appear excessive. Temperature distribution in the mantle will be discussed in detail in Section 7.

In view of the above factors the presence of a substantial transition region would be a necessary consequence of an olivine–spinel transition in the mantle. Accordingly it may be concluded that the Jeffreys–Bernal hypothesis is able to explain the seismic data on the mantle, and is consistent with Birch's thermodynamic analysis.

5. Elasticity of the Lower Mantle (Region *D*)

Birch deduced that the ratio of initial compressibility to density for the material of region *D* was about 60 (km/sec)^2 at room temperature. It is of some interest to compare this ratio with that to be expected for Mg_2SiO_4 spinel.

The compressibility of the spinel is unknown. The approximate value can be found from a study of analogous compounds, however. The compressibility of a substance is largely dependent upon the closeness with which its constituent ions or atoms are packed together. In oxygen compounds the closeness of packing of the large oxygen ions is a particularly important factor. In general, the closer the packing, the smaller the compressibility. This relation holds best for fairly close-packed compounds such as those under consideration. Anomalies may occur with the more open structures.

On these grounds, the inversion from olivine to spinel, involving as it does a considerable volume decrease, would be expected to produce a substantially smaller compressibility in the spinel modification. The initial compressibility of magnetite, which has a spinel structure is $5{\cdot}5 \times 10^{-7}$ bar^{-1} (Birch *et al.*, 1942). In magnetite the Fe^2 and Fe^3 ions are both larger and more compressible than Mg^2 and Si^4 in Mg_2SiO_4 spinel. The initial compressibility of Mg_2SiO_4 spinel is therefore probably somewhat less than that of magnetite. The most closely packed oxide structure known is that of corundum, and as might be expected, this has the smallest compressibility. The packing in Mg_2SiO_4 spinel would approach that of corundum, but would be somewhat less. This is evident from the respective postulated densities and lattice geometry. It is unlikely that the compressibility of Mg_2SiO_4 spinel will be as low as that of corundum. From these considerations

a value for the initial compressibility of Mg_2SiO_4 between 5·5 and 3·6 seems indicated. The value selected is $4{\cdot}5 \pm 1 \times 10^{-7}$ bar^{-1}. It is noteworthy that the compressibility of pyrope, the only silicate comparable in density and packing with Mg_2SiO_4 spinel has a compressibility within this range ($5{\cdot}45 \times 10^{-7}$ bar^{-1})*.

Using this estimate for the compressibility of Mg_2SiO_4 spinel and taking $3{\cdot}54 \pm 0{\cdot}10$ g/cm^3 for the density (derived from Part I), the ratio K/σ is found to be about 65 ± 15 (km/sec)^2, in excellent agreement with the value of 60 (km/sec)^2 found by Birch for the material of region *D*.

6. Density Variation in the Mantle

From a consideration of the distribution of moment of inertia within the earth, and depth variation of seismic velocities, Bullen (1936, 1947) has been able to calculate the density distribution within the earth. His principal results are:

(1) That the mantle must be inhomogeneous.

(2) That a substantial increase in density is required at a relatively shallow depth.

Bullen suggested that this increase in density was associated with the seismic discontinuity found by Jeffreys in the 400 km region. Using the Jeffreys depth–velocity distribution, and assuming that the density immediately below the Mohorovicic discontinuity was that of magnesian olivine (3·32 g/cm^3) Bullen found, by extrapolating the densities of regions *B* and *D* that they must differ in density by 0·54 g/cm^3. If the 20° discontinuity occurs at a smaller depth than 413 km the density difference between the two regions will be reduced.

In Part I, the density increase associated with the olivine–spinel transition in Mg_2SiO_4 was placed at $(0{\cdot}35 \pm 0{\cdot}10)$ g/cm^3. This is in reasonable agreement with the geophysical value which is subject to appreciable variance according to the depth at which the transition is assumed to occur, the density assumed beneath the *M*-discontinuity, and the assumed density of the core. The gap between the two values could be eliminated if the spinel phase became slightly enriched in Fe_2SiO_4. Solid solution and transitions of subsidiary pyroxene and garnet of region *B* as previously discussed could also cause an increase in density greater than that calculated.

7. Temperature Distribution in the Mantle

In the previous section it was pointed out that the inhomogeneity in region *C* of the mantle could be explained by the effect of a temperature gradient spreading out the phase transition region. Although the width of the transition zone at constant *P*-*T*, can only be guessed at, and there is a substantial range of possible error in both the position and slope of the transition curve in forsterite, it turns out that the model implies a rather specific type of temperature distribution. The width of region *C* depends upon whether the Jeffreys or Gutenberg depth-velocity curves are adopted (Section 4). In the following discussion Jeffreys'

* Birch, and Yoder (personal communication) have recently separately determined the compressibility of two samples of $MgAl_2O_4$ spinel as 4·6 and $4{\cdot}1 \times 10^{-7}$ bar^{-1}. The first value refers to a sample containing a large stoichiometric excess of Al_2O_3. The higher compressibility is probably due to the large number of holes which must be present in this crystal.

curves are selected. According to them, region *C* begins at about 400 km. If the GUTENBERG curves, implying that region *C* starts at 200 km are more correct, there is little difficulty in modifying the model to accord with them.

In Fig. 2, the location of the transition phenomena in the mantle is indicated. The basic control is the position of the transition in Mg_2SiO_4 which was determined in Part II. A pressure range of 150 km for the transition region at constant

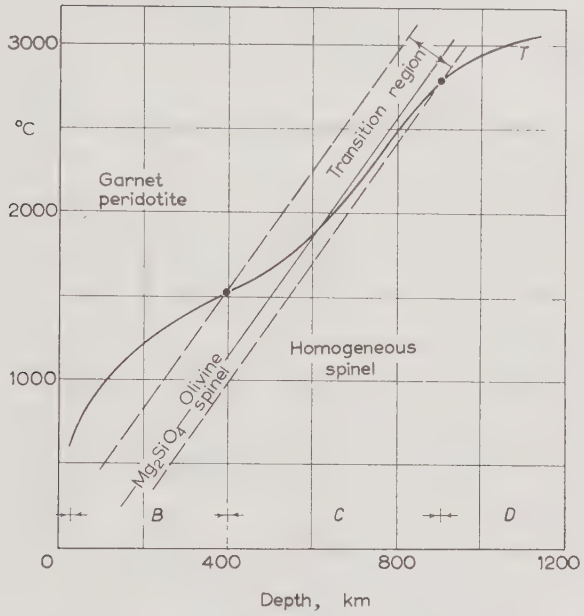

Fig. 2. Structure of mantle showing suggested relationship between temperature gradient (T) and width of transition zone.

temperature corresponding to 500°C at constant pressure, has been assumed. Accordingly the transition region takes the shape of a band with slope 100 bars/°C. Fayalite, which enters preferentially into the spinel solid solution, will spread out the transition to lower pressures. So will other components which are likely to be preferentially soluble in the spinel (CaO, Al_2O_3, Cr_2O_3, Na_2O and excess SiO_2). Accordingly most of the width of the band falls on the low pressure side of the Mg_2SiO_4 transition line. The principal transition which may extend the band to the high pressure side of this line is the breakdown of pyroxene:

$$\underset{\text{pyroxene}}{2(MgFe)\,SiO_3} \rightarrow \underset{\text{spinel}}{(MgFe)_2SiO_4} + \underset{\text{coesite}}{SiO_2}$$

which was studied in Part II.

From Fig. 2, it may be seen that in order to have a transition region between 400 and 900 km, the internal temperature–depth curve should enter the transition zone at 400 km equivalent to 1500°C and leave it at 900 km and 2700°C. Although the above figures may be subject to substantial variance owing to experimental

error, uncertainty of the width of the transition zone, and uncertainty of the width of region C in the earth, there is one important feature which appears to remain the same no matter what reasonable combination of variables is chosen.

It is usually assumed (Verhoogen, 1956) that temperatures in the shallow mantle rise rather rapidly and may be in the neighbourhood of 1000°C at depths around 100 km. This necessitates a high initial temperature gradient in this zone. If the earth's temperature–depth curve is to enter the transition region at 400 km the temperature gradient must decrease rapidly (Fig. 2). This implies a relatively low temperature gradient in the region between 200 and 400 km.

When the transition region is entered, however, the temperature gradient must rise considerably in order to stay in the inhomogeneous region until 900 km. The gradient in this region must therefore be about 3°C/km. On moving out of the transition region at 900 km the gradient should lessen in order not to lead to excessively high temperatures in the core.

The previous discussion indicates that a marked increase in the earth's temperature gradient in region C is a probable consequence of the proposed model. It could be escaped by assuming the transition zone at constant pressure or temperature to be very much wider, but this appears improbable. An alternative escape from this conclusion would be to assume a mantle in which chemical composition changes markedly in region C. However, there is no need to make these assumptions. There is independent evidence suggesting that the temperature gradient may indeed increase sharply in region C, and it is possible to find plausible reasons for this behaviour.

Lahiri and Price (1939) have studied the variation with depth of electrical conductivity in the mantle. They found that conductivity in the upper mantle was about $10^{-4}\ \Omega^{-1}\ \mathrm{cm}^{-1}$, but in the vicinity of 600 km it rose rapidly to $10^{-2}\ \Omega^{-1}\ \mathrm{cm}^{-1}$. The rate of increase of conductivity must flatten out below this depth in order to obtain a reasonable value near the core-mantle boundary. The depth at which the conductivity begins to rise is not known definitely, but may be between 300 and 600 km. More recent studies of conductivity in the mantle by Rikitake (1950) and MacDonald (1957) place the beginning of the region of rapid increase around 400 km.

Runcorn (1955) has studied the Lahiri and Price distribution and concludes that currently advocated temperature distributions in a mantle composed principally of olivine will not explain the rapid increase of conductivity between 700 and 900 km. He concludes that a phase change to a more densely packed structure in this region could explain the data. The high-pressure phase is assumed to have higher electronic conductivity than the olivine modification. Runcorn does not examine the other alternative of determining the type of temperature distribution which would cause the observed conductivities, assuming that large changes in the conductivity constants do not occur.

Tozer (manuscript) has recently completed a study of the relation between electrical conductivity and temperature in the mantle and has kindly informed the author of his results. Assuming a mantle dominantly of olivine composition, he finds that the average temperature gradient in the upper mantle is about 1·5°C/km, leading to a *maximum* temperature at 400 km of about 1700°C. In the

model a value of 1500°C is suggested for this depth. These estimates are in reasonable agreement.

Tozer has also examined the effect of phase transitions on electrical conductivity at high temperatures. He agrees with Runcorn that an olivine–spinel transition will involve an increase in conductivity but is doubtful whether this is large enough to be responsible for the rapid rise of conductivity in region *C*. Making a reasonable assumption regarding the effect of phase changes on conductivity, Tozer finds that a substantial increase in temperature gradient is required somewhere below 400 km. The increase is compatible with the 3°C/km suggested in this paper for region *C*.

Additional considerations support this conclusion. Tozer finds from the electrical conductivity of the lower mantle that temperatures higher than 3000°C extend outwards from the core for 2000 km. This conclusion is essentially independent of the nature of the phase changes in region *C*. In order to reach a temperature of 3000°C at 1000 km from the 400 km region, where an average gradient of 1·5°C/km is reasonably well established, a marked increase of gradient is required. This may exceed 3°C/km.

Thus it may be seen that the evidence from electrical conductivity, which constitutes almost the only specific source of information on temperatures in the upper mantle, supports the temperature distribution in the proposed model. This distribution is required to explain region *C* in terms of phase changes in a chemically homogeneous mantle of garnet peridotite. Inquiry may next be directed towards the cause of this distribution.

Present ideas on temperature distribution are partially controlled by views about the mechanism of heat transport—whether it be by convection or conduction. It appears that both mechanisms are able to account for the presence of a high gradient in region *C*. This may be regrettable since it rules out the possibility of deciding which mechanism occurs in the earth.

Estimates of internal temperatures are commonly made by considering the cooling of a hot radioactive earth. These estimates are usually based upon the assumption of a constant thermal conductivity in the mantle. In view of recent work, this appears most unlikely. Clark (1956, and in press), Preston (1956) and Ringwood (1956) have independently pointed out that at the high temperature occurring in the mantle, heat transport may occur by direct radiation as well as through lattice vibrations, and may well be of considerable importance. A detailed investigation of this effect has been made by Clark, who finds that the conductivity due to radiative transfer in the upper mantle may be as much as three times the normal lattice conductivity. Below about 600 km however, radiative conductivity becomes greatly reduced because of absorption owing to the high electrical conductivity in this region. The temperature gradient is largely dependent upon the thermal conductivity and becomes greater as the conductivity decreases. According to these results, the temperature gradient should increase in the region around 600 km. The uncertainty is such as to allow appreciable variance in this depth and is in reasonable agreement with the requirements of the model.

Convection currents are considered by many to be the prime means of heat transport in the mantle. For a convection current to occur the thermal gradient

must exceed the adiabatic gradient in the mantle given by:

$$\frac{dT}{dr} = \frac{\alpha g T}{C_p}$$

where α is the coefficient of thermal expansion and C_p is the specific heat at constant pressure. In the upper mantle (region *B*) Verhoogen (1956) has estimated this gradient to approximate 0·3°C/km. For a convection current to penetrate the transition zone it is apparent however that the gradient must be much higher since a considerable increase in density occurs. At the same time, latent heat estimated in Part II as 100 cal/g is evolved. Since there is a range of transition it is sufficient for a first approximation to consider the term $\Delta v/t$ equivalent to thermal expansion in the transition range, where Δv is the total volume change in the transition (estimated as 11 per cent in Part I) and t is the temperature interval across which the transition is considered to extend at constant pressure. In Fig. 2, this has been taken as 500°C. Similarly the specific heat might be regarded as $(\Delta H/t) + C_p$ where ΔH is the latent heat of transition (estimated as 100 cal/g) and C_p is the normal specific heat. Substituting these values the adiabatic gradient in the transition region is found to be about 2°C/km, thus exceeding the normal adiabatic gradient by a factor of 6. Accordingly for a convection current to penetrate the transition region, the temperature gradient must increase as much as sixfold through the region. When (and if) a current has passed out of the transition zone the adiabatic gradient decreases to 0·3–0·2°C/km (Verhoogen, 1956).

The preceding discussion shows that both in a non-convecting mantle in conductive equilibrium and in a convecting mantle, the temperature gradient may increase considerably in region *C*. Evidence for this increase is provided by studies of the electrical conductivity of the mantle. This is in agreement with the requirements of the proposed model.

8. Summary, and Conclusion

This study was stimulated by the Jeffreys–Bernal hypothesis which suggested that the 20°C discontinuity was caused by an olivine–spinel inversion in the mantle. In Parts I and II, the P–T conditions governing this inversion in forsterite and fayalite were investigated. It was found that natural olivine should invert to a spinel in the upper mantle, in a region where phase changes and inhomogeneity have been inferred to other grounds (region *C*). A thermochemical study of pyroxene, indicated that it should break down to spinel and coesite under these conditions.

A model of the mantle was suggested on geochemical and petrological grounds in which the region immediately below the *M*-discontinuity consisted of dunite–peridotite. This graded downwards into material of uniform and primitive chemical composition approximating a garnet–peridotite. On this model it was found that the phase transition phenomena dominated by the olivine–spinel transition should be spread out over an appreciable depth range. The precise location and width of this range was determined by temperature distribution in the mantle. By choosing a specific temperature distribution the experimental

transition range can be made to coincide with the boundaries of region *C*. Recent studies on electrical conductivity and temperatures in the mantle support the temperature distribution adopted.

The known properties and data on the mantle have been examined in order to find out whether they were consistent with an olivine–spinel transition in region *C*. The following conclusions were drawn:

(1) The olivine–spinel transition and related transition phenomena are able to explain the relevant seismic data, particularly the fact that seismic data seem to suggest a transition range.

(2) The elastic properties of the mantle below 900 km deduced by Birch do not agree with those of any known silicate but are in good agreement with the probable elastic properties of the spinel modification of Mg_2SiO_4.

(3) The rapid increase of density with depth below the 20° discontinuity deduced by Bullen is in reasonable agreement with that which would be expected on the basis of an olivine–spinel transition.

(4) The temperature distribution implied by the transition phenomena is in agreement with that inferred from a study of electrical conductivity in the mantle. Both the conduction and convection mechanisms of heat transport in the mantle can account for this distribution.

It is believed that this combined evidence furnishes strong support for the Jeffreys–Bernal hypothesis and that justification exists for proposing a more specific model of the mantle than is usually attempted.

Using Bullen's depth classification, the following model is suggested:

Region A. Crust; surface—*M*-discontinuity.

Region B. *M*-discontinuity—400 km (Jeffreys) or 200 km (Gutenberg). Dunite–peridotite grading downwards into garnet peridotite. Both layers contain irregularly distributed segregations of eclogite. Temperature at 400 km about 1500°C.

Region C. From 400 km (or 200 km) to 900 km. Transition zone in garnet–peridotite dominated by inversion of olivine to spinel. Pyroxene breaks down to spinel plus coesite. Coesite dissolves in spinel to form defect solid solution. Garnet dissolves in spinel. Temperature gradient increases as zone is entered and may be around 3°C/km. Temperature at 900 km approximating 3000°C.

Region D. 900 km to 2900 km. Homogeneous spinel phase consisting of a highly disordered solid solution, chemically equivalent to garnet–peridotite.

Acknowledgements—The work described in Parts II and III was largely carried out at the Dunbar Laboratory, Harvard University, whilst the author was the recipient of a Research Fellowship granted by the Committee on Experimental Geology and Geophysics of Harvard, and a travelling scholarship provided by the University of Melbourne. The author has had throughout the privilege of constructive suggestions and stimulating discussion from Professor F. Birch, Dr. S. Clark and Messrs. D. C. Tozer and E. Herrin which have influenced much of the manuscript. For this he is deeply appreciative. However, they are not to be held responsible for any conclusions drawn herein.

References

Ahrens L. H. (1954) The abundance of potassium. *Nuclear Geology* (Edited by Faul). John Wiley, New York.

Birch F. (1952) Elasticity and constitution of the earth's interior. *J. Geophys. Res.* **57,** 227.
Birch F., Schairer J. F. and Spicer H. E. (1942) *Handbook of Physical Constants.* Geol. Soc. Amer. Spec. Paper 36.
Bowen N. L. (1928) *The Evolution of the Igneous Rocks.* Princeton Univ. Press.
Bullen K. E. (1936) The variation of density and the ellipticities of strata of equal density within the earth. *Mon. Not. R. Astr. Soc. Geophys. Suppl.* **3,** 395.
Bullen K. E. (1947) *Introduction to the Theory of Seismology.* Cambridge Univ. Press.
Clark S. P., Jr. (1956) Effect of radiative transfer on temperatures in the earth. *Bull. Geol. Soc. Amer.* **67,** 1123.
Eskola P. (1921) On the eclogites of Norway. Kristiana Videnskap. Sktift I Mat–Nat. Klasse, No. 8.
Gorter E. W. (1954) Saturation magnetism and crystal chemistry of ferrimagnetic oxides. *Philips Res. Rep.* Sept 9, 295.
Gutenberg B. (1948) On the layer of relatively low wave velocity at a depth of about 80 kilometers. *Bull. Seismol. Soc. Amer.* **38,** 121.
Hess H. H. (1955) *Serpentines, Orogeny, and Epeirogeny—in Crust of the Earth* p. 391. Geol. Soc. Amer. Spec. Paper 62.
Jeffreys H. (1939) The times of P.S, and the SKS tables. *Mon. Not. R. Astr. Soc. Geophys. Suppl.* **4,** 498.
Kennedy G. C. (1956) Polymorphism in the feldspars at high temperature and pressures. *Bull. Geol. Soc. Amer.* **67** (Abstract).
Kuiper G. P. (1952) Planetary atmospheres and their origin. *Atmospheres of the Earth and Planets.* Univ. of Chicago Press.
Lahiri B. N. and Price A. T. (1939) Electromagnetic induction in non-uniform conductors and the determination of the electrical conductivity of the earth from terrestrial magnetic variations. *Phil. Trans.* A **237,** 509.
MacDonald G. J. F. (1954) *A Critical Review of Geological Important Thermochemical Data.* Ph. D. Thesis, Harvard Univ.
McDonald K. L. (1957) Penetration of the geomagnetic secular field through a mantle with variable conductivity *J. Geophys. Res.* **62,** 117.
Preston F. W. (1956) Thermal conductivity in the depths of the earth. *Amer. J. Sci.* **254,** 754.
Rikitake T. (1950) Electromagnetic induction within the earth and its relation to the electrical state of the earth's interior. *Bull. Earthq. Res. Inst. Tokyo* **28,** 45, 219, 263.
Ringwood A. E. (1956) Ph. D. Thesis, Univ. of Melbourne.
Ringwood A. E. (1958) The constitution of the mantle, Parts I and II. *Geochim. et Cosmochim. Acta.* **13,** 303 and **15,** 18.
Robertson E. C., Birch F. and MacDonald G. J. F. (1957) Experimental determination of jadeite stability relations to 25000 bars. *Amer. J. Sci.* **255,** 115.
Ross S., Foster M. D. and Myers A. T. (1954) Origin of dunites and olivine rich inclusions in basaltic rocks. *Amer. Min.* **39,** 693.
Rubey W. W. (1951) Geologic history of sea water. *Bull. Geol. Soc. Amer.* **62,** 1111.
Runcorn S. K. (1953) The electrical conductivity of the earth's mantle. *Trans Amer. Geophys. Un.* **36,** 191.
Urey H. C. (1952) *The Planets.* Yale Univ. Press.
Urey H. C. and Craig H. (1953) *Geochim. et Cosmochim. Acta* **4,** 36.
Verhoogen J. (1956) Temperatures within the Earth. *Physics and Chemistry of the Earth* (Edited by Ahrens *et al.*) Vol. 1. McGraw-Hill, New York.
Wager L. R. and Mitchell R. L. (1951) The distribution of trace elements during strong fractionation of basic magma. *Geochim. et Cosmochim. Acta* **1,** 129.
Wagner P. A. (1914) *Diamond Fields of South Africa.* Chap. 2, 3 and 4.
Wagner P. S. (1928) The evidence of the kimberlite pipes on the constitution of the outer part of the earth. *S. Afr. J. Sci.* **25,** 127.
Williams A. F. (1932) *The Genesis of the Diamond* Vols. I and II. E. Benn, London.

Geochimica et Cosmochimica Acta, 1958, Vol. 15, pp. 213 to 217. Pergamon Press Ltd. Printed in Northern Ireland

The α-β inversions in eucryptite and spodumene*

Thelma Isaacs and Rustum Roy
College of Mineral Industries, The Pennsylvania State University, University Park, Pennsylvania

(*Received* 7 *April* 1958)

Abstract—Reversible hydrothermal experiments have allowed the unequivocal determination of the p–t dependence of the $LiAlSiO_{4(willemite)} \rightleftharpoons LiAlSiO_{4(high\text{-}quartz)}$ reaction. This constitutes one of the few reconstructive phase changes so studied. The revised α–β inversion temperature at atmospheric pressure is set at 848 ± 5°C and the enthalpy of inversion is calculated as 3750 cal/mole $LiAlSiO_4$.

It was found impossible to study the α–β spodumene inversion, since in no case could α-spodumene be synthesized from its own composition at pressures up to 4000 atm. The assemblage α-eucryptite + petalite appeared consistently instead.

The mineral "eucryptite" although first described by Brush and Dana (1880) was essentially re-discovered, synthesized and correctly described for the first time by Roy, Roy and Osborn (1950). In that paper mention was already made of the fact that the name eucryptite (Greek: well-hidden) was singularly prescient. Brush and Dana actually gave no optical data for the mineral. As far as we can determine, optical data were actually first reported by Larsen (1921) though only the Brush and Dana reference is usually cited. Larsen reports for eucryptite: $\omega = 1{\cdot}545$, uniaxial negative, showing that he was describing the wrong phase. Winkler (1948) who synthesized large crystals of a phase of composition $Li_2O.Al_2O_3{\cdot}2SiO_2$ expected that these were in fact the true natural eucryptite, although he mentioned several discrepancies between the properties of this phase and those listed by Brush and Dana. He showed the structure of this phase to be analogous to that of high quartz. In the contemporaneous work at Penn State two polymorphs of the 1 : 1 : 2 composition were established. The higher temperature one was shown to be identical with Winkler's form while it was shown that the lower temperature form is identical with a natural mineral which actually occurs in samples from Branchville, Connecticut (the locality where it had been said to occur by Brush and Dana). Since then eucryptite has been found in a large number of localities, and can most easily be recognized in hand specimen by its red fluorescence.

Winkler (1954) using the low temperature eucryptite crystals grown in our earlier study showed the structure of (natural) α-eucryptite to be analogous to that of willemite with (Li^{1+} + Al^{3+}) substituting for (Zn^{2+} + Zn^{2+}). In the previous study (Roy *et al.*, 1950) although the α to β inversion in eucryptite was shown to be reversible under hydrothermal conditions, due to equipment limitations, the inversion temperature was determined in dry runs in which the reaction only goes from $\alpha \rightarrow \beta$. The inversion temperature was said to be 972°C.

In a study of the applicability of thermodynamics to phase transitions in the solid state, this transition was studied in greater detail since it offered a "reconstructive" type change which would be studied experimentally with available

* Contribution No. 57–70. College of Mineral Industries, The Pennsylvania State University, University Park, Pennsylvania.

equipment. Moreover, it represented a change between two of the major silicate structure types. It was hoped that an accurate measurement of p–t dependence of the inversion point could be determined, and using the relatively accurate ΔV term, accurate inversion enthalpy and entropy terms could be determined.

In the α–β spodumene case there was a similar interest in the transition from the dense pyroxenoid to the open quartz structure. It also appeared to take place at a very convenient temperature for study up to very high pressures. Although it had not been possible to make α-spodumene from β-spodumene, nor indeed to synthesize α-spodumene reproducibly, it was felt that with the improved apparatus available now we could encounter no difficulty at all in synthesizing α-spodumene and studying the transition.

Table 1. Powder X-ray diffraction data
(Cu/Ni $\lambda = 1{\cdot}5418$ Å)

α-Eucryptite				β-Eucryptite		
d	I/I_0	d	I/I_0	d	I/I_0	hkl
6·789	33	1·782	5	4·551	22	100
4·160	23	1·723	5	3·90	1	003
3·914	69	1·666	6	3·533	100	102
3·880	24	1·631	5	2·628	9	110
3·570	5	1·543	14	2·621	1	
3·486	24	1·520	4	2·384	3	104
						112
3·368	100	1·500	26	2·274	9	200
3·145	12	1·498	5	2·105	8	113
						202
3·039	12	1·470	5	1·914	38	203
						114
2·736	63	1·460	5	1·763	3	204
2·543	67	1·410	5	1·719	3	106
						210
2·451	5	1·370	33	1·643	24	212
2·377	29	1·321	8	1·515	3	300
2·244	12	1·297	10	1·463	11	214
						302
2·142	5	1·230	4	1·441	16	206
2·090	5	1·180	5	1·332	7	108
						304
2·072	5			1·312	7	220
1·981	4			1·264	8	216
						310
1·945	12			1·247	1	009
1·884	5			1·231	14	118
						312
1·873	15			1·148	2	314
1·799	28			1·136	2	400
		Hexagonal				225
		$a = 5{\cdot}245$				
		$c = 11{\cdot}20$				

Experimental

Mixtures of γ-Al_2O_3, silicic acid and Li_2CO_3 were made and either used as such or melted to glasses, crushed fine and used.

"Gels" of the composition $Li_2O{\cdot}Al_2O_3{\cdot}2SiO_2$ and $Li_2O{\cdot}Al_2O_3{\cdot}4SiO_2$ were also prepared by the method described by Roy (1956) and part of each converted to the "completely" crystalline state. The different starting materials were treated in hydrothermal vessels within sealed gold capsules in the range up to 1000°C and up to 4000 atm. The products were examined by powder X-ray diffractometer techniques and with the petrographic microscope.

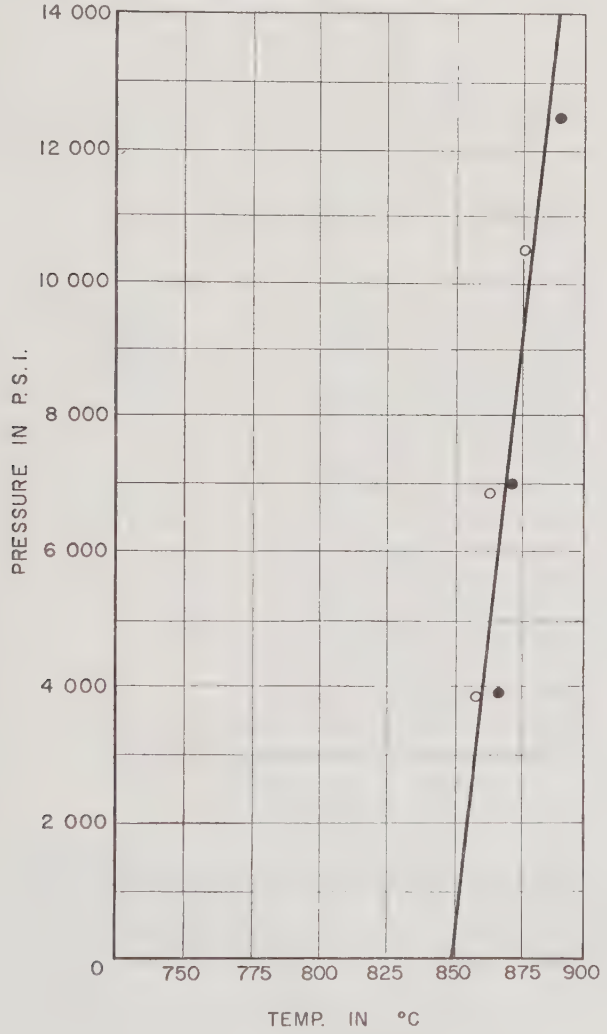

Fig. 1. p–t Curve for the reaction α-eucryptite $\rightleftharpoons$ β-eucryptite. See table for many other points.

Results

"The α–β eucryptite inversion"

Revised X-ray data for the two forms are given in Table 1. They differ substantially from those in the literature: they were obtained on a Philips wide-range

Table 2. Phase equilibrium data on the α–β eucryptite transition

Duration (hr)	Temp. (°C)	Pressure (lb/in^2)	Starting material	Products*
24	897	16,500	α	$\alpha + \beta$
			β	β + tr. α
146	865	3900	α	$\beta + \alpha$
			β	β
190	857	3850	α	α
			β	$\beta + \alpha$
138	878	10,500	α	α
			β	β + tr. α
144	863	6900	α	α
			β	α
140	890	13,300	α	β + tr. α
			β	β
172	870	7000	α	$\beta + \alpha$
			β	β
68	950	2500	Glass	β
19	866	2500	Glass	β
18	805	5400	Glass	$\alpha + \beta$
86	773	5600	Glass	α
			Mixture	α
69	790	5500	Glass	α + some β*
88	800	5350	α	α
			β	α
188	815	6500	α	α
			β	α
92	832	6400	α	α
			β	$\alpha + \beta$
111	847	7500	α	α + tr. β
			β	$\alpha + \beta$
42	820	2000	α	α
			β	β + ?
96	800	2100	α	α
			β	$\alpha + \beta$
75	860	7350	α	α
			β	$\beta + \alpha$
188	870	11,800	α	α
			β	β
283	885	12,200	α	α
			β	β + tr. α

* Some apparently puzzling features of these data were explained by the demonstration of the fact that β-spodumene is partly converted to the α form during the heating up period.

diffractometer with Cu$K\alpha$ radiation and internal calibration. The data are of especial interest since the "a" and "c" dimensions obtained from this sample are about 1 per cent smaller than those given by WINKLER (1948). This brings the measured and X-ray densities into much better agreement, thus removing the puzzling discrepancy found by WINKLER.

The earlier inversion temperature of 972°C was found to be too high. A new

value of 848 $\pm$ 5°C is obtained by extrapolation of the equilibrium data under a few hundred atmospheres water pressure. The interpretation of these data is unequivocal. The p–t slope for the α–β reaction, 43°C/1000 atm was determined with some care and is shown in Fig. 1. This is based on some twenty-five successful runs, with the data shown in Table 2. A ΔH value based on this slope (and a ΔV calculated after allowing for the negative expansion of the high phase and an assumed expansion coefficient of 100×10^{-7} for the α-form taking $\rho_{hi} = 2.32$, $\rho_{low} = 2{\cdot}59$) may be obtained via the Clapeyron relationship. One obtains $\Delta H_{tr} = 3750$ cal/mole ($\pm$750 cal/mole) $LiAlSiO_4$. The quartz–coesite ΔH (a much cruder estimate) is about 450 cal/mole of Si_2O_4. In view of the enormous discrepancy between thermochemical and p–t values on the ΔH_{tr} for quartz–tridymite it would be very worthwhile to obtain thermochemical data on the high and low forms of eucryptite. The enthalpy of transition is rather high compared to, say, the *maximum* value for quartz–tridymite of about 550 cal/mole. Moreover, the experimental value does not agree with the "low" value predicted by Winkler (1954) on crystal chemical grounds. A fuller discussion of the data is deferred to a later paper.

The α–β spodumene inversion

Remarkable results were obtained at the spodumene composition. In several runs in sealed gold capsules at pressures up to 4000 atm we were unable to synthesize low or natural spodumene. It is quite certain that the hundreds of natural occurrences of spodumene were not formed at pressures of over several hundred atmospheres. Hence we have no good explanation for our failure. The only explanation at hand is the one that claims that some other ion such as Na^+, Fe^+ or F^- is necessary for spodumene formation (see Roy *et al.*, 1950), or that α-spodumene is metastable throughout the p–t range.

Instead of α-spodumene we did not obtain β-spodumene but rather the assemblage α-eucryptite + petalite. This assemblage was obtained consistently throughout the p–t range. Yet both these minerals are rare in nature while spodumene is very common.

Acknowledgement—This work was part of a programme on phase transitions supported by the National Science Foundation grant G-1000.

References

Brush G. J. and Dana E. S. (1880) On the mineral locality at Branchville, Conn. 4th Paper. *Amer. J. Sci.* **20,** 257–285.

Larsen E. S. (1921) The microscopic determination of non-opaque minerals. *Bull. U. S. Geol. Survey* No. 179.

MacDonald G. J. F., (1956) Quartz-coesite stability relations at high temperatures and pressures. *Amer. J. Sci.* **254,** 713–721.

Roy R. (1956) Aids in hydrothermal experimentation: II. Methods of making mixtures for both "dry" and "wet" phase equilibrium studies. *J. Amer. Ceram. Soc.* **39,** 145–146.

Roy R., Roy D. and Osborn E. F. (1950) Compositional and stability relationships among the lithium alumino silicates, eucryptite, spodumene and petalite. *J. Amer. Ceram. Soc.* **33,** 152–160.

Winkler H. G. F. (1948) Synthese and Kristallstruktur des Eukryptits, $LiAlSiO_4$. *Acta Cryst. Camb.* **1,** 27–34.

Winkler H. G. F. (1954) Struktur und Polymorphie des Eukryptits (Tief-$LiAlSiO_4$). *Heidel. Beitr.* **4,** 233–242.

Geochimica et Cosmochimica Acta, 1958, Vol. 15, pp. 218 to 228. Pergamon Press Ltd. Printed in Northern Ireland

The deuterium content of water in some volcanic glasses

Irving Friedman and Robert L. Smith
U.S. Geological Survey, Washington 25, D.C.

(*Received* 20 *May* 1958)

Abstract—The deuterium–hydrogen composition (relative to Lake Michigan water = 0·0) of water extracted from coexisting perlite and obsidian from eleven different localities was determined. The water content of the obsidians is generally from 0·09 to 0·29 per cent by weight, though two samples from near Olancha, California, contain about 0·92 per cent. The relative deuterium concentration is from −4·6 to −12·3 per cent. The coexisting perlite contains from 2·0 to 3·8 per cent of water with a relative deuterium concentration of −3·1 to −16·6 per cent. The deuterium concentration in the perlites is not related to that in the enclosed obsidian. The deuterium concentration in the perlite water is related to the deuterium concentration of the modern meteoric water and the perlite water contains approximately 4 per cent less deuterium than does the groundwater of the area in which the perlites occur. The above relations hold true for perlites from northern New Mexico, east slope of the Sierra Nevada, California Coast Range, Yellowstone Park, Wyoming, and New Zealand. As the water in the obsidian is unrelated to meteoric water, but the enclosing perlite water is related, we believe that this is evidence for the secondary hydration of obsidian to form high water content perlitic glass.

Introduction

This research problem is an outgrowth of the work on the water content of rhyolitic glasses by Ross and Smith (1955). At the outset of this study it was believed that any real understanding of the various physical and chemical properties of natural glasses must depend on a very thorough knowledge of their field relations. As our studies progress, it becomes more and more obvious that without this field control the analytical results are difficult or impossible to interpret and have little geologic significance. There are many types of volcanic glass, and the end-product glasses can commonly be formed by different processes. For example, obsidian can be formed by the chilling of a magma extruded on the surface, as in the chilled margin of a rhyolite flow; by the chilling of a magma at some depth, as in the chilled intrusive margin of a rhyolite dome; and as the result of the extreme welding of volcanic-ash fragments. Some of these obsidians can be differentiated only by their field relations.

Our work was begun on samples collected by Ross and Smith in the Valles Mountains of New Mexico, where the deuterium composition of the perlitic glasses is different from that of the obsidians. As a working hypothesis it was assumed that the perlites were obsidians hydrated by meteoric waters (Ross and Smith, 1955); it became necessary to obtain material for study from climatic environments other than New Mexico. It also became evident that the most suitable material for this research would be samples of perlite and obsidian from the same locality. Nature has been kind in this regard by providing perlite and obsidian in the same rock masses in some localities. These are the so-called obsidian–perlite pairs, which form the basis for this paper. We are currently studying all types of volcanic glasses, but the overall problem is so complex, and suitable material so

* Publication authorized by the Director, U.S. Geological Survey.

difficult to obtain, that conclusions drawn on any materials except the coexisting low-water obsidians and high-water perlites would be premature.

Discussion

The materials considered in this paper are, with the exception of material from two localities,* samples of obsidians and perlites of rhyolitic composition which occur together in the same rock body. This material consists of obsidian "cores" surrounded by perlite. The "cores", which at one time were commonly called "marekanite" from the type locality of Marekanka, Siberia, range in size from microscopic spheres to large angular to subrounded blocks 15 cm or more in diameter. These cores always have a hydrated outer surface, the maximum thickness of which seems to be approximately 50 μ on the smaller cores. The relation is well illustrated in the paper of Ross and Smith (1955). In the obsidian–perlite pairs that we have examined, the obsidian cores usually contain about 0·25 per cent water, while the surrounding perlite contains about 3 per cent water by weight. The term "marekanite" has no official standing either as a rock or mineral name. However, for our purpose it is a convenient term to use to characterize obsidians peculiar to the obsidian–perlite environment on which this study is based. We refer to this environment as the marekanite zone. This zone will be described more fully in a paper on the field relations of rhyolite domes and flows, but for the purpose of this paper it can be defined as a zone of shatter within a dome or flow. Fig. 1 illustrates some of this material in a rhyolite flow near Clear Lake, California.

The perlite has the same bulk chemical composition as the obsidian, with the exception of the higher water content. The perlite produced in the marekanite zone of rhyolite domes or flows always has a pearly lustre, which is partly due to concentric "onion skin" cracking and partly to subparallel shatter cracks. This zone is found in the transition between the region where the glass flows plastically and the region where the glass has solidified to the point where it is strong enough to remain rigid.

In this transition region, the semiplastic glass yields by both fracture and plastic flow, resulting in a region where the glass is highly fractured. Subsequent hydration then proceeds inwardly from these fracture surfaces. From an examination of many of the cores under the microscope, it is highly probable that the water enters the obsidian to produce a rim of hydrated glass containing about 3·0 per cent H_2O by weight. This hydration results in a change in volume of the glass, and the resulting strain pattern is easily visible under polarized light, where it contrasts with the weaker strain birefringence in the original unhydrated obsidian core. When the hydration proceeds to the point where the stress exceeds the strength of the hydrated glass, the strained rim cracks away (in an onion skin pattern) from the core, the strain in the hydrated rim is released (Fig. 2), and hydration continues on the glass surface.

* The samples from Steamboat Springs, Nevada, and from Yellowstone National Park, Wyoming, differ from all the other samples reported here, in that they do not represent obsidian and perlite from the same outcrop. However, they do represent obsidian and perlite from the same general area, and we have evidence that these samples may be considered in the same manner as the other samples.

To check this theory of the formation of perlite by secondary hydration, we determined the deuterium–hydrogen ratio of the water extracted from the glasses. In most cases, we were able also to obtain samples of modern meteoric water of the region. We realize that this modern water may, in some cases, not be representative of meteoric water of earlier geologic epochs, but it does give us a convenient starting point from which to work.

Experimental Procedure

Preparation of sample

For our deuterium analysis, it was desirable to choose a sample of sufficient size to yield between 3 and 10 mg of water upon fusion. For the average obsidian a 5 to 10 g sample was used for each determination. As perlite contains more water than does obsidian, a small sample of approximately 0·3 g was sufficient. Care was taken to select fresh, unaltered specimens, and the hydration rim present on many samples of obsidian associated with perlite was removed by grinding. To minimize the effect of surface contamination, several large pieces were selected for analysis and were introduced into the equipment without crushing or grinding.

Extraction of water

The sample, weighed to $\pm 0{\cdot}01$ g, was placed in a tall platinum crucible (J. Laurence Smith form, approximately 18 mm diameter $\times$ 80 mm long) and covered with a platinum lid. The covered crucible was inserted in a clear quartz tube (Fig. 3) which was then connected to a vacuum system. After reducing the pressure to about 10^{-5} mm of mercury, the sample was heated to 110°C by means of the water-cooled high-frequency induction heater work coil. During this degassing procedure, all gases evolved were pumped off and the pressure in the system seldom rose above 10^{-4} mm. This outgassing was continued until a negligible amount of gas was evolved in a 5 min period. It was found that a 15–30 min period was sufficient for obsidian, and about 1 hr for perlite.

After the vacuum system was degassed the fusion vessel was isolated from the rest of the vacuum system and the temperature of the crucible quickly raised to 700°C. The temperature was then slowly increased to reach $\sim$1450°C in $\frac{1}{2}$ hr and maintained at that temperature 15 min. The water evolved during the fusion was collected by condensing it in the trap (*C*) (Fig. 3). This trap was cooled with liquid nitrogen. At the end of the fusion period, the system was again connected to the vacuum system to pump off any noncondensable gas such as N_2 and H_2. Pumice commonly retained some gas (air?) which was pumped off at this time. The amount of such gas was in the range of from 10^{-1} to 10^{-4} cm^3 N.T.P., the larger amounts being evolved by pumice, while obsidian seldom gave over 10^{-4} cm^3 of noncondensable gas.

After the non-condensable gas was pumped off, the fusion tube was isolated from the system, the liquid nitrogen removed from around trap (*C*) and placed around trap (*E*). Trap (*C*) was allowed to heat to room temperature. The water condensed in this trap evaporated and the water vapour reacted with hot (600°C) uranium metal turnings contained in the Vycor trap (*D*). The hydrogen produced by the reaction, $U + 2H_2O \rightarrow UO_2 + 2H_2$, was continuously pumped off into a

Fig. 1. Marekanite zone in perlitic rhyolite flow, Clear Lake, Lake County, California (grey = perlite, black = obsidian).

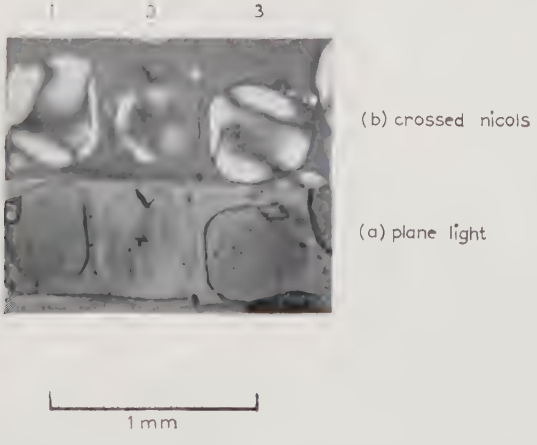

Fig. 2. Photomicrograph of hydration rims showing (1) marekanite with intact hydration rim; (2) marekanite with hydration rim cracked away, with loss of strain birefringence in rim; and (3) similar to (1), but with segment of earlier formed perlitic hydration rim still attached.

manometer (G) by the automatic Toepler pump (F). Any water vapour that passed through the uranium filled Vycor trap (D) was frozen in the liquid nitrogen cooled trap (E). At the completion of the reaction, trap (E) was warmed to room temperature and trap (C) cooled. By turning the appropriate stopcocks, the water vapour was made to pass over the uranium, and the hydrogen was pumped off as before. This process was continued until all of the water had reacted to produce hydrogen.

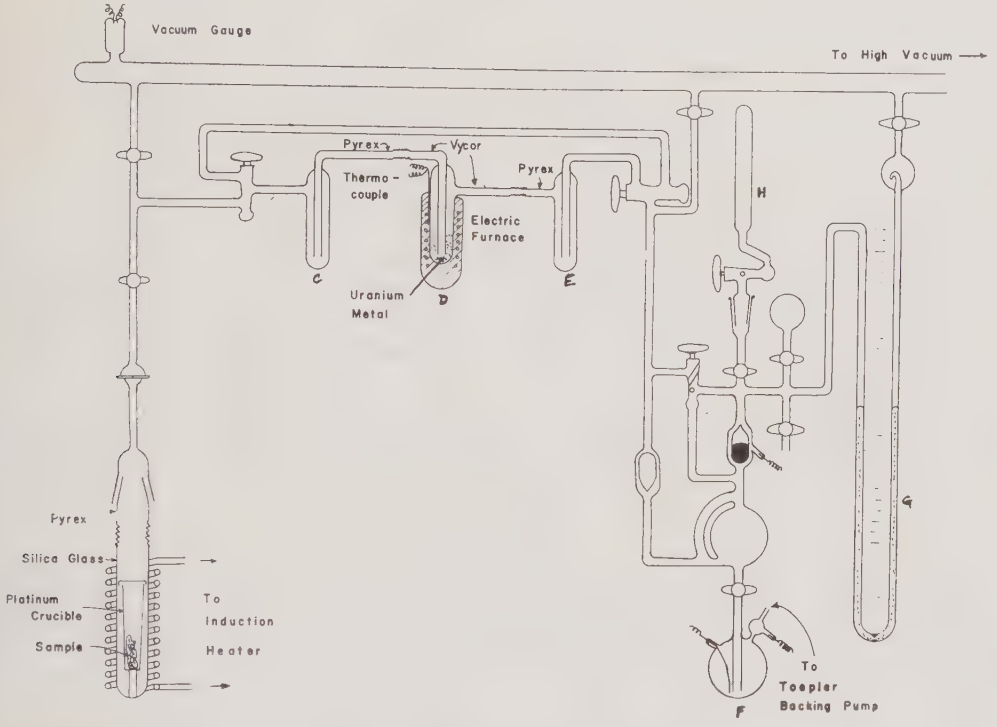

Fig. 3. Sample preparation line.

The hydrogen pressure was measured by the manometer. As the volume of the system was known, the volume of hydrogen, and ultimately the amount of water, could be calculated.

The combined error in weighing the sample and measuring the hydrogen results in an uncertainty in the percentage of water analysis of ± 5 per cent of the amount present. Although a more exact calibration of the volume of the manometer, plus weighing of the sample on a more sensitive balance, would have made possible a water determination accurate to less than 1 per cent of the amount present, it was decided that greater accuracy would have little interpretative value.

After reading the hydrogen pressure, the gas was then pumped out of the manometer into the previously evacuated gas sample tube (H). After all the hydrogen was pumped into the sample tube, the tube was removed from the sample preparation line and attached to the sample inlet system of the mass spectrometer.

Deuterium–hydrogen analysis

The D/H ratio in the hydrogen from the sample was compared to the D/H ratio in hydrogen prepared from a standard water sample. A description of the method has been published by one of the authors (Friedman, 1953), and the mass spectrometer used for the analyses reported in this present paper is very similar to the one described previously. Deuterium values are expressed as deuterium concentrations relative to the same standard Lake Michigan water that was used in that previous study.

The results are expressed, as a percentage:

$$\text{Relative deuterium concentration} = \Delta \text{ per cent} = \frac{\left(\frac{D}{H}\right) \text{sample} - \left(\frac{D}{H}\right) \text{standard Lake Michigan water}}{\left(\frac{D}{H}\right) \text{standard Lake Michigan water}}$$

A value of $\Delta = +5$ per cent indicates that the sample contains 5 per cent more deuterium than does the standard Lake Michigan water, while -5 per cent indicates that the sample contains 5 per cent less deuterium than our standard. Although we can repeat our results on samples of hydrogen gas prepared from duplicate water samples to $\pm 0{\cdot}1$ per cent, the error in these rock-water analyses is $\pm 0{\cdot}25$ per cent.

For purposes of interlaboratory comparison we obtained values for the National Bureau of Standards isotope reference samples (Mohler, 1955) nos. 1 and 1A, of $-0{\cdot}73$ and $-16{\cdot}45$ per cent, respectively.

Results

The results of the analyses of samples of obsidians and perlites are given in Table 1 and Fig. 4. Fig. 5 shows the distribution of deuterium in natural waters and in the rhyolite glass water, as compared with Lake Michigan water (approximately 0·0147 mole per cent D). Average deep ocean water is $+4{\cdot}0$ per cent enriched in deuterium relative to Lake Michigan water, and varies but slightly from place to place. In surface ocean water it varies from about $+5{\cdot}2$ to $+1{\cdot}3$ per cent, the high value being due to deuterium concentration in regions of high evaporation, and the low values to contamination with rain and glacial melt water. Rain varies from about $+5$ to -1 per cent depending upon the origin of the water vapour, the temperature of precipitation, and upon the previous history of the precipitating cloud system. Snow, in general, is lighter (depleted in deuterium), ranging from about -1 to -26 per cent.

The composition of meteoric water, therefore, varies between wide limits, owing first to variations in the original composition of the precipitation from which it was derived, and secondly to the varying enrichment in deuterium due to evaporation that it has undergone between the time of precipitation and the time it is examined.

To assess the influence of meteoric water on the rhyolitic glasses, we must examine the probable deuterium concentration in the meteoric water of various regions, including Iceland, northern New Mexico, east slope of the Sierra Nevada, California Coast Range, and New Zealand.

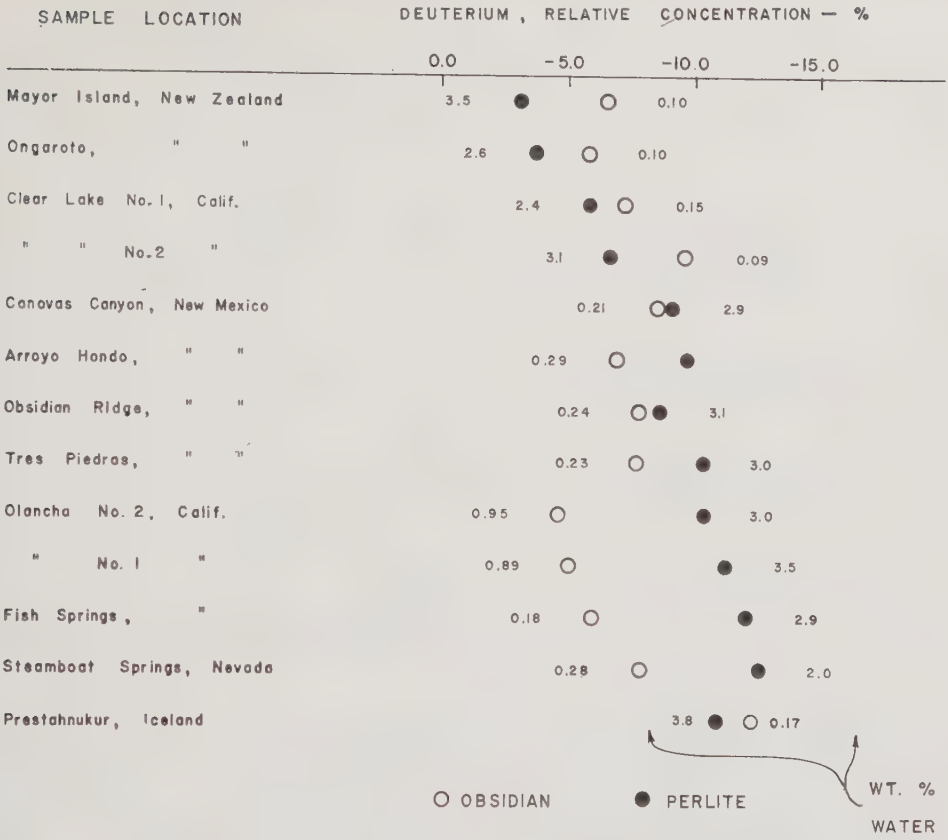

Fig. 4. Water and deuterium content of obsidian–perlite pairs.

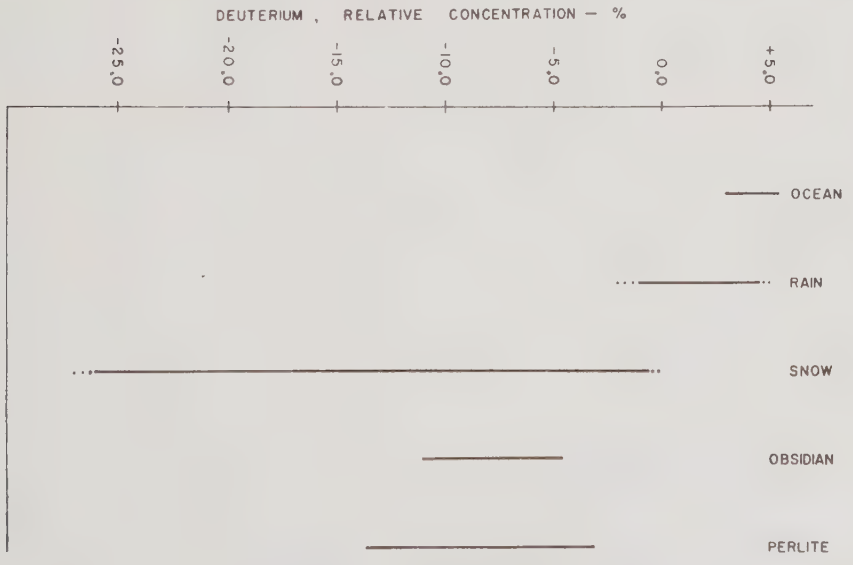

Fig. 5. Distribution of deuterium in natural waters.

Table 1. Water and deuterium content of obsidian and perlite pairs

Sample no.	Location	Age	Type of glass	H_2O (wt.%)	Deuterium (relative concentration %)
	North central New Mexico				
2-3a	Arroyo Hondo, Jemez quad., 35°41′30″ N, 106°34′30″ W	Pliocene?	obsidian	0·29	− 6·9
2-3b			perlite	2·7	− 9·7
20-2	Canovas Canyon, Jemez quad., 35°39′58″ N, 106°34′ W	Pliocene?	obsidian	0·21	− 8·5
20-1			perlite	2·9	− 9·1
36-5	Obsidian Ridge, Bland quad., 35°48′32″ N, 106°24′17″ W	Pliocene–Pleistocene	obsidian	0·24	− 7·8
36-6			perlite	3·1	− 8·0
36-3	Tres Piedras, 36°39′48″ N, 105°50′42″ W	Middle-late Tertiary	obsidian	0·22	− 7·5
36-4			perlite	3·0	−10·3
	East side Sierra Nevada				
65-4	Nevada, Steamboat Springs, 39°20′ N, 119°48′ W	Pliocene–Pleistocene	obsidian	0·28	− 7·8
65-3			perlite	2·0	−12·5
53-9	California, Olancha, Keeler quad., 36°20′ N, 117°50′20″ W (no. 1)	Pliocene–Pleistocene	obsidian	0·95	− 4·6
53-10			perlite	3·0	−10·3
37-16	California, Olancha, Keeler quad., 36°20′ N, 117°50′20″ W (no. 2)		obsidian	0·89	5·0
37-17			perlite	3·5	−11·2
29-8	California, Fish Springs, Big Pine quad., 37°03′17″ N, 118°17′49″ W	Pleistocene	obsidian	0·18	− 5·9
29-9			perlite	2·9	−12·0
	California, Clear Lake area				
52-21	Lower Lake, Sec. 16 and 17, T. 13 N 7W, M.D., 39°0′ N, 122°40′ W (no. 1)	Pleistocene	obsidian	0·09	− 9·6
52-22			perlite	3·1	− 6·6
42-5	Lower Lake, Sec. 16 and 17, T. 13 N, 7 W, M.D., 39°0′ N, 122°40′ W (no. 2)		obsidian	0·15	− 7·2
42-4			perlite	2·4	− 5·8

Table 1. Water and deuterium content of obsidian and perlite pairs (*continued*)

Sample no.	Location	Age	Type of glass	H_2O (wt.%)	Deuterium (relative concentration %)
	Yellowstone National Park, Wyoming				
39-2	Obsidian Cliff, 44°49′48″ N, 110°43′35″ W	Lower Pliocene?	obsidian	0·12	− 8·5
63-18			perlite	2·9	−16·6
	Iceland				
3024-3	Prestahnúkur, 64°35′15″ N, 20°42′ W	Pleistocene	obsidian	0·17	−12·3
3023-2			perlite	3·7	−10·9
70-9	*New Zealand* Mayor Island, North shore, 37°18′ S, 176°15′ E	Pleisto-cene–Recent	obsidian	0·10	− 6·5
70-10			perlite	3·5	− 3·1
70-11	Ongarato, central part of North Island, 38°23′ S, 175°56′ E	Pleistocene	obsidian	0·10	− 5·8
70-12			perlite	2·6	− 3·7

Precipitation west of the Sierra Nevada, California, is heavier (more deuterium) than that east of the Sierra, as the precipitating water vapour originates over the Pacific Ocean and loses deuterium preferentially as it proceeds inland. The meteoric water of the areas in New Zealand under consideration tends to be heavy, since it is derived from oceanic precipitation at relatively low altitudes. These tendencies are borne out by surface- and ground-water data (Table 2).

The Valles Mountains, New Mexico, samples of water are from one well and

Table 2. Deuterium content of ground and surface waters

Region	No. of samples	Deuterium (relative concentration %)	
		Range	Average
Greenland, icecap, 8000 ft	19	−16·6 to −26·4	−20·6
Greenland, ice, sea level	4	−12·3 to −18·1	−14·6
Iceland, Prestahnúkur	6	−3·1 to −5·5	−4·1
New Mexico, Valles Mountains	4	−3·4 to −5·1	−4·5
Wyoming, Yellowstone National Park	5	−10·0 to −15·0	−11·0
Nevada, Steamboat Springs	2	−8·4 to −8·6	−8·5
California, Clear Lake	3	−2·0 to −0·9	−1·3
New Zealand	4	+0·5 to −0·5	+0·0

three springs. The Yellowstone National Park, Wyoming, samples are snow and geyser water. The Clear Lake, California, data were obtained from well and surface run off samples. The New Zealand results were from Mayor Island rain and spring water samples, as well as North Island samples from two streams (Ongarato and Maroa). In all cases, the samples represent an approximation to the present meteoric water, but local and seasonal variations may be superimposed upon these data. However, the values given in Table 2 do show a definite regional trend.

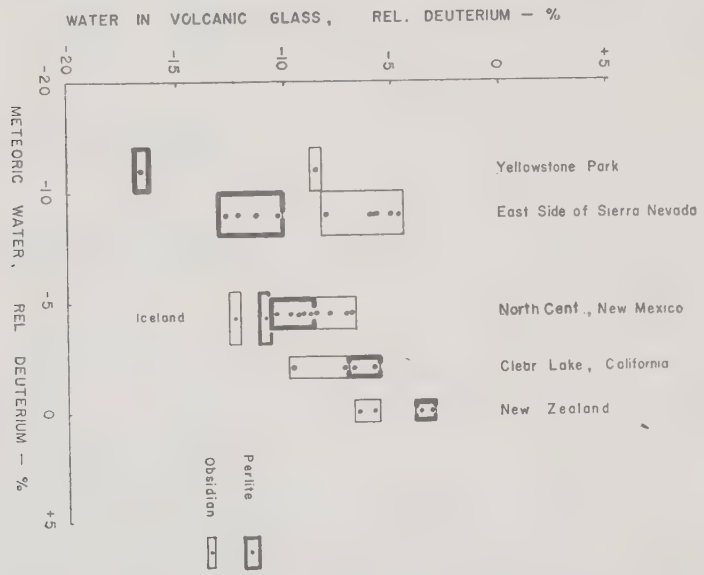

Fig. 6. Deuterium content of rhyolitic glasses related to meteoric waters (heavy rectangles = perlite; light rectangles = obsidian).

That this trend is also followed by the perlites can be seen in Fig. 6. The obsidians have no such trend (Fig. 6), a result that can be explained by either of two possibilities; first, that the water in them is unrelated to meteoric water, and secondly, that whatever the origin of the water, fractionation during the solution and exsolution of water in the magma and in the obsidian during it cooling history, has modified the isotopic composition of the water. Either or both possibilities might explain the random deuterium content of the obsidians.

The fact that the D/H ratio of the water in obsidians falls within a reasonably narrow range (—4·6 to —12·3 per cent) and is definitely lighter than ocean water is significant. Either a large isotopic fractionation occurred upon solution of heavier (sea) water in the magma, or the water is from another, possibly juvenile, source. If one makes this second assumption, the isotopic composition of this juvenile water is depleted in deuterium relative to present average surface water, and one is led to the conclusion that the earth must be losing hydrogen and concentrating deuterium on the surface. One must then assume that either the earth contained a large amount of hydrogen initially, either as free hydrogen or as methane, or that oxygen as well as hydrogen may be escaping. H. C. Urey (personal communication, 1956) has suggested a possible mechanism for the

escape of free oxygen from the earth, since oxygen absorbs radiation in the far ultra-violet, and this energetic radiation would give the absorbing atom enough energy to escape from the outer atmosphere.

The D/H variation in the water in perlite is then interpreted to be due to the fact that this water is secondary and probably mainly of meteoric origin. This is reflected in the wide variation in isotopic composition and in the correlation of isotopic composition with isotopic composition of meteoric waters of the region

Table 3. Relation of deuterium content of perlite to meteoric waters

Region	Deuterium (relative concentration %)		
	Estimated meteoric	Average perlite	Difference
Iceland	−4·1	−11·0	~6·9
New Mexico, north central	−4·5	−9·5	5·0
Wyoming, Yellowstone National Park	−11·0	−16·4	5·4
Nevada, Steamboat Springs	−8·5	−12·5	4·0
Sierra Nevada, east side	−6	−10·8	~4·8
California, Clear Lake	−1·3	−6·6	5·3
New Zealand	0·0	−3·4	3·4

where the material is found. As can be seen from an examination of Table 3, the water in the perlites is approximately 4 per cent depleted in deuterium compared to the meteoric water of the region. This, then is the probable magnitude of the fractionation that occurs when obsidian hydrates to form perlite, uncorrected for any secular change in the isotopic composition of meteoric waters during or since the hydration of the glasses. As the New Zealand area has probably changed least in this respect, 3·5 per cent is probably closest to the true fractionation factor for this reaction.

This fractionation only applies to the water that is loosely bound by the glass and that can be removed by short-term heating below approximately 600°C (Ross and Smith, 1955, p. 1078). The up to ~0·35 per cent water that is tightly bound (Si–OH bonding?) and that is only removed by heating to more than 700°C may have a different deuterium-fractionation coefficient. This is the water that is present in obsidian and remains in the perlite after hydration. While little can be said at this time on the structure of these glasses, the authors are engaged in research into the influence of the volatile content on the physical properties of volcanic glasses and hope that some light will be thrown on the mode of bonding of volatiles in these materials.

The Iceland samples seem to be an exception to our thesis. However, we believe that they are the exception that proves the rule. The fact that the water in the Pleistocene Iceland perlite differs by about 7 per cent from present day meteoric water, suggests that complete exchange between the perlite water and present

day meteoric water has not occurred. From other data we believe that the deuterium content of the meteoric water in Iceland has not changed greatly for the past 5000 to 8000 years.

This time then was insufficient for much exchange to take place. The authors believe that, in general, isotopic exchange between the water in a hydrated rhyolitic glass and water in contact with the glass to be exceedingly slow at surficial temperatures.

Iceland has recently emerged from under an icecap. The climatic regime at the time when the Prestahnúkur glasses began hydrating was probably similar to that in present-day Greenland. The deuterium content of Greenland ice and snow is given in Table 2. From the isotopic data of the Iceland perlites, and assuming a fractionation of 3·5 per cent, a value of $\sim -7{\cdot}5$ would be expected for the meteoric water at the time hydration occurred. Since hydration began with the emplacement of the rock and is proceeding up to the present, this value of $-7{\cdot}5$ represents a mixture of waters varying from icecap water of approximately -14 to present-day water of -4.

None of the other localities covered in this paper has undergone such a great change in climate during the hydration history of the glass found there. The New Zealand localities have always had an oceanic type climate, with precipitation occurring at relatively high wet-bulb temperatures. Northern New Mexico has, since the Miocene at least, been sheltered from maritime air by mountain ranges to the west and south-west and primary precipitation has occurred at low wet-bulb temperatures. (Primary precipitation is here differentiated from locally recycled water as, for example, local air-mass thundershowers. It refers to the major amount of water brought into the region.) The same is true of Yellowstone Park. The east slope of the Sierra Nevada has been similarly sheltered since the Sierra Nevada uplift, at least since late Tertiary time. The deuterium content of the meteoric waters in these regions should not have changed appreciably since the glass was formed.

Acknowledgements—The authors are indebted to T. Sigurgeirsson and T. Tryggvason of Rannsoknarad Ríkisins (The National Research Council) of Iceland; F. R. Boyd of the Geophysical Laboratory of the Carnegie Institution of Washington; to C. W. Chesterman of the California State Division of Mines; D. E. White, and especially to R. A. Bailey of the U.S. Geological Survey. Mr. Bailey, who has spent several seasons in New Mexico in the field with Ross and Smith, kindly collected critical samples in New Zealand.

The authors would also like to thank C. S. Ross for encouraging the research, and for his many stimulating discussions of the problem. A great is debt due to Beatrice Schoen for her assistance with the laboratory work.

This work is part of a programme being conducted by the U.S. Geological Survey on behalf of the Division of Research of the U.S. Atomic Energy Commission.

References

Friedman I. (1953) Deuterium content of natural water and other substances. *Geochim. et Cosmochim. Acta* **4,** 89–103.

Mohler F. L. (1955) Reference samples of isotopic abundance. *Science* **122,** 334–335.

Ross C. S. and Smith R. L. (1955) Water and other volatiles in volcanic glasses. *Amer. Min.* **40,** 1071–1089.

Geochimica et Cosmochimica Acta, 1958, Vol. 15, pp. 229 to 236. Pergamon Press Ltd. Printed in Northern Ireland

On radioactive uraniferous iron oxides

M. D. Karkhanavala
Chemistry Division, Atomic Energy Establishment,
Trombay, Bombay

(*Received* 15 *April* 1958)

Abstract—A study has been made of uranium bearing iron oxides from the shear-zone of Bihar, with particular reference to the nature of the association of uranium with magnetite and hematite. In veins where none or very little hematitization has taken place, the primary magnetite and uraninite coexist. Where hematitization has taken place the uranium is very intimately associated with the hematite, probably as a very limited solid solution. A sample of hematite containing uranium equivalent of 0·15 per cent U_3O_8 was found to be metamict, the reconstitution of which was established by X-ray and differential thermal analysis methods.

It is believed that a primary oxidizing solution containing uranyl ions caused the oxidation of the ferrous hydrosol to magnetite and the simultaneous precipitation of uraninite. A later stage oxidizing solution or normal agents of weathering converted the magnetite to hematite and the uraninite to probably U_3O_8 or UO_3, a small amount of which was then somehow taken up in the hematite lattice, and the rest being converted to secondary uranium minerals, the presence of which is known.

I. Introduction

The occurrences of iron oxide containing small percentages of uranium are widespread (McKelvey, Everhart and Garrels, 1956). They are of magmatic origin occurring as veins formed by filling of open cavities and foliation planes and of hydrothermal and metasomatic origin. With the discovery of such deposits in the shear zone of Bihar, interest was aroused in the nature of the association of uranium with iron. During the preliminary studies by the Ore Dressing Section of this Establishment, it was observed that different percentages of the original radioactivity were being retained in the iron oxide fractions, and that in certain cases this activity could not be separated by usual ore dressing procedures. The present study was therefore initiated to try and elucidate the nature of this association, inasmuch as it would influence the subsequent chemical and physical treatments.

II. Review of Literature

Several hypotheses have been proposed concerning the paragenesis of such deposits. There is more unanimity of opinion regarding the paragenesis than the nature of the association of iron and uranium oxides. It is generally believed that the iron and uranium were introduced at about the same geologic time, and that the uranium was fixed during the oxide phase of mineralization.

Lovering (1955) assumes that uranium minerals dissolve in acid sulphate waters—formed, as for example when pyrite in the absence of H_2S and carbonaceous matter breaks down to ferrous sulphate and sulphuric acid—and are carried as uranyl ions or as uranyl sulphate complex. When these waters become neutralized, iron hydrolyses to form colloidal ferric oxide hydrate, which together

with any colloidal silica, coagulates out; the uranyl ions are probably adsorbed on the colloidal particles and removed from the solution. As the hydrate crystallizes to form goethite, uranium is excluded from the structure and forms secondary uranium minerals scattered through the limonite. According to Lovering uranium or uranium minerals are rarely associated with secondary hematite. On the basis of the older values of the ionic radii of uranium ions, he has concluded that uranium cannot replace or take part in the lattice of iron oxides.

Walker and Osterwald (1956) picture a two-stage process. They support Shand's (1947, pp. 191–192) view that the magnetite was laid down by the self-oxidation of the hydrosol $Fe(OH)_2$:

$$3Fe(OH)_2 = Fe_3O_4 + 2H_2O + H_2 \qquad (1)$$

when the alkalis in solution were extracted from a crystallizing magma rich in alkalis. These magnetite deposits were then affected by late stage solution from a granitic magma that gave out copper, lead, zinc and silver sulphides, oxidized magnetite to hematite, and "deposited pitchblende around pieces of hematized magnetite." They believe that since the spinel (magnetite) lattice can accommodate various ions like Cu, Cd or Zn in the interstices, uranium in sixfold coordination may substitute for these ions and thereby occur "as an impurity in the interstices of the magnetite lattice."

Because of the very uniform distribution of the uranium in the iron oxide McKelvey *et al.* (1956) and Surazhasky (1956) favour the hypothesis that pitchblende and hematite were coprecipitated during the coagulation of the hydrosol when acted upon by a solution containing uranyl ions:

$$3H_2O + 2Fe^{2+} + (UO_2)^{2+} \rightarrow Fe_2O_3 + U^{4+} + 3H_2O \qquad (2)$$

The feasibility of equation (2) has been demonstrated by Naumov and Tobelko (1956), who synthesized uraninite by reacting $Fe(OH)_2$ and a U^{6+} compound in sealed glass ampoules in a nitrogen atmosphere at 150°–200°C in a slightly alkaline medium.

The last hypothesis finds some support in the explanation given by Walker and Osterwald (1956) for the association of uranium with the oxide phase and not with the sulphide phase in the ore. They attribute this occurrence as probably due to the "differences in the sols of the two phases" and add that "metals and metallic sulphides form negatively charged sols in systems with water as the dispersion medium, whereas the sols of the metallic hydroxides are positively charged. It may be that uranium was in the form of positively charged particles, which were coprecipitated with the oxide and not with the related sulphides."

This explanation however is not very clear, because according to the well-known Schulze–Hardy rule for the precipitation of sols, an ion is effective in bringing about coagulation if it is opposite in sign to that of the colloidal particle; coagulating power increases considerably with increasing charge of the ion. It may therefore be that the real reason why uranium occurs with the oxide phase is that at the time of precipitation the uranyl ions were not present as free positive ions, but had perhaps formed, as is now known (Arden and Wood, 1956) negatively charged complex with the sulphate ions.

III. Experimental

(a) *Samples used.* Since this study was primarily aimed at elucidating the nature of the association between uranium and iron oxides, only the ferruginous portion of the ores was studied. The ore samples, though from different localities were all from the shear zone of Bihar. In some cases, both the surface, and the drill-core samples from the same locality were available. The description of the ore body and the colour of the sample separated therefrom are tabulated in Table 1, arranged according to increasing uranium content of the sample.

Samples 1 to 6 represent the products obtained after further cleaning in a wet magnetic separator of the Davis tube type, the magnetics being obtained in the usual dry magnetic separation of a gravity concentration product. Sample 7 was obtained by flotation of the iron oxides. These samples as supplied by the ore dressing section after the treatments mentioned, were all −300 mesh, and hence were used for all subsequent studies without any further grinding.

Table 1. Description of samples

Sample No.	Locality	Description of ore body	Colour of sample
1	A	quartz–biotite schist	black
2	B	apatite–magnetite rock	black
3	C	magnetite–quartzite	black
4	D	quartz–biotite schist (bore-hole core sample)	black
5	E	magnetite–quartzite	brownish black
6	D	same as (4) outcrop sample	dark brown
7	F	gossan of hematite–quartzite	pale brown

(b) *X-ray powder analysis.* Power diffraction patterns were obtained in a G.E. 144 mm powder camera, with filtered Fe$K\alpha$-radiation at 30 kV and 10 mA. The Straumanis–Ievins asymmetric method of film mounting was used. Film shrinkage correction was calculated from a standard pattern of pure calcite obtained under identical conditions.

(c) *Differential thermal analysis (D.T.A.).* An automatic recording D.T.A. apparatus incorporating a Honeywell–Brown Program-Controller-Recorder and a Differential Millivolt Recorder used. The apparatus was essentially similar to the one described by Gruver (1948). Twenty-four s.w.g. chromel and alumel wires were used for the measuring and the differential couples. A heating rate of 400°C/hr, was maintained.

IV. Results

The X-ray patterns indicated that all the samples were essentially mixtures of magnetite and hematite in different proportions. The percentages of the hematite and magnetite in the mixture was estimated by visual comparison of the line intensities. The results of such an estimate, together with the uranium content (measured as U_3O_8 by radiometric assay) for the various samples are given in Table 2.

Table 2. The estimated magnetite and hematite contents and the measured U_3O_8 percentage

Sample No.	Estimated content of			Remarks
	Magnetite (%)	Hematite (%)	U_3O_8 (%)	
1	almost pure	not detected	0·001	very strongly magnetic
2	almost pure	not detected	0·025	very strongly magnetic
3	about 80	about 10	0·04	moderately magnetic
4	about 65	about 25	0·06	weakly magnetic
5	about 50	about 40	0·11	feebly magnetic
6	about 20	about 70	0·15	very feebly magnetic
7	about 10	about 85	0·29*	very very feebly magnetic

* The pattern of this sample was rather weak and showed the presence of chiefly lepidocrocite, with some amounts of goethite, hematite and magnetite. The "hematite" content in this case was taken as the approximate sum of lepidocrocite, goethite and hematite, and was estimated from the X-ray pattern obtained after heating the sample to 1000°C in an inert atmosphere.

V. Discussion

The fact that X-ray diffraction lines of hematite were absent in samples 1 and 2 does not rule out the occurrence of free hematite in amounts less than about 7 per cent. It is evident that the uranium content (expressed as U_3O_8) increases with increasing hematite content. There must therefore exist a preferential association of uranium with hematite rather than with magnetite. That such a close association does exist is clear from the following:

(1) In the "D" district, because of a major thrust, the schists have recumbent closed folds resulting in a surface outcrop and a core. Samples 4 and 6 represent respectively the magnetic portions of a sample from the deep seated unweathered schist obtained from a bore-hole, and of a sample from the outcrop. In the core sample magnetite is predominant indicating a very partial hematitization, and the uranium content is also low, 0·04 per cent U_3O_8. In the outcrop sample, hematitization is nearly complete and the activity is largely concentrated in this fraction.

(2) Not only is the activity concentrated along with the hematite in this sample, but the hematite in it is distinctly metamict, the discovery of which was reported earlier (Karkhanavala, 1956). This was established from X-ray patterns of the original sample-6 and the heat-treated sample shown in Fig. 1. It is further substantiated from the D.T.A. curve (a) shown in Fig. 2. The broad endothermic peak in the region of 75–150°C is due to the loss of water, mainly adsorbed, and the broad exotherm from about 780–1100°C is due to the slow release of the extra energy stored in the metastable metamict lattice as it reverts to the stable hematite lattice of lower energy.

Since sample 6 contains 0·15 per cent U_3O_8 equivalent was metamict, sample 7, containing uranium equivalent of 0·29 per cent U_3O_8 could also be expected to be metamict. In this case, since the hydrated oxides predominated, it was not possible to ascertain whether the weakened and diffused front-reflection X-ray pattern obtained was due to the poorly crystallized hydrates alone or due to metamictization also. The X-ray pattern of the sample after heating to 1000°C

(a)

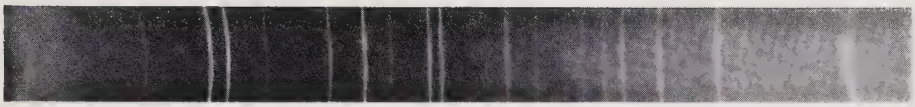

(b)

Fig. 1. X-ray powder pattern of (a) original metamict, and (b) heat-treated sample No. 6.

was quite sharp and was essentially that of hematite. The hematite content of this sample was estimated from this latter pattern.

The nature of this sample is more evident from its D.T.A. curve shown in Fig. 2(b). Apart from the low temperature (70–150°C) loss of absorbed water, the curve shows the characteristic endotherms of lepidocrocite–goethite mixtures in the region 250–390°C and a weak exotherm at about 400°C, corresponding to the $\gamma Fe_2O_3 \rightarrow \alpha Fe_2O_3$ phase transformation. At higher temperatures, it shows a weak but distinct exotherm at about 800°C, indicating that the metamict substance is

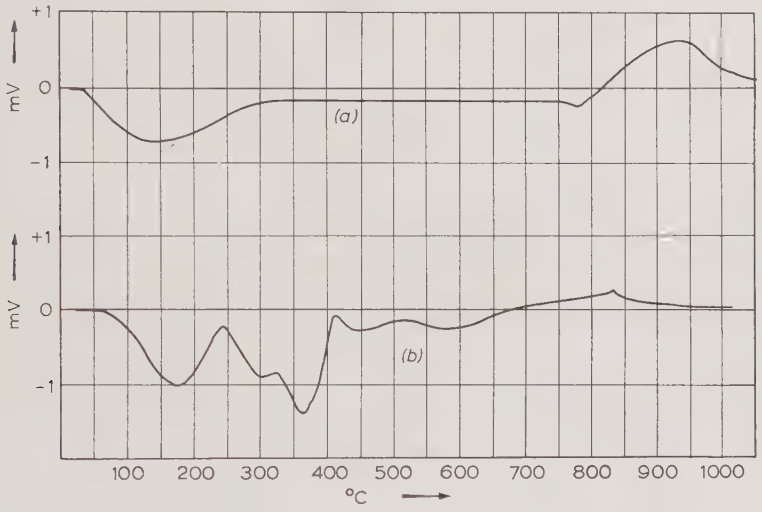

Fig. 2. D.T.A. curves of (a) sample No. 6 and (b) sample No. 7.

present only in small amounts. It is therefore attributed to the small amount of hematite originally present. It is unlikely that either lepidocrocite or goethite could be metamict as in that case a stronger exotherm would have been obtained. Also these hydrates are often so poorly crystallized to begin with, that no assertion can be made as to the extent of radiation damage to their crystal lattice.

(3) A flotation technique primarily aimed at concentrating the iron oxides in samples 6 and 7 also concentrated almost all of the uranium obviously because of its close association with hematite; similar procedures in case of samples 1 and 2 did not yield such a concentration. This is noteworthy since samples 1 and 6 are from essentially similar rocks with comparable mineral composition.

(4) The difference in the behaviour of samples from essentially similar rocks in localities "A" and "D" reflects the fundamental difference in the nature of association of uranium with iron. In the depth samples (1 and 4), where little hematitization had taken place, it was possible to isolate a substantially pure magnetite exhibiting a sharp X-ray diffraction pattern even in the back-reflection regions. The uranium content was very low, and even this was could be attributed to the minute quantities of non-magnetic inclusions traceable petrologically.

In the high grade uranium concentrate of these samples, obtained by successive gravity treatments, the gangue minerals (tourmaline, quartz, apatite and some

zircon) were found from auto-radiographs to be non-active. The uranium mineral isolated from these non-magnetics was identified as uraninite by chemical analysis and leaching characteristics (Bhatnagar, 1957) and by petrographic and X-ray power diffraction methods.

In the case of sample 6, drawn from the altered zone of locality "D", where extensive hematitization had taken place, no such separation of a uranium mineral from the active iron oxide was possible.

It can safely be concluded therefore that at least in the case of the samples studied where the primary magnetite has not been oxidized, primary uraninite coexists and gets associated with the hematite during hematitization. These results do not substantiate the views of Walker and Osterwald (1956) that the uranium is entrapped in the interstices of the magnetite lattice, but clearly indicate the coexistence of magnetite and uraninite, the latter being uniformly distributed throughout the ore body as very fine grained dissemination.

Origin of Deposits

This coexistence of the two primary minerals magnetite and uraninite in veins which have not been subjected to the influence of further oxidizing agents as also the very fine grained, and uniform distribution of uraninite, in magnetite, lead one to believe that both were coprecipitated. This can be visualized by a slight modification of the views of McKelvey *et al.* (1956) and of Surazhasky (1956). It may be that because of conditions then existing the primary ferrous hydrosol instead of being fully oxidized by uranyl ions in a solution to hematite was oxidized to magnetite with the simultaneous precipitation of uraninite. Such a reaction could explain the occurrence of magnetite and uraninite in close juxtaposition.

It is more difficult however to account for the very close, almost chemical association of uranium with hematite. It is very unlikely that in this association uranium is present as uraninite UO_2 because (a) there is a very large difference in the ionic radii of Fe^{3+} and U^{4+} (Table 3), and (b) hematite and uraninite crystallize in different crystal systems, and (c) any weathering agent that altered magnetite to hematite, would also probably convert the UO_2 to either UO_3 or U_3O_8.

The relative reactivity of magnetite and uraninite towards different weathering agents would necessarily play an important part in the selective oxidation but the heats of formation (ΔH_f 298·16°) of hematite from magnetite and of U_3O_8 and UO_3 from UO_2 are very similar:

$$2Fe_3O_4 + \tfrac{1}{2}O_2 = 3Fe_2O_3 - 94{\cdot}7 \text{ kcal/mole}$$

$$3UO_2 + O_2 = U_3O_8 - 88 \text{ kcal/mole}$$

$$UO_2 + \tfrac{1}{2}O_2 = UO_3 - 96 \text{ kcal/mole}$$

These values of ΔH_f 298·16° are calculated from those listed (Rossini, 1952) for the formation from the elements of Fe_3O_4, Fe_2O_3, UO_2, U_3O_8, and UO_3. If it is assumed that simultaneously with the oxidation of magnetite to hematite, uraninite was also oxidized either to U_3O_8 or to UO_3, then a closer association with hematite is more probable.

On the basis of the older ionic radii of uranium and iron, Lovering (1955) had

assumed that uranium cannot substitute for iron in the space lattice of goethite and presumably also of hematite. However, if the more recent values of AHRENS (1952) are accepted (Table 3), then a very limited substitution by U^{6+} is not entirely improbable.

Table 3. Ionic radii and radius ratios (w.r.t. $R_0 = 1{\cdot}40$ Å) of iron and uranium (after AHRENS, 1952)

Ion	Ionic radius R_c	Radius ratio R_c/R_0
Fe^{2+}	0·74	0·53
Fe^{3+}	0·64	0·46
U^{4+}	0·97	0·69
U^{6+}	0·80	0·57

Hematite crystallizes in the hexagonal system—space group $D^6_{3d} = R^-_{3c}$ with cell parameters $a = 5{\cdot}029$ and $c = 13{\cdot}73$ kX (ROOKSBY, 1951, p. 258). U_3O_8 has been shown by SIEGEL (1955) and by HOEKSTRA *et al.* (1955) to exist in two forms, orthorhombic and hexagonal. The latter modification is stable above about 400°C and has cell dimensions $a = 6{\cdot}801$ and $c = 4{\cdot}178$ kX; space group $P_3^- = C^1_{3i}$. α-UO_3 also crystallizes in the hexagonal system, space group $D^3_{3d} = C^-_{3m}$ with cell parameters $a = 3{\cdot}963$ and $c = 4{\cdot}160$ kX (ZACHARIASEN, 1948). UO_2 on the other hand crystallizes in the cubic system—space group C^5_h–F_{m3m}; $a = 5{\cdot}4682$ Å (SWANSON and FUYAT, 1953); it is thus a very different type from hematite. In the hematite lattice, the oxygen ions are arranged in approximately hexagonal close packing and the Fe^{3+} ions fill the interstices leaving every third interstice vacant (BRAGG, 1937, p. 95). Also each Fe^{3+} ion is surrounded by three oxygens at a distance of 1·91 Å and three others at 2·06 Å (WYCKOFF, 1948). In U_3O_8 the uranium oxygen distances are: $U_I—60_I = 2{\cdot}31$ Å; $U_{II}—60_I = 2{\cdot}31$ Å and $U_{II}—20_{II} = 2{\cdot}06$ Å and in UO_3 they are: $U—20_I = 2{\cdot}08$; $U—60_{II} = 2{\cdot}39$ Å. It may therefore happen that a very small amount (not exceeding 0·5 per cent) of U_3O_8 or UO_3 might be taken up in the hematite lattice, with one U^{6+} substituting for two Fe^{3+} to maintain electrostatic balance. The remainder of U_3O_8 or UO_3 which could not be taken up in the hematite lattice would be converted to distinct secondary uranium minerals, the presence of which has been known in the outcrop.

The occurrence of hematite in the metamict state also favours the existence of uranium within the lattice, as it would then be possible that the constant and prolonged bombardment by α-particles from within would cause sufficient disorder, thereby at least partially destroying the long-range order and rendering the mineral metamict. According to the accepted conditions for metamictization (PABST, 1952) magnetite should structurally be more susceptible to radiation damage than hematite. Yet, in spite of the coexistence of magnetite and uraninite, no sample of magnetite was found to be metamict. This is because the magnetite lattice was not subjected to bombardment from within, while the less susceptible hematite lattice was.

It was not possible to prove the existence of a solid solution of uranium in

hematite from a study of the natural samples, because even the sharpest X-ray powder diffraction lines were too broad for precision determination of the cell constants. Also because of the opaque nature of the samples normal petrography techniques could not be used to prove this assumption. A study of artificial mixtures of hematite, magnetite, uraninite and U_3O_8 reacted under dry and hydrothermal condition has, therefore, been undertaken; the results of these will be published later.

The occurrence of large amounts of lepidocrocite in the gossan sample from locality "F" is interesting. It is stated by Rooksby (1951) that lepidocrocite (γ-$Fe_2O_3 \cdot H_2O$) is the crystal form obtained by the oxidation of ferrous compounds, while goethite is the form produced by the ageing of hydrous basic ferric oxides. γ-Fe_2O_3 is cubic, possesses a defect spinel structure and is obtainable by dehydration of the γ-hydrate at about 390°C. Readsorption of water to form the hydrate, is not known. It would be of value to know how in this particular case lepidocrocite was formed together with associated goethite, hematite and magnetite. Magnetite is known to oxidize at low temperatures (about 200°C) into γ-Fe_2O_3, which at 400°C to 500°C irreversibly alters into α-Fe_2O_3. But whether such a stepwise oxidation of the magnetite took place and the γ-hydrate formed from the γ-oxide or directly is not known. It is also not known whether the radioactivity is associated with the hematite alone or is distributed among the hydrates also.

Acknowledgements—The samples used for this study were made available by the Ore Dressing Section and the Raw Materials Division, to whom the author's thanks are due. The author is also indebted to Dr. R. Krishnaswamy, Mr. G. R. Udas and Mr. D. V. Bhatnagar for very useful discussions and suggestions.

References

Ahrens L. H. (1952) *Geochim. et Cosmochim. Acta* **2,** 155.
Arden T. V. and Wood G. A. (1956) *J. Chem. Soc.* 1596.
Bhatnagar D. V. (1957) *Proc. 44th Indian Sci. Cong., Section of Geology,* Abs. No. 55.
Bragg W. L. (1937) *Atomic Structure of Minerals.* Cornell.
Gruver R. M. (1948) *J. Amer. Ceram. Soc.* **31,** 323.
Hoekstra H. R., Siegel S., Fuchs L. H. and Katz J. J. (1955) *J. Phys. Chem.* **59,** 136.
Karkhanavala M. D. (1956) *Curr. Sci.* **25,** 303.
Lovering T. G. (1955) *Econ. Geol.* **50,** 186.
McKelvey V. E., Everhart D. L. E. and Garrels R. M. (1956) *Proc. Int. Conf. Peaceful Uses of Atomic Energy, Geneva, 1955* Vol. VI, p. 551. United Nations.
Naumov G. B. and Tobelko K. I. (1956) *Geokhimiya* **4,** 24.
Pabst A. (1952) *Amer. Min.* **37,** 137.
Rooksby H. P. (1951) *X-Ray Identification and Crystal Structures of Clay Minerals* Chap. 10. Mineralogical Soc., London.
Rossini F. D. (1952) *Selected Values of Chemicals Thermodynamic Properties.* N. B. S. Circular 500, Washington D.C.
Shand S. J. (1947) *Eruptive Rocks.* John Wiley, New York.
Siegel S. (1955) *Acta Cryst.* **8,** 617.
Surazhasky D. Ya. (1956) *Atomnaya Energiya* **2,** 221.
Swanson H. E. and Fuyat R. K. (1953) *Standard X-ray Diffraction Powder Patterns.* N.B.S. Circular No. 539, Vol. II, Washington D.C.
Walker G. W. and Osterwald F. W. (1956) *Econ. Geol.* **51,** 213.
Wyckoff R. W. G. (1948) *Crystal Structures* Vol. I. Interscience, New York.
Zachariasen W. H. (1948) *Acta Cryst.* **1,** 265.

Geochimica et Cosmochimica Acta, 1958, Vol. 15, pp. 237 to 254. Pergamon Press Ltd. Printed in Northern Ireland

Marine geochemistry of germanium and the origin of Pacific pelagic clay minerals*

S. A. El Wardani
Scripps Institution of Oceanography, La Jolla, California†

(*Received* 7 *April* 1958)

Abstract—The germanium content of sea water was found to be 0·05 μg/l. The most abundant organisms of sea water do not take up detectable amounts of germanium. Globigerina ooze and siliceous sponges are devoid of germanium. Diatom frustules may contain some 0·4 p.p.m. germanium. The Pacific northeast equatorial eupelagic clays contain 2 p.p.m. germanium in contrast to shelf material and the south equatorial eupelagic clays, which contain 1 p.p.m. germanium.

Shelf sediments and pelagic clays have an identical germanium content of 1 p.p.m. for their coarse fractions while the clay-mineral size fraction of the Pacific north-east equatorial eupelagic clays has a germanium content at least twice the value for the same fraction of the Pacific south equatorial pelagic clays, shelf sediments, and standard marine clay minerals which have been reported to contain 1 p.p.m. germanium.

The aluminosilicates are primarily responsible for the germanium content of the clays, and partial removal of the element from sea water appears to take place during the hydrogenous growth of such minerals in sea water. The geochemical fractionation of the element between the shelf and deep-sea sediments and their abundant minerals suggests that shelf sediments and the Pacific south equatorial pelagic clays are primarily lithogenous in origin. On the other hand, the Pacific north-east equatorial eupelagic clays have a coarse fraction which is primarily lithogenous in origin and a clay-mineral size fraction which is rich in hydrogenous clay minerals.

I. Introduction

Knowledge of the fractionation of trace elements in Nature can aid not only in understanding the geochemical path and behaviour of such elements but in shedding light on important questions pertaining to more general earth-science problems. The object of the present work was to investigate the distribution of germanium in the marine environment by analysing for the element in sea water, in its more abundant organisms, and in related sediments and their mineral components. Because of close similarity of the ionic radii of Ge^{+4} and Si^{+4}, 0·53 Å and 0·42 Å respectively (Ahrens, 1952), emphasis was placed on silica and aluminosilicates deposited from sea water which may be enriched in germanium. From the observed distribution of germanium, inferences have been drawn during this study concerning the nature and source material of recent marine sediments. This paper also presents geochemical evidence for the hydrogenous growth of clay minerals from sea water.

II. Earlier Work

Our knowledge of the state and behaviour of germanium in the ocean during processes of weathering and sedimentation is only speculative. Bardet (1938)

* Present mailing address: Department of Oceanography, University of Washington, Seattle 5, Washington.

† Contribution from the Department of Oceanography, University of Washington.

reported spectrographic evidence for the presence of germanium in sea water. The Noddacks' (1939) estimate of 10^{-4} p.p.m. germanium in sea water is not based on actual analysis. Their spectrographic data included the analyses of some marine animals for which they presented values of 0·07 to 2·2 p.p.m. germanium. In a single analysis, Goldschmidt (1933) reported a deep-sea red clay (Challenger Expedition, Station 353) as having 3·5 p.p.m. germanium.

III. Analytical Method

A spectrophotometric method was used in which germanium is determined as the phenylfluorone germanium complex. Sedimentary material (0·2–0·5 g 100-mesh) was dissolved in hydrofluoric acid in a platinum evaporating dish to remove

Table 1. Recovery of germanium from pelagic red clay (Red clay Y2P-96, lat. 20°50′ N, long. 125°15·4′ W)

Ge present* (p.p.m.)	Ge found (p.p.m.)
2·5	2·4
5·0	5·2
10·0	9·5
16·0	15·5
20·0	20·0
52·0	50·0

* The original germanium content of this sediment was 2·0 p.p.m., determined independently by the author's method and that of Schneider and Sandell. Germanium was then added to increase the content to the amounts indicated.

silica. The residue was then fused with potassium pyrosulphate. Germanium was separated by distilling it as the tetrachloride from nearly constant boiling HCl, and was finally determined by measuring the absorbancy of its phenylfluorone complex using a Beckman DU spectrophotometer at 505 mμ. For 1 p.p.m. of germanium the error is within 10 per cent, and for higher germanium concentrations the error is proportionately less. The recovery of germanium from the complex matrix of pelagic clays is given in Table 1. The present results were checked by independent analysts using various techniques (El Wardani, 1957).

IV. Germanium in Sea Water

Small quantities of GeO_2 were found to dissolve readily in natural, filtered sea water, indicating that sea water is well undersaturated with respect to the element. The germanium content of sea water is not determined by the solubility product of its compounds and during the processes of weathering the element may enter sea water in association with clay minerals, igneous detritus, and in colloidal or adsorbed form. Doubtless some germanium is present in solution, and its nature is determined by the chemistry of its compounds in the complex medium of sea water. The germanium in true solution may be present as the germanate anion

$GeO_3^{=}$, comparable to the meta-silicate anion $SiO_3^{=}$, a postulate which is not inconsistent with the known aqueous chemistry of the stable germanium (IV).

The germanium content of sea water was determined by first concentrating the element from several litres of sea water using hydrated ferric oxide as a carrier, and then analysing the carrier for its germanium content. The results obtained for control experiments and natural sea water are reported in Table 2.

While this manuscript was being prepared Burton and Riley (1958) published

Table 2. Recovery of germanium from control media and natural sea water

Experiment	Ge (μg added)	Ge (μg recovery)
Distilled water + 0·5 g $FeCl_3$	0·0, 0·0	0·0, 0·0
1 l. filtered sea water + 0·5 g $FeCl_3$	0·0, 0·0	0·0, 0·0
1 l. filtered sea water + 0·5 g $FeCl_3$	1·0, 1·0, 1·0	1·1, 0·98, 1·2
1 l. filtered sea water + 0·5 g $FeCl_3$	0·5, 0·5, 0·5	0·55, 0·60, 0·42
12 l. of filtered sea water + 0·5 g $FeCl_3$*	0·0	0·50
8 l. of filtered sea water + 0·5 g $FeCl_3$*	0·0	0·40
Filtrate from above sample + 0·5 g $FeCl_3$	0·0	0·0

Average Ge content of sea water is 0·05 μg/l.†

* Pacific Ocean water, integrated sample from 1000–1500 m, collected June 1955, and delivered in a polyethylene carboy.

† This concentration is for sea water including particles not retained by millipore filters (Hydrosol assay type) with effective pore size of 0·45 μ.

the results of their germanium analysis in a few samples of sea water from the Irish Sea, the English Channel and North Atlantic. They reported 0·06–0·07 μg of germanium per kg of sea water.

If we take the amount of weathered igneous rocks to be $1{\cdot}6 \times 10^5$ g/cm^2 of the earth's surface (Goldschmidt, 1933) and take 1 p.p.m. for the average germanium content of igneous rocks (El Wardani, 1957) and assume that all germanium from weathered igneous rocks entered into solution in sea water, the calculated concentration of the element in sea water is approximately 6 p.p.m. as compared to the observed concentration of 5×10^{-5} p.p.m. This suggests that most of the germanium is removed from sea water.

Controlled experiments in a medium as complex as sea water for the investigation of possible mechanisms responsible for the removal of trace metals from sea water are time consuming. On the other hand, sometimes significant results and much suggestive information may be obtained from analyses of the associated organisms and the sediments.

V. Germanium in Organisms and Common Trace-metal Scavengers of the Ocean

Many plants and animals of the sea are known to concentrate trace metals from their aqueous medium, and concentration factors of several hundreds or thousands are reported (Noddacks, 1939; Black and Mitchell, 1952). Minerals

Table 3. Germanium content of organisms and trace-metal scavengers of the ocean

Material	Ge (p.p.m.)	
Marine organisms		
Diatom frustules, collected July 1949, S.I.O. Cruise D. V., Station 108, separated from salps.	0·3	
Siliceous frustules (diatoms and Radiolaria), separated from a bottom sample (Gulf of California) rich in siliceous ooze.	0·5	
Siliceous sponge, from Henderson Guyot.	0·0,	0·0
Siliceous sponge, from Pratt Guyot.	0·0,	0·0
Offshore mixed plankton (ash), S.I.O. Cruise 42–63·55.	0·0,	0·0
Offshore mixed plankton (ash), S.I.O. PAS Cruise.	0·0,	0·0
Offshore mixed plankton (ash), provided by Dr. T. W. Thomas.	0·0,	0·0
Macrocystis (ash of four entire small plants), collected February 1956, La Jolla, California.	0·0,	0·0
Macrocystis (ash of one entire large plant), collected February 1956, La Jolla, California.	0·0,	0·0
Laminaria (ash of entire plant), collected February 1956, La Jolla, California.	0·0,	0·0
Laminaria (ash of thick stalks only), provided by Dr. N. Rakestraw, Atlantic Cruise, Gulf of Maine, July 1933.	0·0,	0·0
Marine scavengers		
Manganese nodules		
PAS 19–121, from red clay area, lat. 19°49′ N, long. 121°4·5′ W, depth 4350 m.	0·0,	0·0
Horizon nodule, from red clay area, lat. 40°14′ N, long. 155°52′ W, depth 5500 m.	0·0,	0·0
MP43A (Sylvania Guyot), lat. 12° N, long. 165° E, depth 4600 m.	0·0	
Henderson Sea Mt., lat. 25°15′ N, long. 119°40′ W.	0·0,	0·0
*Phillipsites**		
PAS 19–121, separated from Manganese Nodules, lat. 19°49′ N, long. 121°4·5′ W, depth 4350 m.	0·0,	0·0
MP43A (Sylvania Guyot), Euhedral crystals from vugs in palagonitized tuff breccia, lat. 12° S, long. 165° E, depth 4600 m.	0·0,	0·0
Horizon nodule phillipsite, from red clay area, lat. 40°14′ N, long. 155°52′ W, depth 5500 m.	0·0,	0·0
Apatites†		
MP37C (Cape Johnson Guyot), lat. 17°10′ N, long. 177°10′ W, depth 2200 m.	0·0,	0·0
MP43A (Sylvania Guyot), veins in palagonitized tuff.	0·0,	0·0
Phosphorite nodule from Coronado Bank, lat. 32°40′ N, long. 117°39′ W, depth 300 m.	0·0,	0·0
EDTA-*soluble fraction of red clays*		
Fraction of Ch-6, lat. 12°03·2′ N, long. 125°26·3′ W.	0·0,	0·0
Fraction of Ch-10, lat. 10°21·4′ N, long. 125°26·3′ W.	0·0,	0·0
Fraction of Y2P-96, lat. 20°50′ N, long. 125°14·5′ W.	0·0,	0·0

* Phillipsite separated by acetone wash and tetrabromoethane heavy liquid flotation, followed by magnetic and electrostatic treatment to remove impurities. Purity confirmed by X-ray diffraction. (PAS 19–121 given final cleaning with EDTA (pH = 8) to remove all Fe, Mn and exchangeable cations.) Samples provided by Dr. R. Rex.

† Apatite separated by heavy liquid fractionation with tetrabromoethane followed by magnetic treatment to remove impurities. Purity confirmed by X-ray diffraction. Samples provided by Dr. R. Rex.

such as hydrated oxides of iron, aluminium and manganese; hydrogenous apatites; and authigenic phillipsites, are commonly referred to as marine scavengers, and are also powerful agents in removing trace metals from sea water (Murray and Renard, 1891; Goldberg, 1954: Arrhenius and Goldberg, 1955, and Krauskopf, 1956). Table 3 shows the germanium content for some marine organisms

Table 4. Germanium in shelf and basin sediments

Sample*	Latitude	Longitude	Depth of water above core (m)	Ge (p.p.m.)
Pacific Ocean				
Green mud	32°32′ N	117°27′ W	1300	1·5
Fine mud	32°38′ N	117°24′ W	296	1·1
Fine sand	32°41′ N	117°12′ W	58	0·8
Unidentified	32°39′ N	117°22′ W	208	1·1
Unidentified	32°38′ N	117°17′ W	72	1·4
Sea of Japan				
Blue mud	41°34′ N	130°26′ E	2791	1·0, 1·0
Blue mud	37°47′ N	133°43′ E	517	1·0
Blue mud	39°49′ N	133°15′ E	1622	1·1
Blue mud	41°24′ N	131°53′ E	3394	1·2
Gulf of Mexico				
Offshore clay	29°28′ N	88°32′ W	336	1·2, 1·2
Unidentified	25°19′ N	84°40′ W	2280	1·3
Unidentified	28°40′ N	89°45′ W	120	1·1
Unidentified	29°40′ N	89°45′ W	120	1·1
Clay and silt	29°21′ N	89°09′ W	9	1·0
Carribbean Sea				
Green mud (stagnant basin)	10°37′ N	65°24′ W	1436	1·2, 1·1
Green mud	10°55′ N	65°36′ W	290	1·1
Green mud	10°46′ N	64°52′ W	480	1·1
			Average	1·1

and for the common marine scavengers of trace elements. Clay minerals are considered later in the text.

It is evident from the results shown in Table 3 that the most abundant organism of the marine environment do not take up detectable amounts of germanium. Marine amorphous silica contains little or no germanium, as shown from the analyses of diatom frustules and siliceous sponges. It is evident also that marine scavengers, which concentrate titanium, cobalt, nickel, copper, radium, zircon and other trace elements from sea water, do not concentrate germanium in the marine environment.

VI. Germanium in Shelf and Basin Sediments

Table 4 shows the concentration of germanium in shelf and basin sediments, together with the description and location of the samples. An average of 1·1 p.p.m. germanium is found in the shelf sediments. This concentration is similar to that obtained by the author for igneous rocks (El Wardani, 1957).

VII. Germanium in Deep-sea Sediments

Table 5 shows the location and description of cores analysed as well as a key of

Table 5. Description of deep-sea cores used in this investigation

Core	Latitude	Longitude	Depth of water above core (m)
	Pacific north-east equatorial pelagic clays		
Cap-50BP	14°55′ N	124°12′ W	4270
Cap-49BP	9°17′ N	124°09′ W	4410
Ch–G	12°03·2′ N	125°26·3 W	4636
Ch–10	10°21·4′ N	125°26·3′ W	4645
Y_2P	20°50′ N	125°14·5′ W	5000
Y_4P	20°49·5′ N	125°15′ W	4900
Y_7P	20°50′ N	125°11′ W	4940
Y_3G	20°51′ N	125°14′ W	5020
MP–36	16°48′ N	176°27′ W	5400
PAS	19°49′ N	121°4·5′ W	4350
NH12	22°49′ N	156°50·3′ W	4484
NH13	23°21·8 N	156°28·7′ W	4254
NG3	27°08·5′ N	119°29·0′ W	4480
NG2	28°41·5′ N	120°12′ W	3900
SW46	8°22′ N	108°0′ W	3775
	Pacific south equatorial pelagic clays		
Cap–31BG	17°29′ S	158°40′ W	4890
Cap–33BG	12°46′ S	143°33′ W	4380
Cap–34BG	11°20′ S	142°25·5′ W	4500
Cap-Hg-composite of five cores	16°26′ S	162°43′ W	5125
	16°40′ S	162°15′ W	4675
	16°58′ S	161°35′ W	5140
	16°44′ S	161°22′ W	4685
	16°53′ S	159°08′ W	5040
	Atlantic pelagic clays		
AT–60	27°45′ N	61°54′ W	5670
	Globigerina ooze		
SW–60	1°35′ N	134°57′ W	4540
SW–61	0°06′ S	135°58′ W	4437

Cap = Capricorn Exp.; Ch = Chubasco Exp.; SW = Swedish Deep Sea Exp.; Y = Yoyo Exp.; MP = Mid-Pacific Exp.; PAS = Pacific Area Studies Exp.; NH = North Hawaii Exp.; NG = Navy Guadalupe Exp.; At = Atlantic Cruise; P = Piston Core; B = R. V. Baird; H = R. V. Horizon.

nomenclature used for the samples. The germanium content of the deep-sea sediments analysed is shown in Table 6.

The Pacific south equatorial pelagic clays show an average of 0·9 p.p.m. for their germanium content, which is similar to that of igneous rocks. The Pacific

Table 6. Germanium in deep-sea sediments

Sample*	Ge (p.p.m.)
Pacific north-east equatorial pelagic clays	
Cap–50BP–28	2·4, 2·5
Cap–50BP–48	2·0
Cap–50BP–92	2·1
Cap–50BP–216	2·2
Cap–50BP–280	1·2
Cap–50BP–688	1·9
Cap–50BP–760	1·9
Cap–49BP–28	2·5
Cap–49BP–integrated	2·3
Cap–49BP–188	2·1
Cap–49BP–372	2·2
Cap–49BP–813	2·1, 2·2
CH6–integrated	2·5
CH10–integrated	2·1
Y2F–96	2·0‡
Y2P–31	2·1
Y4P–integrated	2·0
Y7P–integrated	2·0
Y3G–21	2·0
MP–36 (2 in.–3 in.)	1·8
MP–36 (57 in.–61 in.)	2·0
PAS–surface	2·0, 2·0
NH12–integrated	2·0
NH13–integrated	2·0
NG3–integrated	2·1
NG2–integrated	2·0
SW46(0–10)	2·0§
Average	2·0
Pacific south equatorial pelagic clays	
Cap–31BG–integrated	1·7
Cap–33BG–integrated	0·9, 0·9
Cap–34BG–integrated	0·9, 1·0
Cap–HG–composite of five cores (21–25)	0·9
Average (not including Cap–31BG)	0·9

Table 6—*continued*

Sample*	Ge (p.p.m.)
Atlantic pelagic clays	
AT60–13	2·1
Globigerina ooze	
SW60–1007	0·0, 0·0
SW60–1011	0·0
SW61–200	0·0, 0·0
SW61–240	0·0
Average	0·0

* Numbers given after the name of the core refer to depth of sample below surface of core in centimetres.
† Sample below the unconformity.
‡ Average of five separate analyses giving 2·0, 2·1, 2.1, 2·0, 1·95 p.p.m.
§ Corrected for $CaCO_3$ content of 50 per cent.
¶ Unusually high in unaltered pyroclastics.

north-east equatorial pelagic clays, on the other hand, have an average germanium content of 2 p.p.m., which is twice the value for shelf material, Pacific south equatorial pelagic clays, and igneous rocks. Globigerina ooze is devoid of germanium.

VIII. Immediate Source Material for Germanium in Deep-sea Sediments

The absence of germanium in globigerina ooze (Table 6) and its low concentration or absence in biological silica (Table 3) leave the pelagic clays and their mineral phases as concentration sites for germanium from sea water. The ratio of germanium concentration in pelagic clays to that of sea water is of the order of 10^4.

The slow rate of accumulation of pelagic clays results in a relative concentration of components which are otherwise masked in sediments of higher rate of accumulation. These components are: quartz, detrital igneous minerals, manganese nodules, meteoritic dust, biological remains and, in high latitudes, ice-rafted material. However, the bulk of material is formed of clay minerals.

The relative abundance of the non-clay-mineral fraction in the pelagic clays varies from one sample to another, but rarely exceeds from 25 to 50 per cent by weight of the total material. Of this fraction, quartz is probably an abundant mineral of the lithogenous contribution (Rex, personal communication). Quartz was found to be practically devoid of germanium (El Wardani, 1957), and the present work indicates that biological contribution of germanium to the sediments is nil or negligible (Table 3). Manganese nodules, apatite and phillipsites, which are common concentration sites for trace metals also do not contain

detectable amounts of germanium. The cosmogenous part* (meteoritic dust), being less than 1 p.p.m., can scarcely contribute to the germanium content of the pelagic clays. Of the remaining building blocks of pelagic clays, the clay minerals, whether hydrogenous or lithogenous, together with the lithogenous igneous detritus may account for the observed germanium content of the sediments. The lithogenous contribution to sediments is defined as material derived from terrestrial erosion, submarine volcanoes and underwater weathering. The hydrogenous fraction is defined as the solid phases formed in the ocean and partly from ionic and molecular

Table 7. Germanium content of Pacific north-east equatorial pelagic clay size fractions

Pelagic clays	Size (μ)	Ge (p.p.m.)
Ch. 6 integrated	<3	3·1
Ch. 6 integrated	>3	1·3
Cap 49 BP integrated	<1	3·6
Cap 50 BP (tertiary portion)	<1	1·8
Y7P integrated	<1	3·0
Y2P–96	<2	3·0
Y2P–96	>2	1·0
Ch. 10 integrated	<3	2·0
Ch. 6 integrated	<3	3·1
Ch. 6 integrated	>3	1·3
Average Ge content of size fraction predominately of clay minerals not including Cap. 50 BP		3·0
Average Ge content of size fraction poor in clay minerals		1·2

solutions in sea water. An example of hydrogenous contribution is the precipitation of hydrated oxides of iron and manganese, the formation of calcium carbonate, and the coarsening and growth of aluminosilicates from sea water.

To determine the relative importance of clay and non-clay-mineral contributions of germanium to the sediments, pelagic clays were separated into two fractions, one containing most of the clay minerals and the other containing little or no clay minerals. The size fractions separated by settling and centrifuging were analysed for their germanium content and the results are given in Table 7.

The observed concentration of germanium in the size fractions which are predominantly clay minerals suggests that germanium is essentially confined to the aluminosilicates of the clay-mineral size fraction. The removal of the element from sea water may therefore be associated with the mode of formation of such minerals.

* Cosmic spherules are known to be present in pelagic clays (Murray and Renard, 1891; Mellis and Laevastu, 1955; Pettersson, 1955; Bruun *et al.*, 1955). Since iron meteorites are high in their germanium content (El Wardani, 1957), an attempt was made to separate and analyse the cosmic fraction of the deep-sea sediments. The cosmic fraction was separated by settling, magnetic separation and solution of the ferromanganese fraction by EDTA. The final strong magnetic fraction, believed to be magnetite and cosmic material, was a few milligrams and the germanium content was below the limit of detectability.

IX. Adsorption vs. Structural Incorporation

Sea water is undersaturated with respect to many of the trace metals, including germanium. Goldschmidt (1937) suggested that rare-metal concentrations in sea water are kept low by adsorption on hydrated iron oxides. Harvey (1955) reported that copper salts are readily soluble in sea water and that copper can be removed by adsorption on clay or organic matter. Goldberg (1954) suggests that titanium, zirconium and cobalt are adsorbed on hydrated iron oxide, while nickel appears to be removed from sea water by adsorption on hydrated manganese oxide.

Table 8. Germanium content of pelagic clays and their clay minerals before and after EDTA treatment

Pelagic clay	Ge (p.p.m.)	
	Before	After
Ch. 6, integrated	2·5	2·5, 2·6
Ch. 6, size fraction less than 3 μ	3·1	2·8, 3·0
Ch. 10, integrated	2·1	2·1
Ch. 10, size fraction less than 3 μ	2·0	2·0
Cap 33 BG size fraction less than 3 μ	0·9	1·0

More recently, Krauskopf (1956) discussed the factors controlling the concentrations of thirteen metals in sea water and emphasized the importance of adsorption by hydrated oxides of iron and manganese, apatite, clay and organic matter in removing trace metals.

Deep-sea clays and their size fractions rich in clay minerals were extracted with ethylenediaminetetraacetic acid (EDTA) at pH 7 and 50°C for several hours. After treatment with EDTA, the germanium content of the clays was again determined and the results are given in Table 8. Under the above conditions EDTA complexes readily with adsorbed cations on the surface of clay minerals, but does not readily attack the aluminosilicate structure of such minerals. The results shown in Table 8 indicate, therefore, that germanium in the pelagic clays is not totally available for complexation with EDTA and that the element is probably structurally bound in the aluminosilicates, perhaps proxying for silicon in the tetrahedral sheets.

If germanium enrichment in the clay mineral fractions of the sediments (Table 7) results from adsorption of the element from sea water on the surface of clay minerals precipitated from sea water, the residence time of germanium in the oceans may approximate that of aluminium. Using the equation given by Goldberg and Arrhenius (1958) to calculate the residence times of elements in the oceans, the average residence time of germanium is 10^5 years as compared to 10^2 years for aluminium.

Further evidence indicating that germanium enrichment in the clay minerals is not totally a surface adsorption phenomenon is given later in the text.

If part of the clay minerals in pelagic clays is formed from sea water (Arrhenius, 1954a), and as shown by the author later in the text, then the structural incorporation of trace elements during the hydrogenous growth of such minerals is a plausible mechanism for removal of trace elements from sea water and their ultimate concentration in the sediments.

X. Origin of Pelagic Clay Minerals

Murray and Renard (1891, p. 339), discussing the origin of marine clays, note:

> "The clays of marine deposits may, from the point of view of their origin, be divided into two varieties: first, those in which one clayey matter has been chiefly transported by rivers from continental and other land surfaces, and second, those in which it has principally been formed *in situ* from the decomposition of rocks and minerals scattered over the bottom of the ocean. The former corresponds to the clayey matter in all terrigenous deposits in close proximity to the land, while the latter corresponds generally to the clayey matter in all truly pelagic deposits laid down towards the central regions of the great ocean basins."

Kuenen (1950, p. 360), amplifying the concept of terrigenous source of clay minerals points out that minerals of the pelagic "red" clays are similar to those in blue mud and globigerina ooze. He also notes that these fine grains of subaerial chemical weathering on land have spent a long time in oceanic circulation before finally settling in the pelagic regions of the deep sea. Kullenberg (1953) assumed that the size of the clay particles now observed in pelagic sediments has remained essentially unchanged during transport and deposition, pointing to them as products of subaerial weathering.

Goldschmidt (1932) demonstrated that certain minerals are formed in the ocean, and are characterized by a high boron content which he ascribed to adsorption. Murray and Gravenor (1953) suggested that a combination of negatively charged colloidal silica, the $SiO_3^=$ ion and positively charged aluminium hydroxide form clay minerals and thus responsible for removal of part of the silica from sea water. Arrhenius (1954a, p. 1228) pointed out that the structural distribution of boron in pelagic clay minerals suggests that a considerable fraction of these minerals is precipitated from solution in the ocean. Arrhenius in a later publication (1954b) also emphasized the hydrogenous origin of part of the clay minerals in the Pacific north-east equatorial eupelagic clays.

The present investigation on the localization and geochemical fractionation of germanium between shelf and deep-sea sediments indicates that the element may serve as a tracer for the origin of pelagic clay minerals. The germanium content of Pacific north-east equatorial eupelagic clays is twice that of shelf sediments (Tables 4 and 6) and of greater significance is the germanium content of the fine fractions* in these two types of sediments and of standard API† clay minerals of marine origin (Table 9), assuming the latter has not undergone diagenesis.

It is evident from Table 9 that the clay-mineral fraction of Pacific north-east equatorial eupelagic clays is about three times higher in its germanium content, as compared to standard API marine clay minerals, and the fine fraction of shelf

* The fine fraction of the sediments includes the principal portion of the clay minerals (Grim, Dietz and Bradley, 1949), and it is here referred to as the clay-mineral fraction.

† American Petroleum Institute.

Table 9. Germanium content of standard A.P.I. marine clay minerals and fine fractions of shelf and eupelagic clays

Material	Ge (p.p.m.)
Standard A.P.I. marine clay minerals	
Illite, Morris, Ill.	1·2, 1·2
Illite, Fithian, Ill.	1·2
Kaolinite, Murfreesboro, Ark.	1·3, 1·4
Kaolinite, Macon, Ga.	1·3, 1·3
Kaolinite, Bath, S.C.	1·1, 1·1
Kaolinite, Mesa Alta, N. Mex.	1·0
Montmorillonite, Polkville, Miss.	0·5
Montmorillonite, Upton, Wyo.	0·5
Montmorillonite, Little Rock, Ark.	0·5
Average	1·0
Fine fractions of shelf sediments	
$<2\ \mu$, lat. 32°38′ N, long. 117°17′ W	0·8, 0·8
$<2\ \mu$, lat. 32°39′ N, long. 107°22′ W	0·9, 1·0
$<2\ \mu$, lat. 32°38′ N, long. 117°24′ W	1·0, 1·0
Average	0·9
Fine fractions of Pacific north-east equatorial eupelagic clays Individual analysis are given in Table 7	
Average	3·0

sediments. This, together with the structural bonding and localization of germanium in the clay-mineral fractions, suggests that the eupelagic clay minerals are not entirely terrigenous clay minerals transported in suspension to the site of deposition.

Volcanic material is a possible source of clay minerals in the ocean (Murray and Renard, 1891, p. 340). If clay minerals of the Pacific north equatorial eupelagic clays result primarily from the alteration of volcanic material, it may be expected that volcanic material such as Pacific oceanic basalts and pumice, as well as pelagic clays and their fine fractions from areas of high relative volcanic contribution, exhibit a germanium content similar to that observed in the former. Oceanic volcanic material and pelagic clays and their clay-mineral fractions from areas of high relative volcanic contribution were analysed for their germanium content and the results are given in Table 10.

The results indicate that oceanic volcanic material has a germanium content similar to that of continental igneous rocks, 1 p.p.m. germanium (El Wardani, 1957). Of greater significance is the average germanium content of Pacific south

Table 10. Germanium content of oceanic volcanic material and pelagic clays from areas of high relative volcanic contribution

Material	Ge (p.p.m.)
Oceanic basalts	
Henderson Sea Mt., Pacific, lat. 25°34·3′ N, long. 119°33·3′ W	1·1, 1·2
Fieberling Bank, Pacific, lat. 32°24′ N, long. 127°47′ W	1·1
Socorro Island, Pacific. lat. 18°43′ N, long. 111°57′ W	0·9
Sylvania Sea Mt., Pacific, lat. 12° N, long. 165° E	1·2
Erbem Bank, Pacific, lat. 37°50′ N, long. 132°32′ W	1·1
Mytilus Sea Mt., Atlantic, lat. 39°50′ N, long. 67°12′ W	1·1
Bear Sea Mt., Atlantic, lat. 39°55′ N, long. 67°27′ W	1·0
Average	1·0
Volcanic ash and pumice	
Ash, Borcenia Volcano, Pacific	1·2
Oceanic pumice (provided by Dr. A. F. Richards)	1·0
Pacific south equatorial eupelagic clays (*entire material*)	
Individual analyses given in Table 6.	
Average	0·9
Pacific south equatorial eupelagic clays (*fine fractions*)	
Cap. 33 BG integrated sample size fraction $<3\mu$	0·9
Cap. 31 BG integrated sample size fraction $<1\mu$	1·8
Cap. HG, composite of five cores (21–25 m) size fraction $<3\ \mu$	1·2
Average	1·3

equatorial pelagic clays and their clay-mineral fraction, being at most one-half the germanium content in the corresponding material of the Pacific north-east equatorial eupelagic clays. Clay minerals of the Pacific north-east equatorial eupelagic clay cannot therefore be primarily alteration products of volcanic contributions nor do they appear to be entirely transported from land.

To further investigate this conclusion, material from core Capricorn 50 BP was fractionated into size fractions ranging from 0·03 to 10 μ by settling and ultracentrifuging. The germanium content of each size fraction is given in Table 11 and Fig. 1 shows the germanium in p.p.m. plotted against the logarithm of particle diameter.

It is obvious from Fig. 1 that the germanium content increases with decreasing particle diameter. Nevertheless, this increase in germanium with decreasing

particle diameter is not characteristic of a pure surface adsorption phenomena. The germanium content per unit area and the germanium concentration in p.p.m. (assuming the element to be totally adsorbed) were calculated and the results are

Table 11. Germanium in size fractions of core Capricorn, 50 BP

Size fraction, (μ)*	Ge (p.p.m.)
0·03–0·1	3·7
0·1–0·32	3·1
0·32–1·0	2·6
1·0–3·2	2·0
3·2–10	1·0

* Size fractions were provided by Dr. G. O. S. Arrhenius.

given in Table 12, along with the particle diameter and the observed germanium content for the different size fractions. In calculating the data in column 3 the surface area of particles 2·1 μ in diameter was normalized to unity and their germanium content normalized to the observed value of 2 p.p.m.

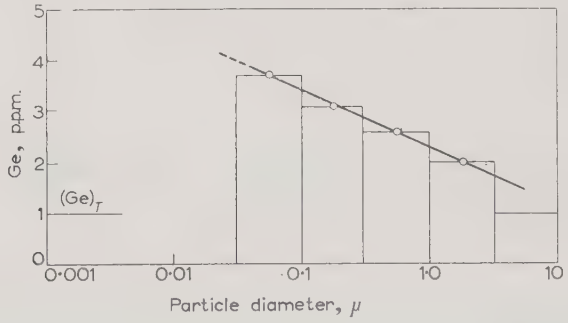

Fig. 1. Germanium concentration as a function of particle diameter
$(Ge)_T$ = Germanium concentration of terrigenous contribution.

It is evident from the above data and previous findings that germanium in the pelagic clay minerals is not totally a surface adsorption phenomenon. The germanium in the pelagic clay minerals most probably proxies for silicon in the tetrahedral sheets suggesting that the observed increase in germanium concentration with decrease of particle diameter results from an increased proportion of germanium-rich hydrogenous clay minerals formed in sea water.

Few minerological analyses of the fine fractions of recent marine sediments are available in the literature. In the fine fractions (<1 μ) terrigenous clay minerals and quartz are undoubtedly present along with the hydrogenous aluminosilicates, and quantitatively represent the bulk of the material. While the terrigenous clay mineral contribution is difficult to assess quantitatively, data are available on the quartz content of the fine fractions. Correns (1925), in his work on the sediments

of the Equatorial Atlantic Ocean, found from 10 to 15 per cent quartz in the $<1\ \mu$ fraction and the mineral was present in the majority of samples examined. Grim *et al.* (1949) found quartz to be present in the $<1\ \mu$ fraction of almost every sample studied from recent marine sediments of the Pacific. They estimated from 5 to 10 per cent and from 1 to 2 per cent quartz in the 1–0·01 μ and $<0{\cdot}1\ \mu$ fractions respectively.

Table 12. Calculated and observed germanium content of size fractions of core Capricorn, 50 BP

Particle diameter (μ)	Ge (μg/unit area $\times 10^{18}$)*	Ge assuming total surface physical adsorption (p.p.m.)	Ge, observed (p.p.m.)
6·5	8·3	0·7	1·0
2·1	6·2	2	2·0
0·65	2·0	8	2·6
0·21	1·0	20	3·1
0·06	0·3	78	3·7

* Data in this column are calculated by taking 2 g/cm^3 for the density of the material and assuming the particles to be spherical in shape.

Quartz, both continental and separated from deep-sea sediments, was found to be practically devoid of germanium (El Wardani, 1957) and, unless there is an unknown phase that is highly specific for germanium in the fine fraction ($<1\ \mu$), the aluminosilicates of this fraction in the Pacific north-east equatorial eupelagic clays appear to be largely hydrogenous in origin. In the light of the present investigation the possibility that clay minerals of fractions $<0{\cdot}1\ \mu$ are essentially lithogenous, with a negligible amount being hydrogenous but highly specific for germanium to bring about the observed germanium content, is unlikely.

XI. Relative Abundance of Hydrogenous and Lithogenous Aluminosilicates

The present work demonstrates that the germanium content of hydrogenous clay minerals is at least twice that of lithogenous clay minerals. It is therefore possible that both lithogenous and hydrogenous clay minerals be detected in pelagic sediments by their low and high germanium content respectively. If the concept of hydrogenous origin of part of the clay minerals is accepted, then a pure hydrogenous clay would exhibit a characteristic germanium content and the relative abundance of such minerals could then be evaluated. Assuming that pure hydrogenous aluminosilicates give approximately 6 p.p.m. for their germanium content, obtained by extrapolation of Fig. 1, and, since clay minerals transported from land have 1 p.p.m. germanium, the relative abundance of both components in the clay-mineral size fractions can be estimated from the germanium content of the latter. The relationship $6(1 - x) + 1(x) =$ germanium, p.p.m. (where x is the percentage

of lithogenous clay minerals) is used to calculate the relative abundances given below:

Size fraction (μ)	Ge, observed (p.p.m.)	Lithogenous content (%)	Hydrogenous content (%)
0·03–0·1	3·7	46	54
0·1–0·32	3·1	58	42
0·32–1·0	2·6	68	32

If we take 3·3 p.p.m. for the germanium content of the fraction $<1\ \mu$ in the Pacific northeast equatorial eupelagic clays (Table 7) the hydrogenous clay minerals amount to 46 per cent of this fine fraction or at least 23 per cent of the total clay material. Of course it is assumed that particles with 6 p.p.m. germanium are entirely pure hydrogenous aluminosilicates, and the relative percentages given are therefore, only approximations.

XII. Sediments of the Pacific

The observed geochemical distribution of germanium between the shelf and deep-sea sediments and their size fractions substantiates our knowledge of the nature and origin of the sediments from lithological and mineralogical investigations. The average germanium content of shelf and deep-sea sediments and their fine* and coarse† fractions are given below:

Sediment	Ge, entire material (p.p.m.)	Ge, fine fraction (p.p.m.)	Ge, coarse fraction (p.p.m.)
Shelf	1·0	1·0	1·0
NE equatorial Pelagic clays	2·0	3·0	1·0
S equatorial Pelagic clays	1·0	1·3	1·0
Globigerina Ooze	0·0	—	—

The germanium distribution in shelf sediments is similar to that of igneous rocks (El Wardani, 1957) and suggests that shelf materials are essentially lithogenous in origin. The south equatorial pelagic clays and their coarse fraction as well as the coarse fraction of northeast equatorial pelagic clays exhibit a germanium content also characteristic of igneous material and are therefore essentially lithogenous.‡

* Fine fractions contain most of the clay minerals.

† Coarse fractions contain little or no clay minerals.

‡ Authigenic and hydrogenous minerals such as zeolites, goethite, barite, etc., and the biogenous contribution are quantitatively of minor importance in the eupelagic clays.

It is significant that the germanium content of north-east equatorial pelagic clays and their fine fraction is twice the value for corresponding material in the south equatorial pelagic clays, an area of high relative contribution of pyroclastics. This difference may be partially attributed to different sources of clay minerals. Clay minerals of the south equatorial pelagic clays may predominantly be of lithogenous origin arising from *in situ* decomposition and alteration of water-borne pumice and other volcanic rocks and minerals. On the other hand a significant fraction of the clay minerals of the north-east equatorial eupelagic clays appears to be hydrogenous material formed in sea water.

In the light of the present investigation it may be said that the north-east equatorial pelagic areas of the Pacific are more truly oceanic environments receiving a smaller lithogenous contribution compared to the south equatorial pelagic areas.

Acknowledgement—The author wishes to thank Dr. G. Arrhenius who provided many of the deep-sea sediments and their fine fractions and for his valuable suggestions and help during the investigation.

The author is particularly grateful to Dr. N. W. Rakestraw who kindly encouraged this work at the Scripps Institution of Oceanography. The author is indebted to Dr. I. A. Breger for his valuable criticism and comments and to Dr. E. B. Sandell who read the manuscript.

References

Ahrens H. L. (1952) The use of ionization potentia's. Part I. Ionic radii of the elements. *Geochim. et Cosmochim. Acta* **2,** 155–169.

Arrhenius G. (1954a) Significance of carbonate stratification in pelagic deposits. *Bull. Geol. Soc. Amer.* **65,** 1228.

Arrhenius G. (1954b) Origin and accumulation of aluminosilicates in the ocean. *Tellus* **3,** 215–220.

Arrhenius G. and Goldberg E. D. (1955) Distribution of radioactivity in pelagic clays. *Tellus* **7,** 226–231.

Bardet J., Tchakirian A. and Lagrange R. (1938) Recherche spectrographique des elements existant a l'etat de traces dans l'eau de mer. *C. R. Acad. Sci., Paris,* **206,** 450.

Black W. A. P. and Mitchell R. L. (1952) Trace elements in the common brown algae and in sea water. *J. Mar. Biol. Ass. U.K.* **30,** 575–584.

Bruun A., Langer E. and Pauly H. (1955) Magnetic particles found by raking the deep-sea bottom. *Deep-Sea Res.* **2,** 230–246.

Burton J. D. and Riley J. P. (1958) Germanium and gallium in sea-water. *Nature, Lond.* **181,** 179–180.

Correns C. W. (1925) Die Sediments des äquatorialen atlinischen ozeans. *Deutsche atlanische Exped. Meteor.* **27,** Wiss, Erq. Bd. III, Teil III.

El Wardani S. A. (1957) On the geochemistry of germanium. *Geochim. et Cosmochim. Acta,* **13,** 5–19.

Goldberg E. D. (1954) Marine geochemistry. I. Chemical scavengers of the sea. *J. Geol.* **62,** 249–265.

Goldberg E. D. and Arrhenius G. O. S. (1958) Chemistry of Pacific pelagic sediments. *Geochim. et Cosmochim. Acta* **13,** 209.

Goldschmidt V. M. (1932) Zur Geochemie des Bors. I, II, *Nachr. Ges. Wiss. Gottingen.*

Goldschmidt V. M. (1933) The enrichment of rare elements in coals. *Nachr. Gesell. Wiss., Gottingen* **4,** 371–387.

Goldschmidt V. M. (1937) Geochemische Verteilungsgesetze der elemente. IX. Die Mengenverhaltnisse der Elemente und der Atom-Arten. *Norske Videnskaps-akad. Oslo, Skr., Mat.-Nat. Kl.* **4,** 148.

Grim R. E., Dietz R. S. and Bradley W. F. (1949) Clay mineral composition of some sediments from the Pacific Ocean off the California Coast and the Gulf of California. *Bull. Geol. Soc. Amer.* **60,** 1785–1808.

Harvey H. W. (1955) *The Chemistry and Fertility of Sea Waters.* Cambridge University Press.

Krauskopf K. B. (1956) Factors controlling the concentrations of thirteen rare metals in sea-water. *Geochim. et Cosmochim. Acta* **9,** 1–32.

Kuenen Ph. H. (1950) *Marine Geology.* John Wiley, New York

Kullenberg B. (1952) Absolute chronology of deep-sea sediments and the deposition of clay on the ocean floor. *Tellus* **5,** 302.

Mellis O. and Laevastu T. (1955) Extraterrestrial material in deep-sea deposits. *Trans. Amer. Geophys. Un.* **36,** 385–389.

Murray H. H. and Gravenor G. P. (1953) Colloidal-size silica in sediments. *Science* **118,** 3053, 25–28.

Murray J. and Renard A. (1891) Deep-sea deposits. *Rep. Challenger Exp.* Vol. IV.

Noddack I. and Noddack W. (1939) Die Häufigkeiten des Schwermetalle in Meerestieren. *Ark. Zool.* A **32,** 4, 1–35.

Pettersson H. (1955) Shooting stars. *Sartryck ur Sjofartsmuseet i Goteborg,* Festskrift for Tot E. J:son Brostrom.

Geochimica et Cosmochimica Acta, 1958, Vol. 15, p. 225. Pergamon Press Ltd. Printed in Northern Ireland.

BOOK REVIEW

Gmelin-Institut, Frankfurt a.M. **Gmelins Handbuch der anorganischen Chemie.** 8. Auflage. System Nummer 28: Calcium. Teil A—Lieferung 2. Verlag Chemie, Weinheim/Bergstrasse, 1957. 420 S. mit 29 Fig. DM 232.

Die vorliegende Lieferung 2 des Bandes Calcium des Gmelin' schen Handbuches behandelt auf 132 Seiten das Vorkommen des Calciums, davon Kosmochemie auf 4 Seiten. Die Literatur über die Geochemie des Calciums ist wohl nahezu vollständig aufgeführt, und zwar wenigstens in einzelnen Fällen bis 1955. So findet man z.B. umfangreiche Tabellen über den Calciumgehalt von Mineralen (9 Seiten), von Eruptiven und Sedimenten des Grundwassers und der Böden (8 Seiten). Am Schluss des geochemischen Teiles wird des Kreislauf des Calciums besprochen und in einem anschaulichen Bild dargestellt. An die Geochemie schliesst sich eine topographische Übersicht an, in des die nutzbaren Lagerstätten von Flusspat auf 41 Seiten, von Gips und Anhydrit auf 39 Seiten, von optischem Kalkspat auf 5 Seiten und von Calciumphosphaten auf 76 Seiten behandelt sind. Auf 27 Seiten werden die Ca-Minerale besprochen. Des Rest der Lieferung (104 Seiten) befasst sich mit den Eigenschaften des Elementes Calcium und seinen *Legierungen*.

Die Lieferung enthält für den Geochemiker eine Fülle von wertvollen Literaturhinweisen.

C. W. Correns

Geochimica et Cosmochimica Acta, 1958, Vol. 15, p. 256. Pergamon Press Ltd. Printed in Northern Ireland.

Papers to be published in future issues

S. Ďurovič: Contribution to the lognormal distribution of elements

Marjorie Hooker: Data of rock analyses—V. Australian periodical and serial literature

A. E. Ringwood: On the chemical evolution and densities of the planets

A. Heydemann: Adsorption aus sehr verdünnten kupferlösungen an reinen tonmineralen

K. J. Murata, C. V. Dutra, M. Teixeira da Costa and J. R. Branco: Composition of monazites from pegmatites in eastern Minas Gerais, Brazil

K. S. Heier and S. R. Taylor: Distribution of Li, Na, K, Rb, Cs, Pb and Tl in southern Norwegian pre-Cambrian alkali feldspars

W. S. Brocker and Alan Walton: Geochemistry of C^{14} in the fresh water systems

R. A. Edge, R. R. Brooks, L. H. Ahrens and S. Amdurer: Some reconnaissance observations on the combined use of ion exchange enrichment and spectrochemical analysis for the determination of trace constituents in silicate rocks

D. Greenhalgh and P. M. Jeffery: A contribution to the pre-Cambrian chronology of Australia

N. Sen, S. R. Nockolds and R. Allen. Trace elements in minerals from rocks of the S. Californian Batholith

J. V. Jizba: Frequency distribution of elements in rocks

D. Carroll and H. C. Starkey: Leaching of clay minerals in a limestone environment

R. E. Belin: Radon in the New Zealand geothermal regions

G. L. Bate, J. R. Huizenga and H. A. Potratz: Thorium in stone meteorites by neutron activation analysis

W. U. Ault and J. L. Kulp: Isotopic geochemistry of sulphur

H. H. Le Riche: The distribution of certain trace elements in the lower lies of southern England

J. F. G. Wilkinson: The geochemistry of a differentiated teschenite till near Gunnedah, New South Wales

J. C. Vogel: Uber den Isotopengehalt des Kohlenstoffs in Süsswasser-Kalkablagerungen

J. L. Snyder: Distribution of certain elements in the Duluth complex

J. D. Burton, F. Culkin and J. P. Riley: The abundances of gallium and germanium in terrestrial materials

INFORMATION FOR CONTRIBUTORS

I. GENERAL

1. Papers on geochemistry should be submitted to the appropriate Executive Editor. Papers submitted for publication will naturally be judged from the standpoint of scientific originality and novelty. Technical details of apparatus used in scientific investigation can, however, be presented in brief notes. Critical comments or preliminary results requiring early publication should be submitted as letters to the editors. Where possible, letters should be confined to 500 words. The preparation of progress reports and review articles will be invited by the editors from time to time. The journal appears as independent and complete numbers, which are combined into volumes of about 300 pages.

2. Only papers which have not been previously published can be accepted. Authors must agree not to publish elsewhere a paper submitted to and accepted by *Geochimica et Cosmochimica Acta*.

3. Fifty reprints of each paper are provided free. Additional copies can be purchased if ordered at the time the first proofs are returned. A reprint order form will accompany first proofs.

II. SCRIPT REQUIREMENTS

1. Scripts must be written in one of the three official languages—English, French, or German.

2. The script should be typed (not a carbon copy). The text must be ready for printing and should be carefully checked for errors. Authors will receive proofs for correction.

3. Illustrations should accompany the script, mounted on separate sheets. Line diagrams that require to be redrawn should include all relevant details. Half-tone illustrations should be restricted to the minimum necessary. Photographs should be enlarged sufficiently to permit their clear reproduction, and if words or numbers appear on them, two copies should be sent, one clearly printed and the other without inscription. All illustrations should be provided with descriptive legends, which should be given on a separate sheet. Any lettering on diagrams—other than Greek letters, symbols, etc.—should be stencilled and should be sufficiently large and bold to permit reproduction when the diagram has been reduced to a size suitable for inclusion in the journal.

4. References in the text should be given by quoting the author's name and year of publication, i.e. AHRENS (1952). **Full references should be listed at the end of each paper, in alphabetical order, in the following manner:**

AHRENS, L. H. (1952) The use of ionization potentials—I. Ionic radii of the elements. *Geochim. et Cosmochim. Acta* **2**, 155–169.

and should include the full title of the article, standard abbreviated title of the journal, year, volume number and inclusive page numbers. References to books should include the total number of pages.

5. The text of articles submitted should be concise and in a readily understandable style. The technical description of the methods used should only be given in detail when such methods are new. The essential contents of each paper should be briefly recapitulated in an abstract in English. Such an abstract may, however, be submitted by the author in the language of the original typescript for translation into English by the editorial staff.

6. To conserve space, authors are requested to mark less important portions of the paper (such as description of methods, record of experimental results, etc.) for printing in smaller type.

7. Indices of refraction should be denoted by the symbols α, β, γ, ω, ε, n, and vibration directions by X, Y, Z, O and E.

Pergamon Press are also publishers of the following Journals:

JOURNAL OF NUCLEAR ENERGY (*including* THE SOVIET JOURNAL OF ATOMIC ENERGY*). PART A: REACTOR SCIENCE. PART B: REACTOR TECHNOLOGY
HEALTH PHYSICS (*The Official Journal of the Health Physics Society*)
JOURNAL OF INORGANIC AND NUCLEAR CHEMISTRY
TETRAHEDRON (*The International Journal of Organic Chemistry*)
TALANTA (*An International Journal of Analytical Chemistry*)
INTERNATIONAL JOURNAL OF APPLIED RADIATION AND ISOTOPES
BIOCHEMICAL PHARMACOLOGY
* BIOPHYSICS
* JOURNAL OF MICROBIOLOGY, EPIDEMOLOGY AND IMMUNOBIOLOGY
* PROBLEMS OF HEMATOLOGY AND BLOOD TRANSFUSION
* PROBLEMS OF VIROLOGY
* PROBLEMS OF ONCOLOGY
* SECHENOV PHYSIOLOGICAL JOURNAL OF THE U.S.S.R.
* BULLETIN OF THE ACADEMY OF SCIENCES OF THE U.S.S.R.; GEOPHYSICS SERIES
* ELECTRIC TECHNOLOGY, U.S.S.R.
* RADIO ENGINEERING
* RADIO ENGINEERING AND ELECTRONICS
* TELECOMMUNICATIONS
* PHYSICS OF METALS AND METALLOGRAPHY
* THE ABSTRACTS JOURNAL OF METALLURGY
* APPLIED MATHEMATICS AND MECHANICS
CHEMICAL ENGINEERING SCIENCE
JOURNAL OF ATMOSPHERIC AND TERRESTRIAL PHYSICS
PLANETARY AND SPACE SCIENCE
BULLETIN GÉODÉSIQUE
ANNALS OF THE INTERNATIONAL GEOPHYSICAL YEAR
SPECTROCHIMICA ACTA
JOURNAL OF THE MECHANICS AND PHYSICS OF SOLIDS
ACTA METALLURGICA (*for the Board of Governors of Acta Metallurgica*)
INTERNATIONAL JOURNAL OF THE PHYSICS AND CHEMISTRY OF SOLIDS
DEEP-SEA RESEARCH
JOURNAL OF NEUROCHEMISTRY
JOURNAL OF PSYCHOSOMATIC RESEARCH
JOURNAL OF INSECT PHYSIOLOGY
JOURNAL OF AIR POLLUTION
INTERNATIONAL ABSTRACTS OF BIOLOGICAL SCIENCES (*for Biological and Medical Abstracts Ltd.*)
RHEOLOGY ABSTRACTS
VACUUM
OPERATIONAL RESEARCH QUARTERLY
ANNALS OF OCCUPATIONAL HYGIENE

* *Translations of Russian journals published on behalf of the Pergamon Institute, a non-profit-making foundation*

Leaflets giving further details and subscription rates of each of these journals are available on request

THE GEOCHEMICAL SOCIETY

OFFICERS

FARRINGTON DANIELS, President
JOHN F. SCHAIRER, Vice-President
KONRAD B. KRAUSKOPF, Secretary
GEORGE T. FAUST, Treasurer

COUNCILLORS

WILLARD F. LIBBY, 1956–1958
HATTEN S. YODER, 1956–1958
JOHN A. S. ADAMS, 1957–1959
ALFRED O. NIER, 1957–1959
E. F. OSBORN, 1958–1960
H. G. THODE, 1958–1960

REGIONAL VICE-PRESIDENTS

LOUIS H. AHRENS
RUI RIBEIRO FRANCO
ING. GEORGES ORDOÑEZ
C. W. CORRENS
WILLIAM S. FYFE
KEN SUGAWARA

COMMITTEES

Auditing Committee:
JOSEPH J. TREGONING, Chairman
WILLIAM L. HILL
C. R. NASSER

Constitution and By-Laws Committee:
MICHAEL FLEISCHER, Chairman
JULIAN R. GOLDSMITH
DENIS M. SHAW

Education Committee:
H. D. HOLLAND, Chairman
J. A. S. ADAMS
D. M. HENDERSON
KURT E. LOWE
G. D. NICHOLLS

Membership Committee:
R. M. GARRELS, Chairman
HARVEY C. DIEBL
CHESTER B. SLAWSON
JAMES E. SLOSSON

Nominating Committee:
D. E. WHITE, Chairman
GEORGE EDWARDS
A. E. ENGEL
W. D. KELLER
T. G. SAHAMA
D. M. SHAW

Programme Committee:
H. T. EVANS, Chairman
GORDON J. F. MACDONALD
H. E. LOWENSTAM

Publications Committee:
E. W. HEINRICH, Chairman
JULIAN R. GOLDSMITH
JOHN C. MAXWELL
N. W. RAKESTRAW
S. C. ROBINSON
L. R. WAGER

Research Committee:
C. G. DODD, Chairman
LOUIS H. AHRENS
W. F. BRADLEY
C. W. CORRENS
RUI RIBEIRO FRANCO
WILLIAM S. FYFE
ING. GEORGES ORDOÑEZ
R. A. ROWLAND
KEN SUGAWARA
T. G. THOMPSON
G. W. WETHERILL

Russian Translations Committee:
EARL INGERSON

Seal Committee:
ALVIN VAN VALKENBURG, JR., Chairman
MARGARET D. FOSTER
JEWELL GLASS
EDWIN ROEDDER

Standards Committee:
HARRY A. BRIGHT, Chairman
FELIX CHAYES
ALBERT E. J. ENGEL
SAMUEL S. GOLDICH
KIGUMA J. MURATA
GEORGES S. SWITZER

Tellers Committee:
CHARLES MEYER, Chairman
HENRY R. CORNWALL
COLIN O. HUTTON